ชั้นกั้นการแพร่โลหะฐานโครเมียมสำหรับแพลเลเดียมเมมเบรนบนตัวรองรับเหล็กกล้าไร้สนิม

นายเจริญพร โชคบริบาล

วิทยานิพนธ์นี้เป็นส่วนหนึ่งของการศึกษาตามหลักสูตรปริญญาวิทยาศาสตรมหาบัณฑิต
สาขาวิชาปิโตรเคมีและวิทยาศาสตร์พอลิเมอร์
คณะวิทยาศาสตร์ จุฬาลงกรณ์มหาวิทยาลัย
ปีการศึกษา 2550

Cr-BASED INTERMETALLIC DIFFUSION BARRIER FOR STAINLESS STEEL SUPPORTED PALLADIUM MEMBRANE

Mr. Jaroenporn Chokboribal

A Thesis Submitted in Partial Fulfillment of the Requirements
for the Degree of Master of Science Program in Petrochemistry and Polymer Science
Faculty of Science
Chulalongkorn University
Academic year 2007

Thesis Title	Cr-BASED INTERMETALLIC DIFFUSION BARRIER FOR STAINLESS STEEL SUPPORTED PALLADIUM MEMBRANE
By	Mr. Jaroenporn Chokboribal
Field of Study	Petrochemistry and Polymer Science
Thesis Advisor	Associate Professor Supawan Tantayanon, Ph.D.
Thesis Co-Adviser	Assistant Professor Sukkaneste Tungasmita, Ph.D.

Accepted by the Faculty of Science, Chulalongkorn University in Partial Fulfillment of the Requirements for the Master's Degree

S. Hannongbua
.....Dean of the Faculty of Science
(Professor Supot Hannongbua, Ph.D.)

THESIS COMMITTEE

.....Chairman
(Professor Pattarapan Prasassarakich, Ph.D.)

.....Thesis Adviser
(Associate Professor Supawan Tantayanon, Ph.D.)

Sukkaneste Tungasmita
.....Thesis Co-Adviser
(Assistant Professor Sukkaneste Tungasmita, Ph.D.)

W. Trakarnpruk
.....Member
(Associate Professor Wimonrat Trakarnpruk, Ph.D.)

Korbratna Kriausakul
.....Member
(Assistant Professor Korbratna Kriausakul, Ph.D.)

เจริญพร โชคบริบาล: ชั้นกั้นการแพร่โลหะฐานโครเมียมสำหรับแพลเลเดียมเมมเบรนบนตัวรองรับเหล็กกล้าไร้สนิม (Cr-BASED INTERMETALLIC DIFFUSION BARRIER FOR STAINLESS STEEL SUPPORTED PALLADIUM MEMBRANE)
อ.ที่ปรึกษา: รศ.ดร.ศุภวรรณ ตันตยานนท์, อ.ที่ปรึกษาร่วม: ผศ.ดร.สุคคเณศ ตุงคสมิต, 102 หน้า

การศึกษานี้มีจุดประสงค์เพื่อพัฒนาชั้นกั้นการแพร่โลหะฐานโครเมียมที่มีประสิทธิภาพโดยเตรียมชั้น Cr_2O_3 สามรูปแบบและชั้น CrN หนึ่งรูปแบบโดยใช้วิธี (1) การออกซิไดซ์ตัวรองรับเหล็กกล้าโดยตรง (2) การออกซิไดซ์ชั้นโครเมียมที่สร้างจากกระบวนการอิเล็คโทรเพลทติง (3) การออกซิไดซ์ชั้นโครเมียมที่สร้างจากกระบวนการสปัตเตอร์ริงโลหะโครเมียมในบรรยากาศอาร์กอนและ (4) การสปัตเตอร์ริงโลหะโครเมียมในบรรยากาศไนโตรเจน ขั้นตอนการออกซิไดซ์ทำในบรรยากาศออกซิเจนและสภาวะ (อุณหภูมิและเวลา) ที่เหมาะสมที่สุดศึกษาโดยใช้เอ็กซ์เรย์โฟโตอิเล็คตรอนสเปกโตรสโกปีคือที่อุณหภูมิ 600 องศาเซลเซียสเป็นเวลา 6 ชั่วโมง การทดสอบประสิทธิภาพการป้องกันการแพร่ระหว่างชั้นโลหะทดสอบโดยใช้เอสอีเอ็ม-อีดีเอสเพื่อวิเคราะห์ธาตุองค์ประกอบที่พบในชั้นแพลเลเดียมหลังจากที่ให้ความร้อน 450 500 หรือ 550 องศาเซลเซียสเป็นเวลา 24 ชั่วโมง ชั้นสารประกอบโครเมียมทุกชนิดสามารถป้องกันการแพร่ของโลหะเข้าสู่ชั้นแพลเลเดียมได้แต่ด้วยระดับที่แตกต่างกัน ชั้นกั้นการแพร่โลหะชนิด Cr_2O_3 มีประสิทธิภาพสูงกว่าชนิด CrN ชั้น Cr_2O_3 สามารถสร้างได้ดีกว่าโดยใช้วิธี (2) หรือ (3) เพราะชั้นสารประกอบที่สร้างโดยใช้วิธี (1) บางมากและไม่สามารถปกคลุมผิวหน้าตัวรองรับได้ต่อเนื่องเนื่องจากปริมาณโครเมียมที่มีไม่เพียงพอในเหล็กกล้าไร้สนิม ผลการศึกษาอื่นๆครอบคลุมถึงผลของชั้นกั้นการแพร่โลหะต่อสัณฐานของชั้นแพลเลเดียมซึ่งกระทบโดยตรงต่อสมบัติและการใช้ประโยชน์โดยรวมของแพลเลเดียมเมมเบรนได้กล่าวถึงไว้ในการศึกษานี้ด้วย

สาขาวิชา...ปิโตรเคมีและวิทยาศาสตร์พอลิเมอร์.....ลายมือนิสิต.....เจริญพร โชคบริบาล.....
ปีการศึกษา.....2550.....ลายมือชื่ออาจารย์ที่ปรึกษา.....
ลายมือชื่ออาจารย์ที่ปรึกษาร่วม.....

#4872252523 : MAJOR PETROCHEMISTRY AND POLYMER SCIENCE
KEYWORD : INTERMETALLIC DIFFUSION / CHROMIUMOXIDE / ELECTROLESSPLATING / CHROMIUM SPUTERRING

JAROENPORN CHOKBOLIBAL: Cr-BASED INTERMETALLIC DIFFUSION BARRIER FOR STAINLESS STEEL SUPPORTED PALLADIUM MEMBRANE THESIS ADVISER: ASSOC. PROF. SUPAWAN TANTAYANON, Ph.D., THESIS CO-ADVISER: ASST. PROF. SUKKANESTE TUNGASMITA, Ph.D., 102 pp.

Aimed at developing an effective Cr-based intermetallic diffusion barrier, this study prepared three Cr_2O_3 and one CrN films employing: (1) direct oxidation of the stainless steel support, (2) oxidized Cr-electroplating, (3) oxidized Cr-sputtering in argon atmosphere and (4) Cr-sputtering in nitrogen atmosphere. The oxidation step was performed in oxygen atmosphere and the most suitable condition (temperature and time) was determined by X-ray photoelectron spectroscopy to be at 600°C for 6 hours. The efficacies in preventing intermetallic diffusion were assessed employing SEM-EDS to analyze the elemental content of the palladium layer after being heated for 24 hours at 450, 500 or 550°C. All Cr-based thin films can, at varying degrees, protect the palladium layer from metal diffusion. The Cr_2O_3 intermetallic diffusion barriers were more effective than the CrN. The Cr_2O_3 film was better prepared by either (2) or (3) since the film formed via (1) was extremely thin and did not continuously cover the surface of the support due to the inadequate availability of Cr in the stainless steel. Other results including the effects of the barrier on morphology which directly influence the properties and overall usefulness of the palladium layer were also reported.

สาขาวิชา...ปิโตรเคมีและวิทยาศาสตร์พอลิเมอร์..... ลายมือนิสิต Jaroenporn Chokboribal
ปีการศึกษา.....2550..... ลายมือชื่ออาจารย์ที่ปรึกษา.....
ลายมือชื่ออาจารย์ที่ปรึกษาร่วม Sukkaneste Tungasmita

ACKNOWLEDGEMENTS

First of all I would like to express my sincere gratitude and appreciation to my adviser, Associate Professor Supawan Tantayonon, for her support, guidance, and encouragement throughout my education at Chulalongkorn University. She has given me the great opportunity for every thing. I also would like to thank my co-adviser, Assistant Professor Sukkaneste Tungasmita, who helped and gave the thin film sputter knowledge. His wealth of information and input has been proved invaluable to this project. Moreover, I would like to thank my committee members, Professor Pattarapan Prasassarakich, Associate Professor Wimonrat Trakarnpruk, and Assistant Professor Korbratna Kriausakul. I would like to thank analysts at the Synchrotron center, Suranaree University, who helped and analyzed the oxidized film by XPS method. I would like to thank Mrs. Sirirat Phuangthong for her help with SEM-EDS instrument

I would like to extend my deepest gratitude to Mrs. Titinat Sukhonkate for her sincere help and her standing beside me. Next I would like to thank all my friends especially, Mr. Sonchai Wannatess for giving me a hand in preparing this report, Mr. Nattachai Kengpipat, Mr. Sittichai thongworn, Mr. Sakda Sriphumee and Miss Wannarudee Temnin. I would like to thank my roommate at Chulalongkorn dormitory, Mr. Wattana Phummali, Mr. Surichat Jongjit and Mr. Phumarin taowarodom. Without all direct or indirect supports from them this thesis can not be completely successful.

Last but not the least; I would like to thank my parents and my family for all the love, trust, support, worries and encouragement. Their great influence made me who I am today.

CONTENTS

LIST OF TABLES

Page

LIST OF FIGURES

LIST OF ABBREVIATION

C	Substance Concentration
D	Diffusion coefficient (m^2s^{-1})
J	Diffusion Flux (atoms $m^{-2}s^{-1}$)
X	the distance (m)

CHAPTER I

INTRODUCTION

Alternative energy sources are the topic of much interest due to the increasing demand of energy and the major energy sources relied on today are non-renewable. Hydrogen gas is the energy source of choice for it has many merits. It is a clean energy and has high energy release per unit compared to other sources [1]. It also has many applications, for instance, fuel cell.

1.1 Hydrogen Production

Production of hydrogen gas from petroleum hydrocarbon employs hydrolysis, dry reforming, steam reforming, partial oxidation or gasification in which reformings are the most common. Methane reacts with either steam or carbon dioxide as shown in the following equations.

1. Steam Reforming

   $CH_4 + H_2O \longrightarrow CO + 3\,H_2$ $\quad \Delta H\ 298) = 206 KJ/mol$

2. Dry Reforming

   $CH_4 + CO_2 \longrightarrow 2CO + 2H_2$ $\quad \Delta H\ (298) = 247\ KJ/mol$

3. Partial Oxidation

   $CH_4 + \frac{1}{2}CO_2 \longrightarrow CO + 2H_2$ $\quad \Delta H\ (298) = -36\ KJ/mol$

4. Gasification Reaction

   $C + H_2O \longrightarrow CO + H_2$

5. Electrolysis of water

   $2H_2O(l) \longrightarrow 2H_2(g) + O_2(g)$

1.2 Hydrogen Purification and Intermetallic Diffusion

Both processes require a purification step to obtain a high-purity product and typically employ a membrane reactor in which the reforming and purification steps can be operated in a single unit. The membrane in the reactor is a palladium for it is specifically permeable to hydrogen gas so obtaining product of high purity can be easily achieved. The palladium membrane is also stable at high operation temperatures [2].

Palladium layer of limited thickness is coated on a support by electroless plating [3]. The permeability of palladium membrane to hydrogen gas is in inverse proportion to its thickness [4]. The supports are including ceramics and glass but the most common is stainless steel primarily due to its cheapness, ease of welding and high strength. However, while dry reforming of methane over Al_2O_3 catalyst takes place at temperatures 670-700°C [5], diffusions of metal

components of the support into the membrane, this phenomenon called 'intermetallic diffusion' and becomes the major drawback of the stainless steel support, at temperature above 400°C [6] and results in contaminated, poor-selective and shorter-life membrane.

A barrier between the membrane and the support is an effective solution. Such an intermetallic diffusion barrier can be coated on the support by (1) thermal oxidation of the stainless steel support, (2) electroplating of metal atom followed by thermal oxidation and (3) sputtering of metal or compound species with or without thermal oxidation.

1.3 Objective

This study aims to develop an effective Cr-based intermetallic diffusion barrier on stainless steel (SS) support. The extents of intermetallic diffusion from four Cr_2O_3 and one CrN-coated SS supports were examined and compared to that of the unoxidized stainless steel. The Cr_2O_3-coated supports were formed either by (1) thermal oxidation, (2) electroplating of Cr with oxidation, (3) sputtering of Cr with post oxidation or (4) sputtering of Cr in O_2 atmosphere and the CrN-coated by reactive sputtering of Cr in N_2 atmosphere. The testing condition was dry reforming of methane [7].

CHAPTER II

THEORY AND LITERATURE REVIEWS

2.1 Preparation of Intermetallic Diffusion Barriers

Plating is the general name for surface-covering techniques in which a metal is deposited onto a conductive surface. Plating is indispensable as a corrosion inhibitor for the manufacture of computers, mobile phones, and electronic devices as well as other uses such as solder ability, hardness, wear ability, friction loss, paint adhesion, conductivity, shielding, etc. Moreover, it is a key technology for the development of new machines. It is also used for decoration, for example in jewelry, typically to provide a silver or gold exterior. Thin-film deposition techniques have accomplished plating on scales as small as the width of an atom, so it is appropriate to call some plating applications nanotechnology.

There are several plating methods. For example, in one method, a solid surface is covered with a metal sheet, and then heat and pressure are applied to fuse them together (a version of this technique is called Sheffield plate). Other plating techniques include vapor deposition under vacuum, sputter deposition, and methods using vacuum conditions or gas. Recently, however, only plating techniques using a liquid tend to be called "plating". Metallizing refers to the process of coating metal on non-metallic objects.

2.1.1 Electroplating

Electroplating is the process of using electrical current to reduce metal cations in a solution and coat a conductive object with a thin layer of metal. The primary application of electroplating deposits a layer of a metal having some desired property (e.g., abrasion and wear resistance, corrosion protection, lubricity, improvement of aesthetic qualities, etc.) onto a surface lacking that property. Another application uses electroplating to build up thickness on undersized parts.

The process used in electroplating is called **electrodeposition**. It is analogous to a galvanic cell acting in reverse. The part to be plated is the cathode of the circuit. In one technique, the anode is made of the metal to be plated on the part. Both components are immersed in a solution called an "Electrolyte" containing one or more dissolved metal salts as well as other ions that permit the flow of electricity. A rectifier supplies a direct current to the cathode causing the metal ions in the electrolyte solution to lose their charge and plate out on the cathode. As the electrical current flows through the circuit, the anode slowly dissolves and replenishes the ions in the bath.

Other electroplating processes may use a non consumable anode such as lead. In these techniques, ions of the metal to be plated must be periodically replenished in the bath as they are drawn out of the solution.

2.1.1.1 Electroplating Process

The anode and cathode in the electroplating cell are connected to an external supply of direct current, a battery or, more commonly, a rectifier. The anode is connected to the positive terminal of the supply, and the cathode (article to be plated) is connected to the

negative terminal. When the external power supply is switched on, the metal at the anode is oxidized from the zero valence state to form cations with a positive charge. These cations associate with the anions in the solution. The cation are reduced at the cathode to deposit in the metallic, zero valence state. Example: In an acid solution, Palladium is oxidized from an anode to Pd^{2+} by losing two electrons. The Pd^{2+} associates with the anion SO_4^{2-} in the solution to form sulfuric acid. At the cathode, the Pd^{2+} is reduced to metallic Pd by gaining two electrons. The result is the effective transfer of Pd from the anode source to a plate covering the cathode [8].

The plating is most commonly a single metallic element, not an alloy. However, some alloys can be electrodeposited, notably brass and solder.

2.1.1.2 Current density

The current density (amperage of the electroplating current divided by the surface area of the part) in this process strongly influences the deposition rate, plating adherence, and plating quality. This density can vary over the surface of a part, as outside surfaces will tend to have a higher current density than inside surfaces (e.g., holes, bores, etc.). The higher the current density, the faster the deposition rate will be, although there is a practical limit enforced by poor adhesion and plating quality when the deposition rate is too high.

While most plating cells use a continuous direct current, some employ a cycle of 8–15 seconds on followed by 1–3 seconds off. This allows high current densities to be used while still producing a quality deposit. In order to deal with the uneven plating rates that result from high current densities, the current is even sometimes reversed, causing some of the plating from the thicker sections to re-enter the solution. In effect, this allows the "valleys" to be filled without over-plating the "peaks." This is common on rough parts or when a bright finish is required.

2.1.1.3 Electroplating

A closely-related process is brush electroplating, in which localized areas or entire items are plated using a brush saturated with plating solution. The brush, typically a stainless steel body wrapped with a cloth material that both holds the plating solution and prevents direct contact with the item being plated, is connected to the positive side of a low voltage direct-current power source, and the item to be plated connected to the negative. The operator dips the brush in plating solution then applies it to the item, moving the brush continually to get an even distribution of the plating material. The brush acts as the anode, but typically does not contribute any plating material, although sometimes the brush is made from or contains the plating material in order to extend the life of the plating solution.

Brush electroplating has several advantages over tank plating, including portability, ability to plate items that for some reason can't be tank plated (one application was the plating of portions of very large decorative support columns in a building restoration), low or no masking requirements, and comparatively low plating solution volume requirements. Disadvantages compared to tank plating can include greater operator involvement (tank plating can frequently be done with minimal attention), and inability to achieve as great a plate thickness.

Electroplating is the deposition of a metallic coating onto an object by putting a negative charge onto the object and immersing it into a solution which contains a salt of the metal to be deposited. The metallic ions of the salt carry a positive charge and are attracted to the part. When they reach it, the negatively charged part provides the electrons to "reduce" the positively charged ions to metallic form.

2.1.2 Electroless deposition

Usually an electrolytic cell (consisting of two electrodes, electrolyte, and and external source of current) is used for electrodeposition. In contrast, an electroless deposition process uses only one electrode and no external source of electrical current. However, the solution for the electroless process needs to contain a reducing agent so that the electrode reaction has the form: In this work, an electroless process is used for electroless palladium plating.

2.1.2.1 Cleanliness

Cleanliness is essential to successful electroplating, since molecular layers of oil can prevent adhesion of the coating. ASTM B322 is a standard guide for cleaning metals prior to electroplating. Cleaning processes include solvent cleaning, hot alkaline detergent cleaning, electro cleaning, and acid etch. The most common industrial test for cleanliness is the waterbreak test, in which the surface is thoroughly rinsed and held vertical. Hydrophobic contaminants such as oils cause the water to bead and break up, allowing the water to drain rapidly. Perfectly clean metal surfaces are hydrophilic and will retain an unbroken sheet of water that does not bead up or drain off. ASTM F22 describes a version this test. This test does not detect hydrophilic contaminants, but the electroplating process can displace these easily since the solutions are water-based. Surfactants such as soap reduce the sensitivity of the test, so these must be thoroughly rinsed off.

Electroless plating, also known as chemical or auto-catalytic plating, is a non-galvanic type of plating method that involves several simultaneous reactions in an aqueous solution, which occur without the use of external electrical power. The reaction is accomplished when hydrogen is released by a reducing agent, normally sodium hypophosphite, and oxidized thus producing a negative charge on the surface of the part. The most common electroless plating method is electroless nickel plating. See: Electroless nickel plating

2.1.2.2 Chrome plating [9]

Chrome plating is a finishing treatment utilizing the electrolytic deposition of chromium. The most common form of chrome plating is the thin, decorative *bright chrome*, which is typically a 10-μm layer over an underlying nickel plate. When plating on Iron or Steel, an underlying plating of Copper allows the Nickel to adhere. The pores (tiny holes) in the Nickel and Chromium layers also promote corrosion resistance. Bright Chrome imparts a mirror-like finish to items such as metal furniture frames and automotive trim. Thicker deposits, up to 1000 μm, are called *hard chrome* and are used in industrial equipment to reduce friction and wear.

The traditional solution used for industrial hard chrome plating is made up of about 250 g/l of $Cr0_3$ and about 2.5 g/l of $S0_4^-$. In solution, the chrome exists as chromic acid, known as hexavalent chromium. A high current is used, in part to stabilize a thin layer of chromium

(+2) at the surface of the plated work. Acid Chrome has poor throwing power, fine details or holes are further away and receive less current resulting in poor plating. As such reasonable precautions should be taken to minimize exposure of Cr^{6+} to people and environment.

Look at the figure below, and then follow the written explanation.

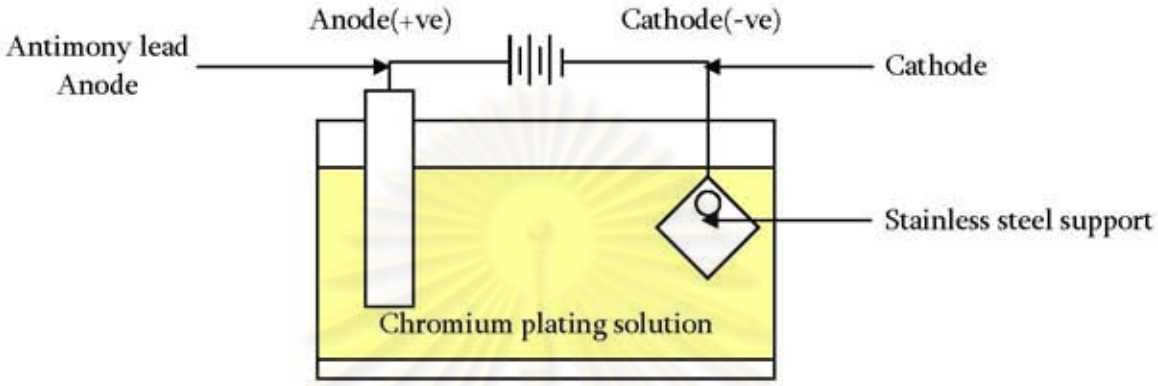

Figure 2.1 Scheme of Chromium electroplating.

Now we fill the cell with a solution of a salt of the metal to be plated. It is theoretically possible to use a molten salt, and in rare cases that is done, but most of the time the salt is simply dissolved in water and acid. The CrO_3 salt ionizes in water to Cr^{6+}

Deposition of chromium

$$Cr_2O_7^{2-} + 14H^+ + 12e^- \longrightarrow 2Cr + 2H_2O \qquad 4.1$$

Evolution of hydrogen gas

$$2H^+ + 2e^- \longrightarrow H_2 \qquad 4.2$$

Formation of chromium (III)

$$Cr_2O_7^{2-} + 14H^+ + 6e^- \longrightarrow 2Cr^{3+} + 7H_2O \qquad 4.3$$

At the anode, liberation of oxygen is accompanied by the oxidation of trivalent of hexavalent chromium, i.e., the regeneration of chromic acid. The reaction was exhibited in equations 4.4 to 4.6.

Evolution of oxygen gas

$$2H_2O \longrightarrow O_2 + 4H^+ + 4e^- \qquad 4.4$$

Oxidation of chromium (III) to chromium (VI)

$$2Cr^{3+} + 6H_2O \longrightarrow 2CrO_3 + 12H^+ + 6e^- \qquad 4.5$$

Formation of lead oxide

$$Pb + 2H_2O \longrightarrow PbO_2 + 4H^+ + 4e^- \qquad 4.6$$

2.1.3 Sputtering

Sputtering is a physical vapor deposition, PVD process whereby atoms in a solid target material are ejected into the gas phase due to bombardment of the material by energetic ions. It is commonly used for thin-film deposition, as well as analytical techniques

2.1.3.1 Physics sputtering

Standard physical sputtering is driven by momentum exchange between the ions and atoms in the material, due to collisions. The process can be thought of as atomic billiards, with the ion (cue ball) striking a large cluster of close-packed atoms (billiard balls). Although the first collision pushes atoms deeper into the cluster, subsequent collisions between the atoms can result in some of the atoms near the surface being ejected away from the cluster. The number of atoms ejected from the surface per incident particle is called the *sputter yield* and is an important measure of the efficiency of the sputtering process. Other things the sputter yield depends on are the energy of the incident ions, the masses of the ions and target atoms, and the surface binding energy of atoms in the solid.

The primary particles for the sputtering process are supplied either by a **plasma** that is induced in the sputtering equipment, or an ion or electron accelerator. In the plasma sputtering devices, a variety of techniques is used to modify the plasma properties, especially ion density, to achieve the optimum sputtering conditions, including usage of RF (radio frequency) alternating current, utilization of magnetic fields, and application of a bias voltage to the target.

Physical sputtering has a well-defined minimum energy threshold which is equal to or larger than the ion energy at which the maximum energy transfer of the ion to a sample atom equals the binding energy of a surface atom. This threshold typically is somewhere in the range 10–100 eV.

Preferential sputtering can occur at the start when a multicomponent target is bombarded. If the energy transfer is more efficient to one of the target components, and/or it is less strongly bound to the solid, it will sputter more efficiently than the other. If in an AB alloy the component A is sputtered preferentially, the solid will during prolonged bombardment become enriched in the B component thereby increasing the probability that B is sputtered such that the composition will approach AB again.

2.1.3.2 Film deposition

Sputter deposition is a method of depositing thin films by **sputtering**, i.e. eroding, material from a "target," e.g., SiO_2, which then deposits onto a "substrate," e.g., a silicon wafer. Resputtering, in contrast, involves re-emission of the depositedd material, e.g., SiO_2, during the deposition also by ion bombardment.

Sputtered atoms ejected into the gas phase are not in their thermodynamic equilibrium state, and tend to deposit on all surfaces in the vacuum chamber. A substrate (such as a wafer) placed in the chamber will be coated with a thin film. Sputtering usually uses argon plasma.

2.1.3.3 Fundamental processes in plasma

Inside plasma, there are electrons, ion of various charge state, neutral atoms and molecules. These particles move around inside the plasma with kinetic energy. The particles may exchange energy when they collide with each other. This collision can be either elastic or inelastic.

For elastic collision, the energy is conserved and the particles only exchange kinetic energy. The magnitude and directions of the velocities of both particles changes after the collision. However, during an inelastic collision, the internal energy of the colliding particles can be changed as well. This leads to various types of processes such as excitation and ionization other than just scattering found in elastic collision.

For a general knowledge of basic mechanics, the fraction of energy transferred during an elastic collision is:

$$\delta = \frac{kinetic\ \ of\ \ m_2\ \ after\ \ collision}{initial\ \ kinetic\ \ energy\ \ of\ \ m_1} = \frac{4m_1m_2}{(m_1+m_2)^2}\cos^2\theta$$

where θ is the angle that m_1 made with m_2 after collision occur. This shows the energy of electron can be transferred to the internal energy of m_2 which may be ion or atom under inelastic scattering process.

As a consequence of collisions among the particles in the plasma, four elementary processes may occur. These are described as follow.

- **Scattering**

$$A + e \longrightarrow e + A \qquad 4.7$$

This is the process caused by elastic collision where the colliding electron will transferred a small fraction of its kinetic energy to the atom or ion.

- **Excitation**

$$e + A \longrightarrow A^* + e \qquad 4.8$$

This process occurs when electron with sufficient energy colliding inelastically with an atom or ion and part of its energy is absorbed by an inner shell electron of the atom or ion. This inner shell electron is raised to a higher energy level where the atom or ion is now deemed to be is an excited state.

Most of the excited states have a short life time. The excited electron will decay back to its original level. In doing so, it emits a photo which is equivalent to the energy difference. This process is called de-excitation or relaxation by spontaneous emission.

- **Ionization**

$$e^- + A \longrightarrow A^+ + 2e^- \qquad 4.9$$

With sufficiently high energy, the colliding electron may transfer enough energy to the target atom or ion to release a bound electron from its level. The atom or ion loses an electron and it is said to be ionized. They will become one charge state higher.

- **Recombination**

$$e^- + A^+ \longrightarrow A + (h\nu) \qquad 4.10$$

Recombination process occurs when electron collides with ion and the electron is captured and occupies the vacancy inside the ion. The charge state if the ion is changed to one level lower than previously. Excess energy of electron is released in a form of photon emitted with energy $h\nu$

By deriving an impact parameter of a collision between atom and electron(in general physics) such that:

$$b_o = \frac{Z_1 Z_2 e^2}{4\pi\varepsilon_o (3KT)}. \qquad 4.11$$

2.1.3.4 The concept of Glow discharge

The sputter deposition process is that the target material, which is bombarded by energetic ions, releases atoms. After gas phase transport through the process chamber, these atoms then condense on the substrate to from a film a film, as shown schematically in Fig. 2.2

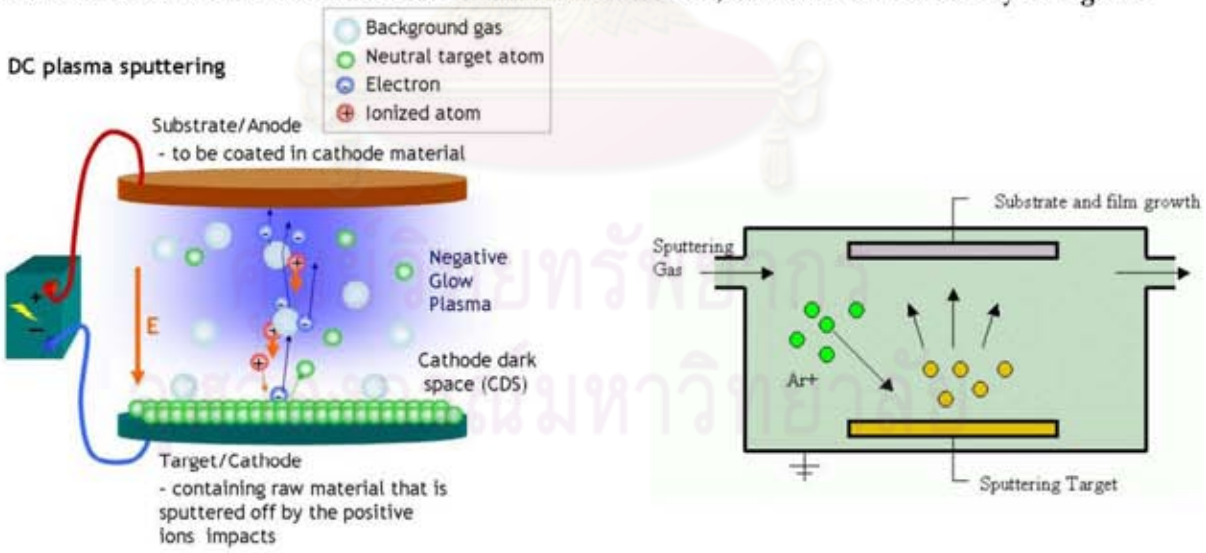

Figure 2.2 Schematic of a basic DC sputtering deposition system.

After a sputtering gas has been introduced into a vacuum chamber, a negative potential is applied to the target. This induces a glow discharge process in the deposition chamber. The ions are accelerated toward the target by the applied potential.

In the collisions between ions and target material, energy and momentum of the incident ions are transferred to the target. If the energy of the target atoms becomes high enough to overcome the surface binding energy, it will cause the atoms of the target to be *sputtered* away and travel to the substrate. This energetic ion bombardment of the target will also cause the generation of secondary electrons that are accelerated away from the target due to the electric field. As we follow the secondary electrons that come out from the target (cathode), they first cross "the dark space," sometime known as the "sheath region" It is name "dark space" because the electron density is very low, reducing excitation of gas atoms in this area, thus reducing glow from their excited states. Due to reduced ionization in the dark-space, most of the applied target potential is dropped over the dark space. The thickness of this dark space depends upon the sputtering pressure and equals the mean free path of the secondary electrons from the cathode. Strong fields, therefore, are formed. Since the secondary electron follows the electric field, which is perpendicular to the cathode surface, they travel in the broad parallel beam and are known as "beam" electrons. After acceleration, they pass into "the negative-glow" region, where they ionize gas molecules and lose their directionally by scattering. In this way, these secondary electrons will sustain the glow discharge process.

2.1.3.5 Thin film synthesis by sputtering

Intermetallic diffusion barriers were grown by using reactive magnetron sputter deposition. Sputtering can be very well controlled and is generally applicable for metals, semiconductors as well as insulators. Furthermore, it gives more degree of freedom to control growth parameters, such as, substrate temperature and kinetic energy of species arriving to the surface of the substrate, than other thin film deposition process. This gives a lot of benefits for many thin film application, such as the growth of alloys and the use of ion-surface interaction for microstructure modification

2.1.3.6 Reactive sputtering

Normally, the sputter deposition of pure metal can be done by using an inert gas, such as argon (Ar). For a compound thin film, as in this work; CrN, chemical reaction between the target material and the sputtering gas are required to be able to form such a film. This process in sputtering is called *reactive sputter deposition* [10] and is commonly used. Generally, a mixture between an inert gas and a reactive gas, such as N_2, O_2 and CH_4, can be used in the process. This gives the possibility to alter compound stoichiometry in sputtering from a compound target or to deposit a compound film from a metallic target. A typical behavior of reactive sputtering upon increasing the content of reactive gas in the gas mixture is the increasing compound coverage of the active target surface. The compound material on the surface is then sputtered away from the surface instead of the pure metal. This will change the deposition process and require an optimization of the process parameters since the compound usually have low sputtering rate. In the CrN thin film synthesis in this work, nitrogen gas with very high purity (99.999999999%) has been used as sputter gas, with reacts with the aluminum target and forms a compound CrN layer on the target surface. The sputtering of this compound layer then creates a 1:1 flux of the Cr and N towards the substrate

2.2 Diffusion

2.2.1 Introduction of diffusion

Simply put, diffusion is the phenomenon of material transport by atomic motion. This unit discusses the atomic methods by which diffusion occurs, the maths behind it, and the influence of temperature and materials used, on the rate of diffusion. This unit will introduce the topic of diffusion, how it occurs, and some examples of its use in industry.
If two pieces of different metal are joined together as shown here in figure2.3 for example, palladium and stainless steel alloy, and they are then heated for a long time (but below their melting points), the atoms from the metals migrate, or diffuse into the other.

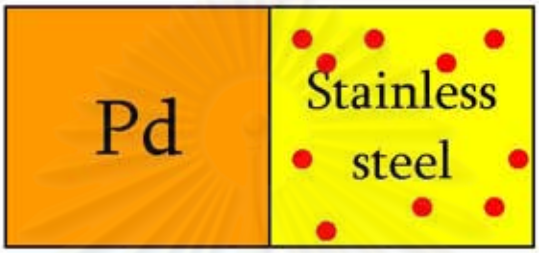

Figure 2.3 Diffusion between two pieces of difference metal.

Concentrations of both metals vary with position. This process is known as *interdiffusion*, and is a time dependent process.

2.2.2 Mechanisms of diffusion

At an atomic level, atoms are arranged in a lattice pattern, e.g. as shown simply in the diagram. Diffusion is just the stepwise migration of atoms from lattice site to lattice site. One type of diffusion involves the exchange of an atom from its normal lattice position, to an adjacent vacant lattice site or vacancy. This is known as substitutional or vacancy diffusion. Of course, this process requires the presence of vacancies, and vacancy diffusion depends on the extent of vacancies in the material. The second type of diffusion involves atoms that migrate from an "interstitial" or "in-between" position, to a neighboring one that is empty. This occurs with the infusion of impurities such as Hydrogen or Carbon, which have atoms that are small enough to fit into the interstitial positions. This process is called, as you might expect, interstitial diffusion. The mechanisms of diffusion have 3 types as shown in Figure 2.4.

Figure 2.4 Three types of diffusion phenomena.

Steady-State Diffusion

Diffusion is a time-dependent process, and often it is necessary to know how fast it occurs, or the rate of mass transfer. This rate is known as the *diffusion flux*, J, and is defined as the mass, M, diffusing through a unit cross-sectional area of solid, per unit of time. Therefore,

$$J = \frac{M}{AT} \qquad 4.12$$

where A is the area across which diffusion is occurring, and T is the elapsed diffusion time. If the diffusion flux does not change with time, a steady state condition exists, and this is called *steady-state diffusion*.

Non-Steady State Diffusion

In real life, most diffusion is non-steady state, i.e. the diffusion "flux", J, varies with time. Look back at the graph showing the concentration gradients between palladium and Stainless steel alloy. It is how "harsh" this concentration gradient is, that determines this flux, which is how quickly diffusion is occurring. The concentration gradient drives diffusion: a high gradient means a high flux.

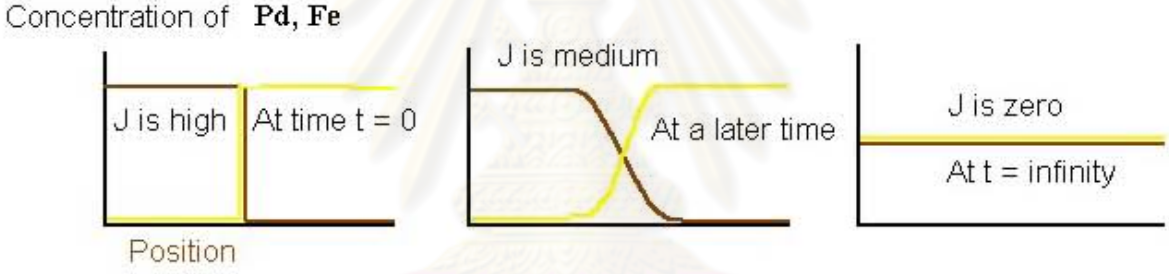

Figure 2.5 Diffusion flux between Pd and metal atoms in SS occurring non-steady state.

This means that the last equation we used is no longer valid. In these situations an equation known as Fick's First Law is used:

States that the rate of diffusion, or flux, J of a species is proportional to the concentration gradient, ∂C/∂x:

$$J = -D\frac{\partial C}{\partial X} \qquad 4.13$$

where D is the diffusivity or *coefficient of diffusion*. For atomic diffusion the units are:

J	atoms m-2s-1
D	m2s-1
∂C/∂x:	atoms m-4.

And the Fick's second Law is used:

$$\frac{\partial C}{\partial t} = D\frac{\partial^2 C}{\partial x^2} \qquad 4.14$$

where C is the concentration of the substance you're looking at (measured between 0 and 1). D is known as the diffusion coefficient, and is given in square metre per second.

In real life some simple boundary conditions can be applied to materials. These are that:

- x is the distance from the interface you're looking at, and=0 at the surface or interface of the material.
- The instant before diffusion starts, time is taken as zero, and
- Before diffusion starts, all the atoms that will be diffusing are evenly distributed. Because of these boundary conditions.

2.2.3 Factors that influence diffusion

2.2.3.1 Diffusing species

The magnitude of the diffusion coefficient, D, is a measure of the rate at which atoms diffuse. The diffusing species, as well as the host material, influences the diffusion coefficient. For example, if a diffusing species has smaller atoms, it will interstitially diffuse through a host material more easily. Also substitution of diffusion is made easier if the host material has lots of vacancies to start with.

2.2.3.2 Temperature

Temperature has the most profound influence on the coefficients and diffusion rates. For example, for the self-diffusion of Fe in alpha Fe, the diffusion coefficient increases about five times, after the temperature is raised from 500 to 900°C. This is because diffusion is a thermally activated process-i.e. there is an energy barrier (activation energy) that has to be overcome, in order for the atoms to move from one lattice site to the other.

The more thermal energy there is around, the easier it is for this energy barrier to be overcome. Therefore, there is an exponential relationship between Temperature (T), and Diffusion Coefficient (D), and this is:

$$D = A \cdot e^{-\frac{Q}{RT}} \qquad 4.14$$

where Q = activation energy, T = temperature in Kelvin, R = Universal Gas Constant, and A is a constant. Taking natural logarithms of this equation,

$$\ln D = \ln A^{-\frac{Q}{RT}}. \qquad 4.15$$

And since A, Q and R are all constants, this expression is similar to the equation of a straight line: y = mx + C.

X-ray Photoelectron spectroscopy, XPS technique

X-ray photoelectron spectroscopy is a surface sensitive spectroscopy technique that allows chemical identification of the elements in the top atomic layers of a sample by recording the binding energies of the electrons associated with these atoms. Furthermore, because the binding energies differ not only from chemical species to species, but also vary with the bonding conditions in which the element is found, this technique also provides information on the actual compounds present on the surface. In essence, it probes the electronic structure of the surface. When used in combination with sputter depth profiling, in

which ions are used to remove surface layers from a sample, XPS provides information about the binding energy spectra of a sample.

The information provided by XPS is complementary to the data obtained with other techniques, as it provides information about the true electronic structure of the surface. Binding energies are sensitive to local environments of atoms or ions in materials, information about which is not accessible through regular (EDS or WDS) spectroscopy techniques.

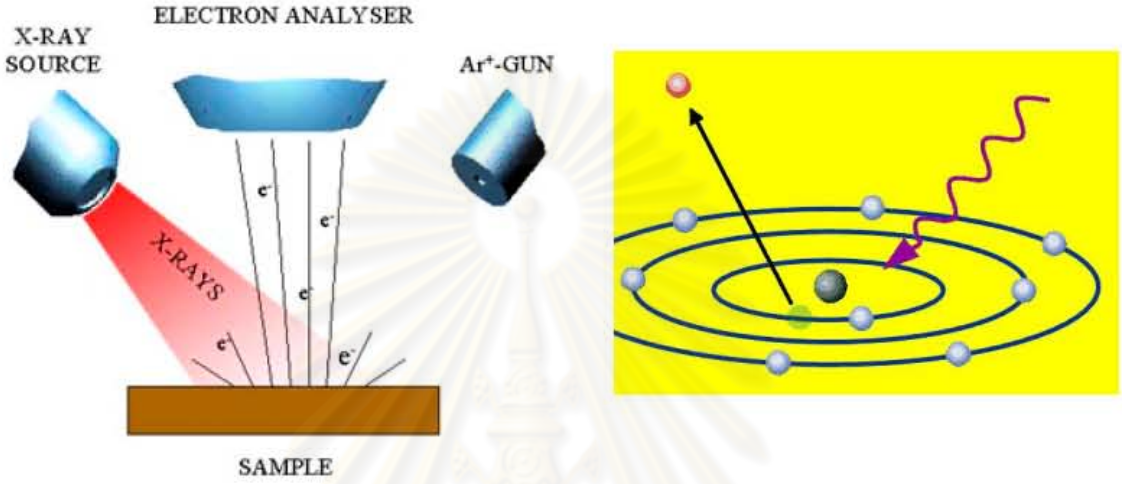

Figure 2.6 Concept of XPS technique.

X-ray photoelectron spectroscopy (XPS), also known as Electron Spectroscopy for Chemical Analysis (ESCA), is a widely used technique for obtaining chemical information of various material surfaces. Core-level electrons are emitted from a surface after it has been irradiated with soft X-ray. The low kinetic energy (0-1500 eV) of emitted photoelectrons limit the depth from which it can emerge so that XPS is a very surface-sensitive technique and the sample depth is in the range of few nanometers. Photoelectrons are collected and analyzed by the instrument to produce a spectrum of emission intensity verse electron binding energy. In general, the binding energies of the photoelectrons are characteristic of the element from which they are emanated so that the spectra can be used for surface elemental analysis. Small shifts in the elemental binding energies provide information about the chemical state of the elements on the surface. Therefore, the high resolution XPS studies can provide the chemical state information of the surface [11].

2.4 Literature reviews

Wang *et al.* [12] reported that metallic particles embedded in the oxide film play an important role in film's optical property. The result showed that metallic phases of Ag, Ti, and Pb can be formed in different oxide films under heating, X-ray photon, and electron radiation. The metallic phase separated from metal oxide film was investigated by X-ray photoelectron spectroscopy technique. Metal oxygen bond breaking and total energy reduction in the film. It is necessary to fully understand the formation mechanism of metallic particles so their shapes and distributions can be tailored to achieve the desired film's properties. Thermal activated metallic phase formation in first two cases can be explained by the bond breaking and reduction of total energy.

Shen *et al.* [13] reported that nanocrystalline chromium nitride (CrN) with the cubic rock-salt structure was synthesized by the arc discharge method in nitrogen gas (N_2). The product was characterized by X-ray diffraction (XRD) and transmission electron microscopy (TEM). It was found that the nitrogen gas pressure is a crucial factor for the synthesis of cubic CrN. At relatively low N_2 pressure, cubic CrN was formed. With the increase of N_2 pressure, hexagonal Cr_2N and metal Cr were gradually formed. It indicated that the formation of CrN is enhanced at a low nitrogen pressure environment, and the diffusion of nitrogen atoms into the Cr was lowered with the increase of N_2 pressure. They explain this experimental observation in terms of the evaporation rate of anode Cr and the ionization of nitrogen. In conclusion, they have synthesized the cubic CrN nanocrystalline at a low nitrogen pressure of 5 kPa by the DC arc discharge method. The sizes of most CrN particles are less than 10 nm, with the increase of the nitrogen pressure, the amount of CrN decreases and the amount of Cr_2N and Cr increases. This indicates that the ability of nitridation falls, and the particle size also becomes much larger. The low-pressure synthesis of cubic CrN should be beneficial to improve nitridation of other transition metals such as, Co, Ta, Mo, and W.

Yan and Roland [14] reported that the integrity of thin composite palladium membranes is influenced by the surface roughness of the porous support. Supports with smooth surface and small pore size are expensive as they are composed of several layers with decreasing pore size which require multiple successive energy and time consuming sintering steps. In addition, smooth surfaces may cause poor membrane adhesion. It is therefore of interest to develop methods for preparation of thin defect-free palladium membranes over supports with rough surfaces. Atmospheric plasma spraying produced relatively thick continuous films, but with some residual open porosity. Electroless plating gave the densest layers. Activation of the support surface by metal organic chemical vapor deposition of palladium instead of the conventional sensitization and activation pretreatment based on successive immersion in $SnCl_2$ and $PdCl_2$ solutions allowed to reduce the membrane thickness without compromising its integrity.

Arias *et al.* [15] reported that thin films of TiN and ZrN were grown on stainless steel 316 substrate using the pulsed cathodic arc technique with different number of discharges (one to five discharges). The coatings were characterized in terms of crystalline structure, microstructure, elementary chemical composition and stoichiometric by X-ray diffraction (XRD), atomic force microscopy (AFM) and X -ray photoelectron spectroscopy for chemical analyses (XPS), respectively. The XRD results show that for both TiN and ZrN, the

preferential direction occurs in the plane (2 0 0), and this observation remained- even when the number of discharges was increased. The grain size is increased with the increase of the number of discharges for both nitrides, the roughness for the TiN film is greater than for the ZrN film. XPS analysis determined that there is a higher nitrogen presence in the ZrN film than in the TiN film.

Stefanov *et al.* [16] reported that the structure and composition of chromium oxide films formed on stainless steel by immersion in a chromium electrolyte have been studied by SEM and XPS. Cr_2O_3 crystallites in the range 30–150 nm are fully developed and cover the whole surface. The chemical compositions in the depth and the thickness of the oxide layer have been determined by XPS sputter profiles. The oxide film can be described within the framework of a double layer consisting of a thin outer hydrated layer and an inner layer of Cr_2O_3.

Lacoste *et al.* [17] reported that implantation of oxygen in stainless steel (15% Cr) via plasma-based ion implantation in a distributed ECR plasma reactor has been studied as functions of ion energy and dose. Due to the formation at the surface of dielectric films with optical index and thickness depending on the implantation time and pulse voltage (up to 44 kV), various colorations can be obtained. The experimental results demonstrate the feasibility of uniform processing, the possibility of reaching perfect control of the coloring through the dose and energy of implanted ions, and that the resulting coloration varies monotonically when increasing the dose and penetration depth of implanted oxygen. Characterization of the films by scanning electron microscopy and X-ray microanalysis shows that oxygen implantation results in strong surface oxidation, but without any significant degradation of the surface aspect. The thickness and composition profiles of the oxide layers determined using X-ray photoelectron spectroscopy, increases with ion energy and dose, but that the composition of the oxide layer resulting from. A uniform iron oxide layer (with a stoichiometry closed to Fe_2O_3), free from chromium, is formed in the near-surface region, while chromium segregates at the interface between the oxide layer and the bulk stainless steel to form chromium oxide Cr_2O_3.

Huiyuan *et al.* [18] reported that thin Pd–Cu membranes were prepared by electroless plating technique on porous stainless steel (PSS) disks coated with a mesoporous palladium impregnated zirconia intermediate layer. This intermediate layer provided seeds for electroless plating growth of Pd–Cu film during synthesis and serves as an inter-metallic diffusion barrier that improved membrane stability for practical application. XPS analyses showed that the average surface compositions of the two membranes were respectively $Pd_{84}Cu_{16}$ and $Pd_{46}Cu_{54}$ (at.%).

Sabioni *et al.* [19] prepared chromium protective layers were formed on many industrial alloys to prevent corrosion by oxidation. The role of such layers was to limit the inward diffusion of oxygen and the outward diffusion of cations. A number of chromium forming alloys contain iron as a major component, such as the stainless steels. To check if chromium is a barrier to the outward diffusion of iron in these alloys, iron diffusion in chromium was studied in both polycrystals and oxide films formed by oxidation of Ni–30Cr alloy in the temperature range 700–1100 .C at an oxygen pressure equal to 10.4 atm. An iron film of about 80 nm thick was deposited on the chromium surface, and after the diffusing treatment, iron depth profiles were established by secondary ion mass spectrometry (SIMS).

Two diffusion domains appear whatever the nature of the chromium material, polycrystals or films. In the first domain, using a solution of the Fick's second law for diffusion from a thick film, effective or bulk diffusion coefficients were determined.

Sato *et al.* [6] investigated the oxidation behaviors of modified SUS316 (PNC316) and SUS316 stainless steels under the low oxygen partial pressure of 10^{-31}- 10^{-22} atm at 600–800°C. Oxygen uptake by these materials parabolically increased with time, and the kinetic rate constants depended on both oxygen partial pressure and temperature. For the duplex layer formed under the low oxygen partial pressure, the inner layer consisted of such oxides as Cr_2O_3 and $FeCr_2O_4$, while the outer layer consisted of non-oxidized a-Fe. Furthermore, oxidation along the grain boundaries was observed for samples oxidized for a longtime. From the point of view of fuel cladding chemical interaction evaluation at high burn-up fuel for fast reactors, it is interesting that formation of non oxidized a-Fe was observed under the low oxygen partial pressure.

Huntz *et al.* [20] reported that the oxidation behaviour of AISI 304 and AISI 439 stainless steels was studied at high temperatures, under various oxygen pressures and in the presence or not of water vapor. Thermogravimetric analyses were conducted in isothermal conditions from 850 to 950°C for 50 h and micro structural and chemical analyses of the oxide films grown by oxidation were performed by SEM and EDX. The oxide films were also analyzed by grazing X-ray diffraction and by X photoelectron spectroscopy (XPS). The AISI 439 steel has higher oxidation resistance than AISI 304, above 850°C, under high oxygen pressures. On the other hand, the AISI 304 steel has higher oxidation resistance under low oxygen pressures in the whole temperature range. In order to check whether the growth kinetics of Cr_2O_3 formed by the oxidation of stainless steels was controlled by oxygen or/and chromium diffusion through the oxide film.

Earl *et al.* [21] studied the rates of oxidation of three heater alloys of nominal composition 80% nickel-20% chromium were studied over the temperature range of 500° to 950°C and at a pressure of 7.6 cm of Hg of oxygen, using the vacuum microbalance method. Temper color films were obtained for all oxidations below 850°C, while gray or gray-green films were obtained at temperatures of 850°C and higher. No evidence was found for scaling or cracking of the oxide from the alloys on cooling at temperatures of oxidation up to 950°C.The parabolic rate law was applied to the data. Reasonable agreement was found for temperatures above 650°C, while below this temperature the parabolic rate law constant varied with time. This time variation was explained in terms of composition changes in the oxide and growth of the oxide crystallite size. The classical theory of diffusion was used to interpret effect of temperature on rate of oxidation, and heats, entropies, and free energies of activation for the overall reaction were evaluated from the data.

CHAPTER III

EXPERIMENTAL

3.1 Materials, Equipments and Instruments

3.1.1 Materials

1. Stainless steel grad 316L
2. Palladium (II) chloride ($PdCl_2$), 99.9% from Alfa Aesar
3. Tetra ammine palladium (II) chloride monohydrate ($Pd(NH_3)_4Cl_2 \cdot H2O$, 98%) from Alfa Aesar
4. Tin (II) chloride dehydrate ($SnCl_2 \cdot 2H_2O$), 98% from Carlo Erba
5. Hydrazine anhydrous (N_2H_4), 99.5% from Aldrich
6. Hydrazine hydrate ($N_2H_4.H_2O$), 99.5% from BDH chemical
7. Disodium ethylenediaminetetraacetrate (Na_2EDTA), 99.5% from Carlo Erba
8. Sodium carbonate, Na_2CO_3
9. Sodium hydroxide NaOH
10. Trichloroethylene, C_2HCl_3
11. Iso-propanol, C_3H_7OH
12. acetone
13. Quartz wool from Alltech
14. Argon gas, 99.999% from Thailand Industrial Gas Co., Ltd
15. Nitrogen gas
16. Cr-Target for sputtering technique.

3.1.2 Equipments

1. Furnace reactor
2. Digital flow meter from Altech
3. Flow meter
4. Plasma sputtering chamber

3.1.3 Instruments

1. Scanning electron microscope (SEM), JEOL model JSM-5800LV with Energy Dispersive Spectrometer (EDS)
2. X-ray photoelectron spectroscopy, XPS

3.2 Experimental Procedures

The experimental procedures were divided into 5 parts:

1. Preparation of stainless steel supports
2. Preparations of intermetallic diffusion barriers
3. Electroless plating of palladium membranes
4. Evaluations of the efficiencies in reducing intermetallic diffusion of the barriers
5. Surface characterizations of the palladium membrane

3.2.1 Preparation of stainless steel supports

100-cm^2 sheets of stainless steel were cut into 1-cm^2 specimen and drilled at one corner. The general procedure for metal plating was shown in Figure 3.1.

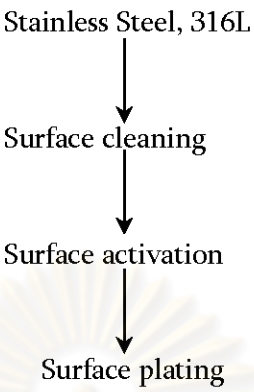

Figure 3.1 General procedure for preparation of the stainless steel supports.

The surface of the stainless steel supports was cleaned prior to activation to remove contaminants such as oil, grease and dirt. The supports were washed either with an alkaline solution if electroplating deposition was subsequently performed or with commercial solvents if plasma sputtering was subsequently performed.

a) Surface cleaning with an alkaline solution.
The supports were immersed in an ultrasonic bath of the solution at ~60°C for one hour and then washed thoroughly three times with deionized water in an ultrasonic bath. Finally, the supports were soaked in iso-propanol to remove any trace amount of water and dried at 100°C for 3 hours. The chemical composition of the alkaline solution is given in Table 3.1.

Table 3.1 Composition of the alkaline solution for cleaning the stainless steel supports.

Compound	Concentration
Sodium phosphate, $Na_3PO_4 \cdot 12H_2O$	45 g/l
Sodium carbonate, Na_2CO_3	65 g/l
Sodium hydroxide, NaOH	45 g/l
Detergent	5 ml/l

b) Surface cleaning with commercial solvents.

Cleaning with commercial solvents was a successive immersion of the supports in three different commercial solvents followed by a rinse in deionized water as given in Figure 3.2. The support was soaked for 5 minutes in each bath containing ~25 ml of solvent. A thoroughly cleaning requires the steps to be repeated four times.

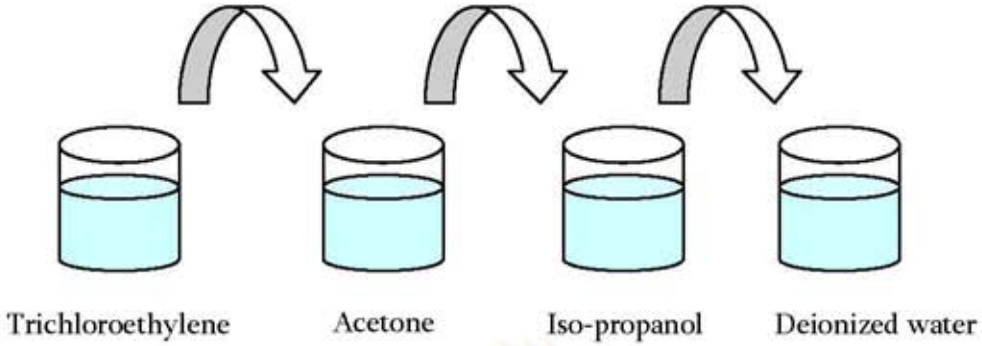

Figure 3.2 One loop of stainless steel cleaning with commercial solvent.

3.2.2 Preparations of intermetallic diffusion barriers

Three techniques were employed in preparing the diffusion barrier:

3.2.2.1 Thermal oxidation,

3.2.2.2 Electroplating followed by thermal oxidation, and

3.2.2.3 Plasma sputtering with or without thermal oxidation.

3.2.2.1 Thermal oxidation [22]

The cleaned support was oxidized at 600°C for 6 hours with heating rate 4°C/min in air in muffle furnace. (Appropriate temperature and time were determined by preliminary XPS study.) The oxidized stainless steel was then weighed and activated.

3.2.2.2 Electroplating/oxidation

The electroplating device setting is depicted in Figure 3.3. The chromium plating solution consisted of 250 g/l chromic acid and 1.25 g/l sulfuric acid as a catalyst in 200:1 ratio. The chromium plating was performed at room temperature with current density ~100-150 A/ft².

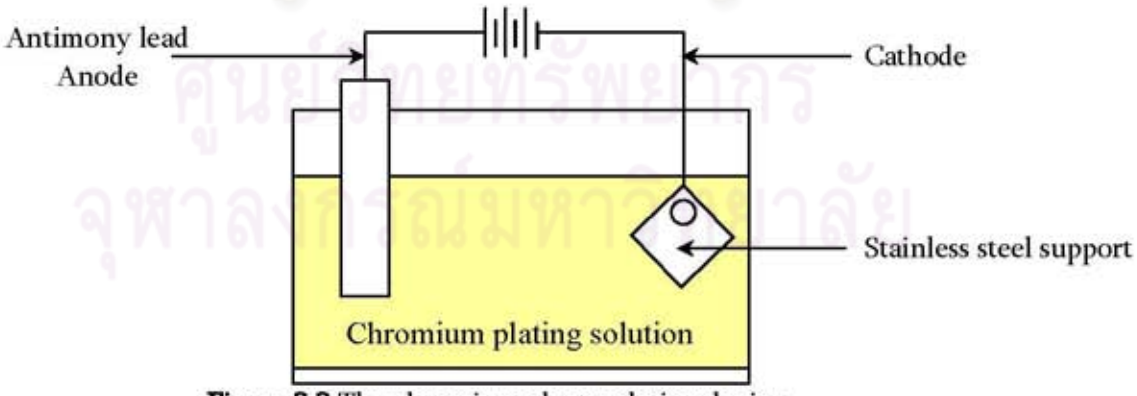

Figure 3.3 The chromium electroplating device.

3.2.2.3 Sputtering

This technique involves bombarding a target with energetic particles that cause surface atoms to be ejected and then deposited on a substrate close to the target [23]. Substrates are placed into the vacuum chamber, and are pumped down to their process pressure. Sputtering starts when a negative charge is applied to the target material (material to be deposited), causing a plasma or glow discharge. The configuration of such an instrument is depicted in Figure 3.4.

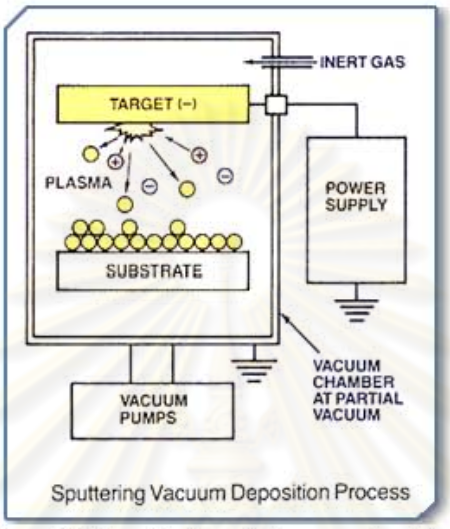

Figure 3.4 Sputtering instrument setting

Two Cr-based diffusion barriers were formed by sputtering as diagramed in Figure 3.5:

(a) sputtering of pure chromium metal in argon atmosphere followed by oxidation at 600°C for ~6 hours,

(b) sputtering of pure chromium metal in nitrogen atmosphere without oxidation.

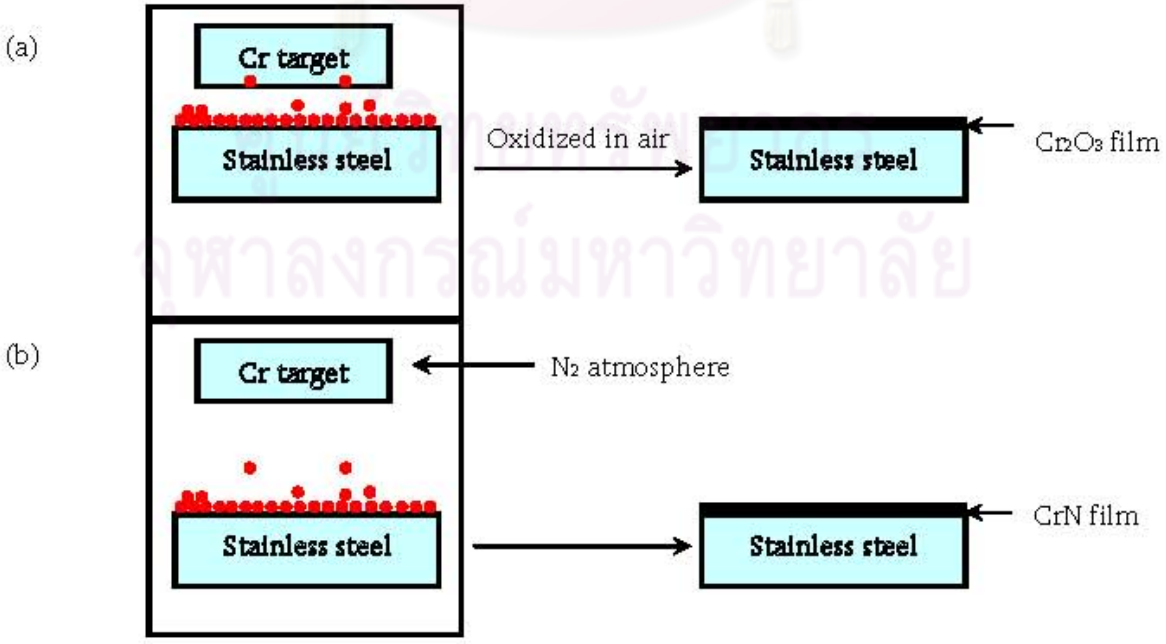

Figure 3.5 Two intermetallic diffusion barriers formed on stainless steel by sputtering.

All the sputtered filmed were prepared in DC high vacuum system, with the background pressure at 1.2 x 10^{-5} Torr. After the substrates were cleaned and introduced into the deposition chamber, the system was pumped down to evacuate the pressure until reached the background pressure. Then the sputter gas (and reactive gas for reactive sputtering for CrN were add to the working pressure of 6.3 x 10^{-3} Torr, before started the plasma glow discharge. The thin film synthesis was done at room temperature and the power of 245W (350V 700mA) was supplied to the magnetron. This gave the deposition rate of about 0.2 nm/sec.

3.2.3 Electroless plating of palladium membranes

The surface of the supports was first activated to initiate the deposition of Palladium atoms.

3.2.3.1 Surface activation

The activation process consisted of successive immersion at room temperature of the supports in 1 g/l $SnCl_2$ solution followed by 0.1 g/l $PdCl_2$ solution with two rinses in deionized water between these baths. After $PdCl_2$ immersion and prior to the first rinse, the supports were briefly dipped in 0.1 M HCl to remove any trace amount of tin compounds on the surface. The schematic diagram of one loop of the activation process is depicted in Figure 3.6. The surface activation in $SnCl_2$ and $PdCl_2$ solutions was generally repeated 6 times and a perfectly activated surface was smooth and grayish brown in color.

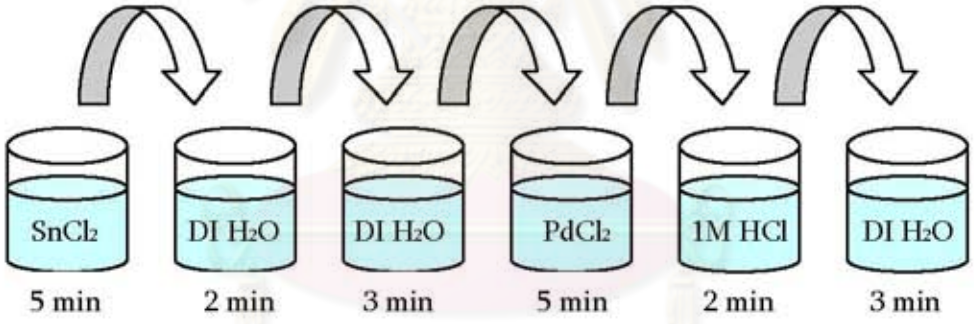

Figure 3.6 One loop of the activation process.

3.2.3.2 Electroless plating deposition of palladium

The plating solution was prepared by mixing the first three compounds given in Table 3.2 [24] at lease one day prior to plating to form stable metal complexes. The palladium plating bath as shown in Figure 3.7. The hydrazine reducing agent was added just prior to plating.

The activated supports were immersed in the plating solution which was renewed every 90 minutes. The supports were rinsed with hot deionized water between plating baths. After deposition was complete the membrane was allowed to cool down at room temperature in deionized water and dried at 100°C for 3 hours.

The layer thickness was measured using gravimetric method given in Equation 3.1.

Table 3.2 Chemical composition of electroless Pd plating solution.

Compound	Concentration
Tetraaminepalladium (II) chloride, $Pd(NH_3)_4Cl_2 \cdot H_2O$	4.0 g/l
Ammonia solution, NH4OH (28%)	198 mg/l
Disodium ethylenediamminetetraacetate, Na_2EDTA	40.1 g/l
Hydrazine hydrate, $N_2H_4 \cdot H_2O$	5.6 – 7.6 ml/l

$$\text{Thickness}\ (\mu\text{m}) = \frac{\Delta\text{Weight (mg)} \times 10}{\text{Plated Area}\ (\text{cm}^2) \times \text{Density of the plated metal}\ (\text{g/cm}^3)} \quad (3.1)$$

Figure 3.7 Palladium plating bath.

3.2.4 Evaluations of the efficiencies in reducing intermetallic diffusion of the barriers

The efficiencies in reducing intermetallic diffusion of the barriers were assessed as diagramed in Figure 3.8. The palladium membrane on the PPS supports with different forms of Cr-based diffusion barrier was heated in argon atmosphere in a muffle furnace at 450, 500 and 550°C for 24 hours and the metal composition of the membranes were quantitatively determined using SEM-EDS. Quantitative SEM-EDS analyses were performed as a part of the surface characterization of the Palladium membrane described below.

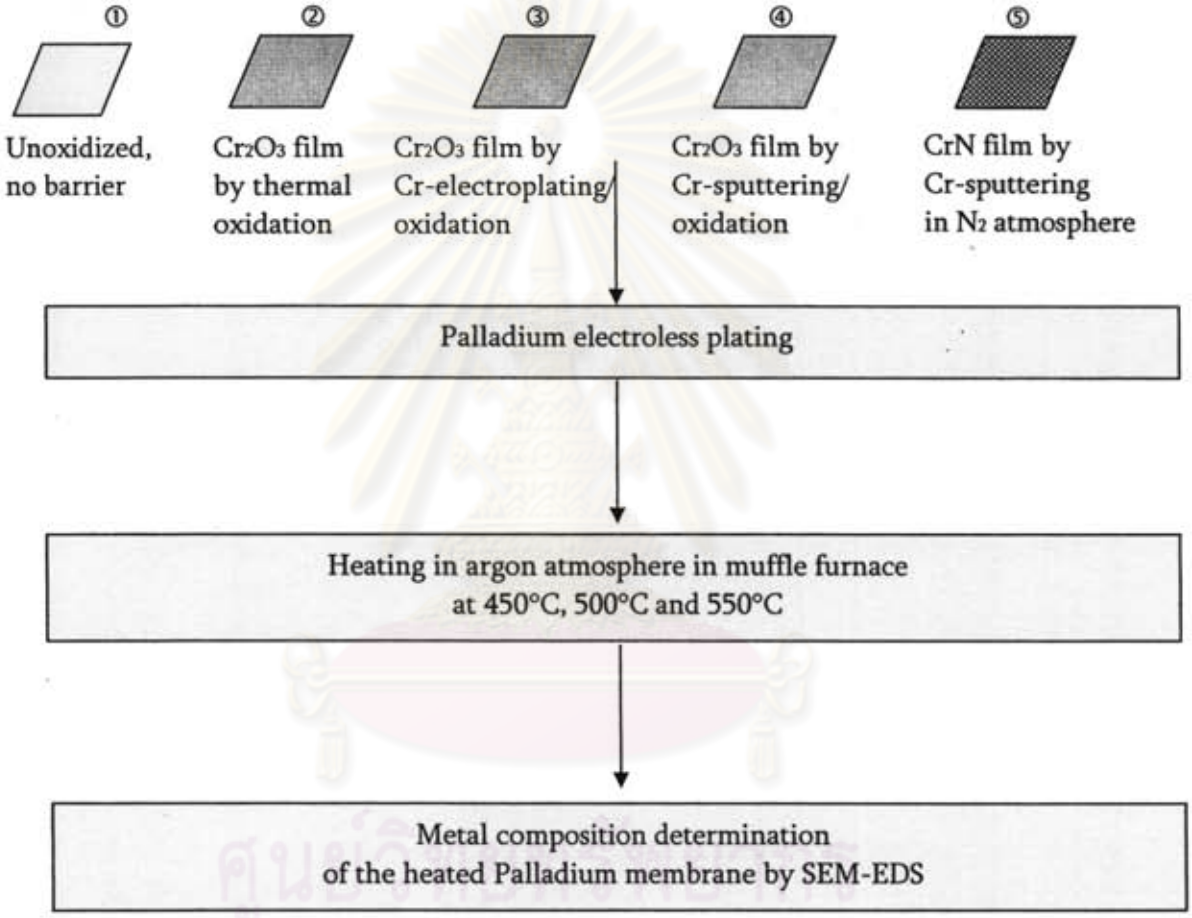

Figure 3.8 Assessment of the efficiencies in reducing intermetallic diffusion by the Cr-based barriers.

3.2.5 Surface characterizations of the palladium membrane

Surface characterizations were performed using scanning electron microscope equipped with electro dispersive spectrometer (SEM-EDS) for both qualitative and quantitative analyses. The spatial resolution for SEM-EDS lied between 0.8-1.2 μm. SEM specimens of the metal deposited stainless steel were cut using a SiC saw blade and ground with phenolic powder in a Smithells II mounting press. The resounding samples were ground with SiC papers with increasing grain fineness from 80 to 400 grits. Grinding was performed using Metaserv 2000 grinder-polisher. Vibromet I automatic polisher was employed to polish the sample to 1-μm thin overnight. Prior to SEM cross-section analyses sample was painted with carbon ink and gold-coated to avoid charging.

CHAPTER IV

RESULTS AND DISCUSSION

4.1 Direct Oxidation of Stainless Steel Disks

Several research groups have reported that, at high temperatures, metal components of stainless steel diffused up and formed an oxide film covering the surface [25]. However, none has ever concerned about how such a film can be used as the protective barrier to intermetallic diffusion. In this regard, although iron is far more present in stainless steel, pure Cr_2O_3 film is more suitable for this function than Fe_2O_3 film due to its much higher melting temperature, i.e. 2435°C versus 1565°C.

In order to successfully develop a Cr_2O_3 protective film through direct thermal oxidation of the stainless steel, a clear picture of how much each metal will diffuse at a particular condition is the first thing to be established. The ideal condition for direct thermal oxidation of the stainless steel support to form Cr_2O_3 film should permit:

(1) The highest diffusion of chromium while keep the diffusion of iron and nickel at minimum, and
(2) The formation of the most stable chromium oxide, the Cr_2O_3.

XPS was employed to examine the degree of diffusion and by varying the time of incubation some clues to further optimize the condition were revealed.

4.1.1 Oxidation at 450°C

Greeff *et al.* [22] prepared oxide film of metal alloy FeCrMo and found that FeO and Cr_2O_3 were present only at temperature higher than 400°C otherwise all oxides were Fe_2O_3. The normal 316L stainless steel used in this study is an FeCrNi alloy having comparable metal percentages to those of the FeCrMo therefore in this study the stainless steel disks were oxidized at 450°C. Metal content in the oxide layer after heating at 450°C and the corresponding XPS spectrum of each metal were shown in Table and Figure 4.1, respectively.

Table 4.1 Metal contents in the oxide layer at the stainless steel surface after heating at 450°C

Heating time (hr)	Percentage of metal*		Ratio of metal to oxygen
4	Cr	1.5417	0.017269
	Fe	9.1828	0.102859
	O	89.2754	
6	Cr	17.4273	0.228045
	Fe	1.8654	0.02441
	Ni	4.2867	0.05609
	O	76.4204	
8	Cr	11.4900	0.142487
	Fe	7.8710	0.097608
	O	80.6389	

*as determined by XPS.

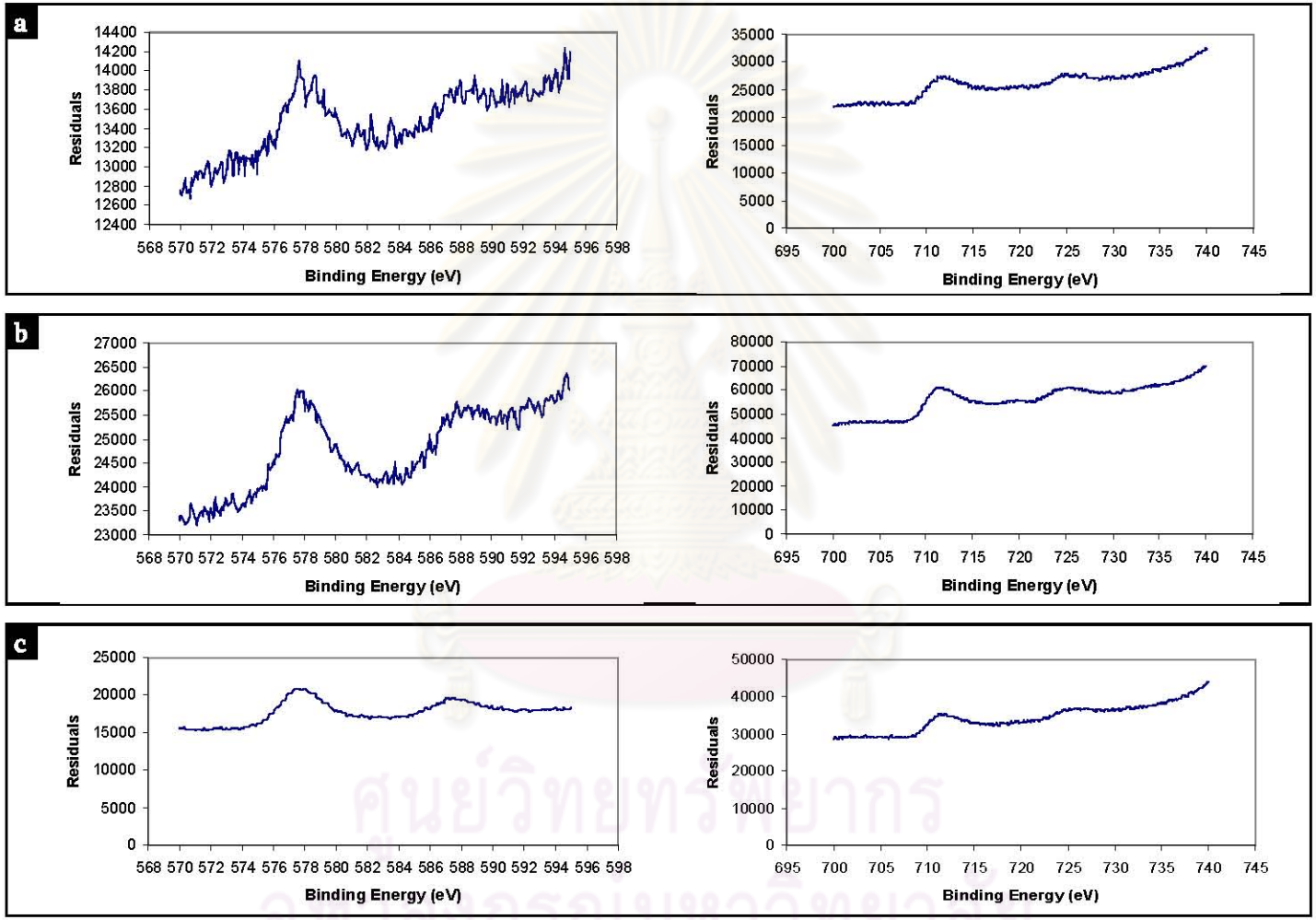

Figure 4.1 XPS spectra of oxides of Cr (left side) and Fe (right side) at the surface of the stainless steel oxidized at 450°C for 4 hr (**a**), 6 hr (**b**) and 8 hr (**c**).

By heating at 450°C for 4 hr, the stainless steel disk became dark and brownish green in colour. Far more iron was oxidized to form a coated film than chromium while, at 6 hr of incubation, the situation was reversed and significant amount of Ni was detected. From 6 to 8 hr of incubation, the diffusion was changed in the opposite direction: accumulation rate of iron oxides began to increase after it first dropped from 4 to 6 hr and no Ni was detected.

These observations can be explained in term of two factors:

(1) The degrees of readiness of metal to diffusion, i.e. how fast each metal diffused at a particular temperature, and

(2) The amount of metal present in the stainless steel, i.e. more percentage means more available for diffusion assuming all metals are evenly distributed.

At 4 hr, the latter factor ruled, that is even though Cr diffusion is faster it cannot compete against Fe that is far more present. This phenomenon was similar to that reported by Greeff *et al.* [22]. Prolonged heating, however, enabled the higher readiness to diffusion of Cr to compensate for its smaller amount. Therefore, in the course of time oxides of Cr outnumbered. At 8 hr, the result seemed to contradict with this explanation, that is percentage of Cr should be even more if the above explanation is correct. But with the fact that Cr is present in smaller amount in the stainless steel, the observation at 8 hr is nothing odd: most of Cr atoms near the surface diffused up and thus longer incubation time leads to the more and more accumulation of iron.

As far as the stability of oxide of Cr is solely concerned, intermetallic diffusion barrier is better prepared at 8 hr of incubation. This is obvious from the left XPS spectra in Figure 4.1. The Cr XPS spectrum of pure Cr_2O_3 as given in Figure A-1 is smooth and has two characteristic peaks at binding energies 577 and 587 eV. The presence of other chromium oxide impurities will be evident as noises resulting in spiky Cr XPS spectra as those observed at 4 or 6 hr. At 8 hr of incubation, however, the Cr XPS spectrum was almost free of noise and its peaks were the characteristics of Cr_2O_3.

4.1.2 Oxidation at 800°C

Ma *et al.* [25] prepared oxide film on porous stainless steel by direct oxidation at 800°C and found that the palladium layer was protected from diffusion at some degrees by the film. However, the form of chromium oxides in the film was not characterized in this study. Therefore, another set of stainless steel disks were heated at 800°C and the results were compared to those obtained at 450°C to establish how metal diffusion changed with temperature. Metal contents in the oxide layer after heating at 800°C and their corresponding XPS spectra were shown in Table and Figure 4.2, respectively.

Table 4.2 Metal contents in the oxide layer at the stainless steel surface after heating at 800°C

Heating time (hr)	Percentage of metal*		Ratio of metal to oxygen
4	Cr	21.70	0.318
	Fe	10.09	0.147
	O	68.19	
6	Cr	16.93	0.178
	Fe	8.47	0.089
	O	74.59	
8	Cr	11.13	0.158
	Fe	18.71	0.266
	O	70.15	
12	Cr	7.93	0.104
	Fe	16.21	0.213
	O	75.84	

*as determined by XPS.

Percentages of metal after heating at 800°C seemed to exhibit the same trend as in the case of 450°C, that is the largest percentage of metal in the oxides film was at first Fe, then Cr and finally Fe. The trend at 800°C was shifted to the left, that is at 450°C the highest percentage of Cr was observed at 6 hr while at 800°C the highest percentage of Cr was shift to 4 hr. Also, the percentage of Cr began to decrease at 4 hr as opposed to 6 hr at 450°C. There is no heating time at 800°C that permit extremely high Cr-to-Fe diffusion ratio as observed at 450°C, 6 hr. At 800°C, Cr-to-Fe ratios ranged from ca. 2 at 4 hr to ca. 0.5 at 12 hr while at 450°C, 6 hr the Cr-to-Fe ratio was ca. 10. By assuming the same trend as that observed at 450°C, this fact suggested that oxides of Fe was at the highest due to greater amount at around 0.5-1 hr, and then the oxides of Cr began to dominate and reached its peak at earlier than 4 hr (probably at 2 hr). At 8 and 12 hr, incubation at 800°C extended the trend to the right. It also underlined the explanation that at some point where most of Cr near the surface diffused up the continuous and constant diffusion of Fe eventually made chromium oxides the minority.

With regard to the forms of chromium oxides, none of the incubation time fulfilled the second requirement. Although the Cr XPS spectra at 4, 6 or 8 hr were free of noise as opposed to the spiky spectrum at 12 hr, their peaks were the characteristics of CrO not the Cr_2O_3. The peaks appeared at binding energies 576 and 586 eV instead of 577 and 587 eV. This observation agreed with that of Greeff *et al.* [22] who characterized the oxide film formed at the surface of stainless steel via oxidation at temperatures higher than 700°C and reported that more Cr were in the form of CrO than Cr_2O_3.

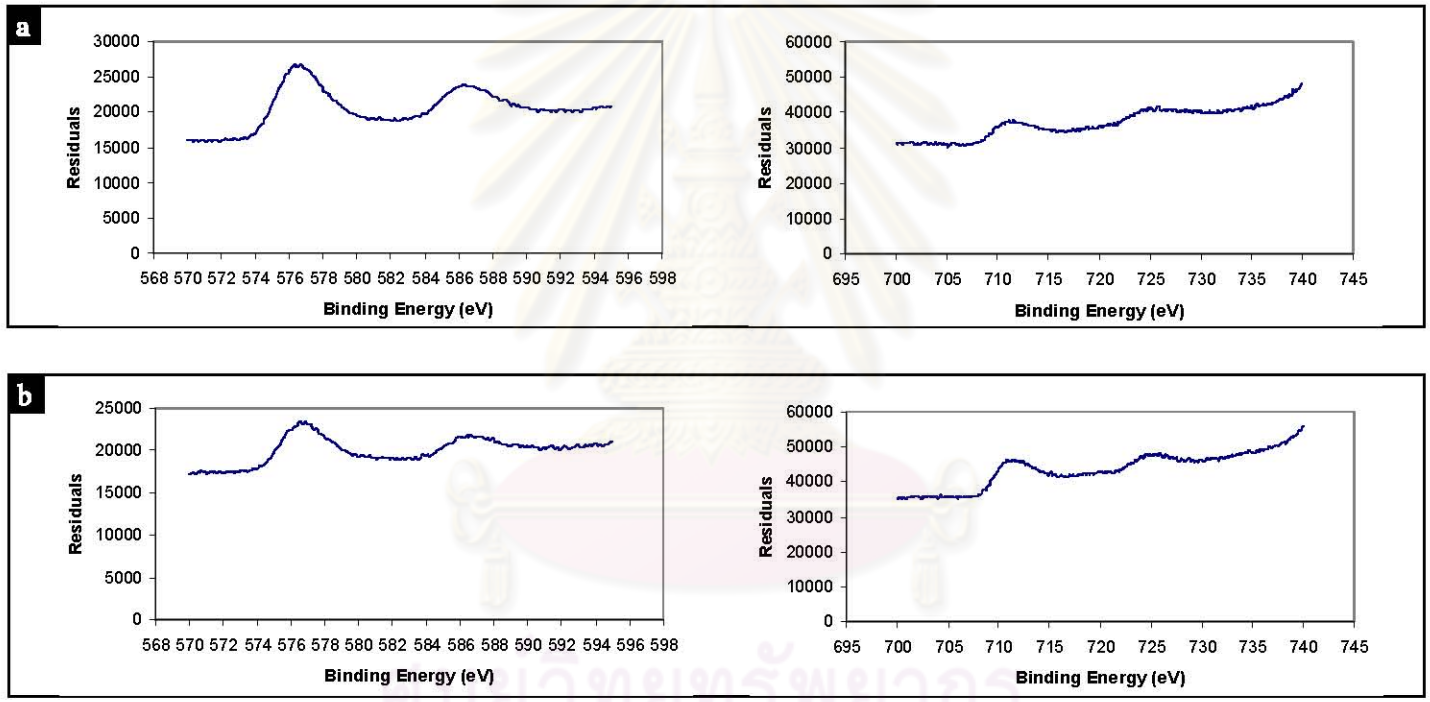

Figure 4.2 XPS spectra of oxides of Cr(left side) and Fe (right side) at the surface of the stainless steel oxidized at 800°C for 4 hr (**a**) and 6 hr (**b**).

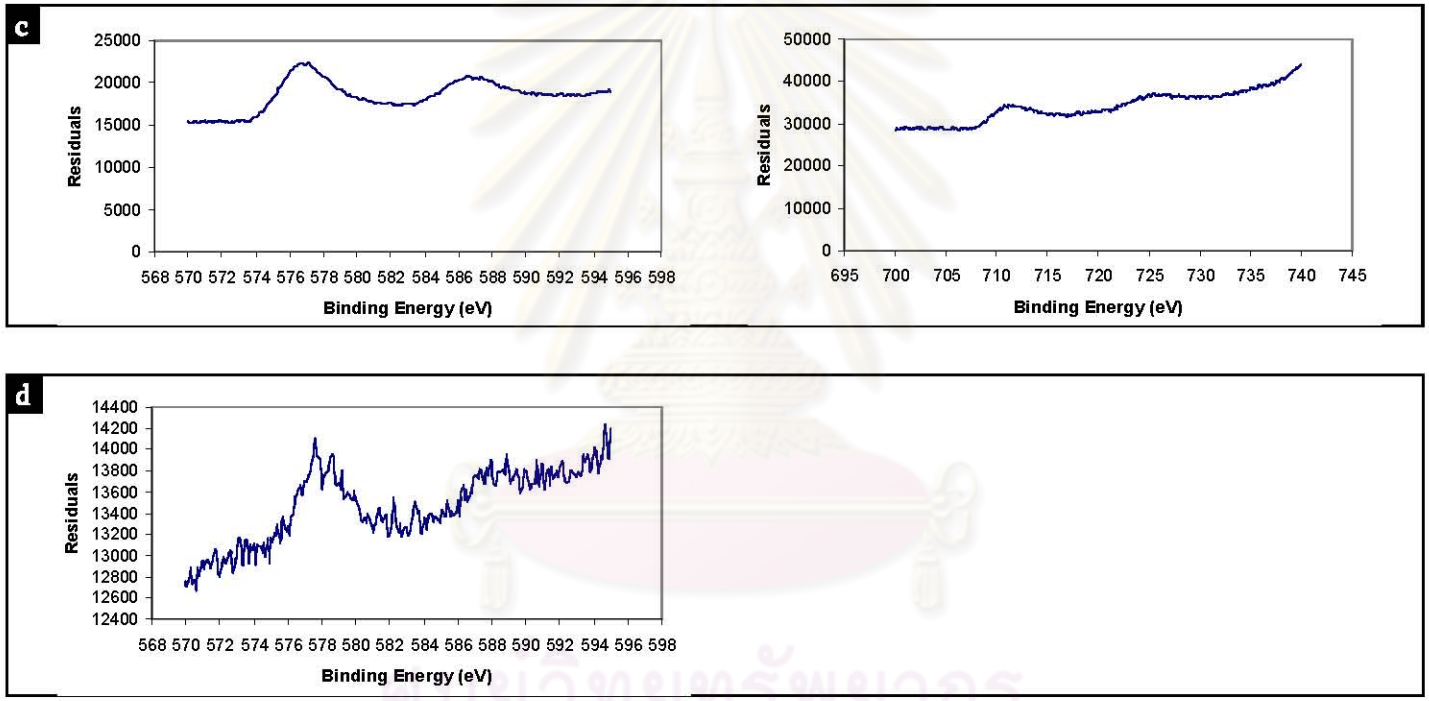

Figure 4.2 (continued) XPS spectra of oxides of Cr (left side) and Fe (right side) at the surface of the stainless steel oxidized at 800°C for 8 hr (**c**) and 12 hr (**d**).

4.1.3 Oxidation at 600°C for 6 hr

From the study at 800°C, it is obvious that, in the range of incubation times examined, heating stainless steel at 800°C was not suitable for preparing stable chromium oxide film. When compare with the study at 450°C, it turns out that 800°C was too high. Heating at 450°C was better but there was no incubation time that fulfilled both requirements. The situation got even worse: since the best incubation time for one requirement was on the worse side for the other requirement, choosing one and leave the other will cost very much. In other word, there must be other temperature-time combinations that better compromise between the two requirements if we cannot get both of them at the same time. There are two routes to solution: fixing the time and varying the temperature, or vice versa. In choosing the former choice, another question was posed. It seemed there are two incubation times to choose from: 6 hr at which the highest Cr content was observed or 8 hr at which the highest Cr_2O_3 content was observed. By recalling that Cr_2O_3 was formed at temperature higher than 400°C [22], only the former choice is possible since choosing 8 hr means lowering heating temperature.

By using 450 and 800°C as the lower and upper temperature limits, the temperature that is exactly in the middle is 625°C. If higher temperature is employed to shift the time for the highest Cr_2O_3 content at 8 to 6 hr, the time for the highest Cr content will be shifted in the same direction as well. Therefore, 600°C was chosen in favour of the lower limit. The stainless steel disk was incubated at 600°C for 6 hr and the XPS results were compared to those at 450 and 800°C in Table and Figure 4.3.

Table 4.3 Comparison of metal contents in the oxide layer at the stainless steel surface after heating at 450, 600 or 800°C.

Metal	Temperature	Percentage of metal*	Ratio of metal to oxygen
Cr	450°C	17.42	0.228
	600°C	15.17	0.195
	800°C	16.93	0.178
Fe	450°C	1.86	0.024
	600°C	7.10	0.091
	800°C	8.47	0.089
Ni	450°C	4.28	0.056
	600°C	-	-
	800°C	-	-
O	450°C	76.42	
	600°C	77.72	
	800°C	74.59	

*as determined by XPS.

As expected, incubation at 600°C fine-tuned the performance of thermal oxidation. At 600°C, the Cr XPS spectrum shifted from the characteristic peaks of CrO observed at 800°C to those of Cr_2O_3 observed at 450°C, i.e from binding energies 576 and 586 eV to 577 and 587 eV. Unlike at 450°C for 6 hr, the Cr XPS spectrum at 600°C was almost free of noise and essentially the same as at 450°C, 8 hr. Although the percentage of Cr was not the highest, the two requirements were better compromised at 600°C. Therefore, 600°C, 6 hr was the condition of choice used throughout in further experiments.

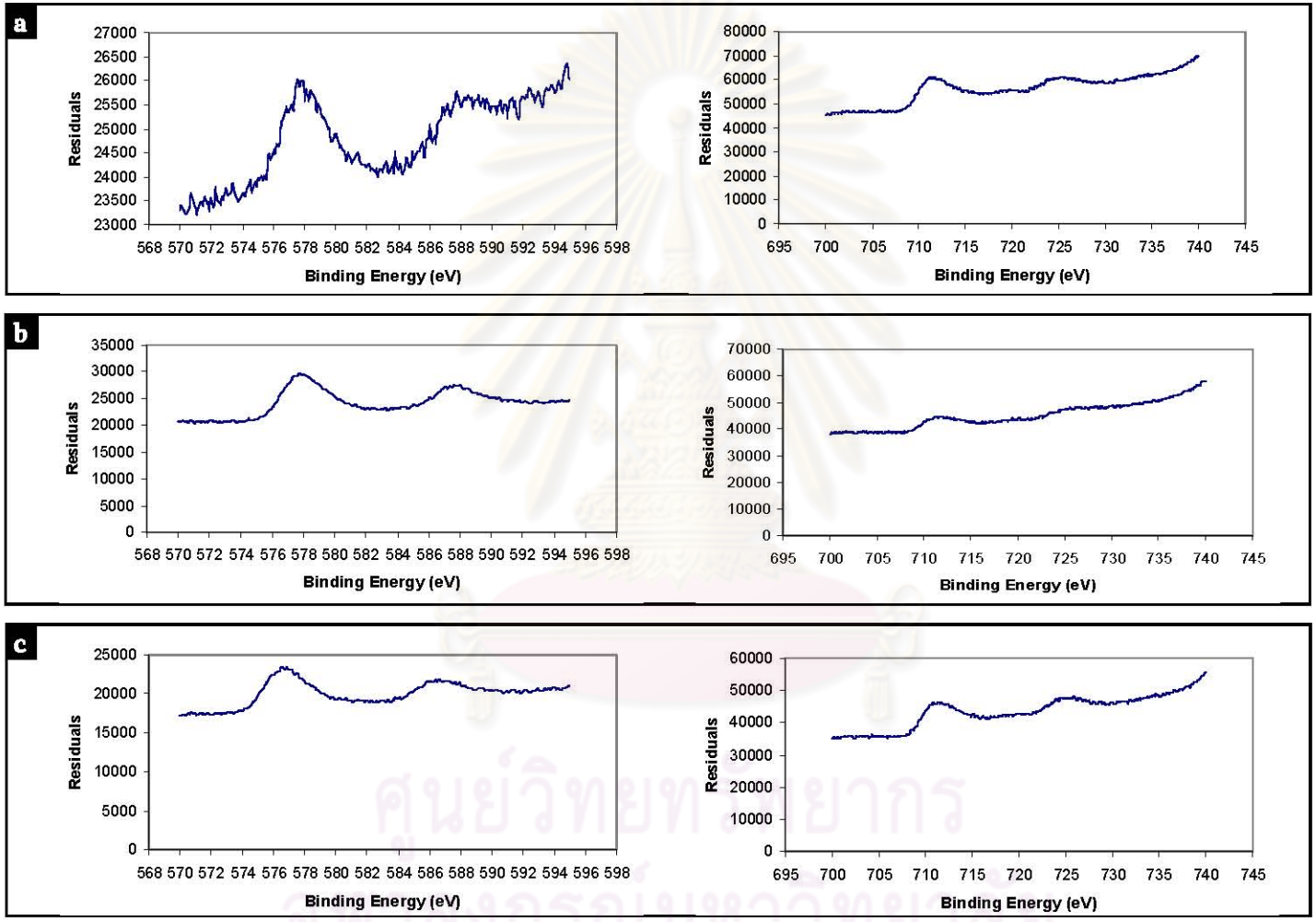

Figure 4.3 XPS spectra of oxides of Cr (left side) and Fe (right side) at the surface of the stainless steel oxidized for 6 hr at (**a**) 450, (**b**) 600 and (**c**) 800°C.

4.2 Cr-Based Intermetallic Diffusion Barriers

4.2.1 Cr_2O_3 intermetallic diffusion barriers

4.2.1.1 Preparation of Cr_2O_3 layer

There are three factors to be considered in preparation of thin film of Cr_2O_3:
(1) Source of Cr,
(2) How to coat Cr on the support, and
(3) How to effectively convert Cr to Cr_2O_3.

With regard to the source of Cr, there are two: internal (Cr inherently in the stainless steel) and external. The external Cr atoms can be coated on the stainless steel support by either (1) electroplating or (2) sputtering. In electroplating, Cr ion was reduced to metal Cr by electrical current and allowed to deposit at the surface of the stainless steel acting as the cathode.

In sputtering, Cr metal was turned to plasma by bombarding with negatively charged particles, the plasma then react with other molecule present in the sputtering chamber, if not inert, forming compound and deposits on the stainless steel substrate. If no reaction occurs, Cr plasma deposits as such forming Cr layer. Reactive Cr-sputtering in oxygen atmosphere is not possible in term of operation setting.

Cr layer prepared by either electroplating or sputtering can be oxidized in a separate step to form Cr_2O_3. Effective oxidation of Cr layer, i.e. throughout its entire thickness, was only possible with a thermal process.

Three methods were employed in this study to prepare Cr_2O_3 intermetallic diffusion barriers on stainless steel.

(1) Direct oxidation of the stainless steel. Since the most abundant metal in stainless steel normal 316L aside from iron itself is Cr which readily diffuses to the surface upon heating, Cr_2O_3 film can be directly formed by thermal oxidation in oxygen atmosphere.

(2) Cr-electroplating/oxidation. The Cr atoms were firstly deposited on the stainless steel support by means of electroplating and then thermally oxidized to form Cr_2O_3 using the same condition as the direct oxidation method.

(3) Cr-sputtering/oxidation. Sputtering of Cr atoms in inert argon atmosphere followed by thermal oxidation using the same condition as the direct oxidation method.

The most effective condition for oxidation of the stainless steel support or the Cr layer to form Cr_2O_3 film was described in section 4.1.

4.2.1.2 Surface characterization of the Cr_2O_3 intermetallic diffusion barriers

SEM micrographs of the surface of the Cr_2O_3 intermetallic diffusion barriers are shown in Figure 4.4. The smooth but grooved surface of the stainless steel (Figure 4.4a) became rough upon thermal oxidation (Figure 4.4b). Fine grains of Cr_2O_3 appeared throughout but the entire surface was not continuously covered by the Cr_2O_3 film as the deep grooves were still there and almost as deep. Within the mass of grains, remnants of the shallow grooves were clearly seen as round dark-grey-to-black spots. Therefore, it is obvious that the stainless steel support provided insufficient amount of Cr and the Cr_2O_3 film was a kind of porous, leaky instead of the intended continuous film.

By contrast, Cr layer produced by electroplating (Figure 4.4c) or sputtering (Figure 4.4e) was continuously formed. No groove previously present on the stainless steel surface was visible even the deepest ones. The surface textures were not changed much after oxidation. Cr_2O_3 grains produced by sputtering/oxidation were extremely fine and the film texture was very smooth as a result (Figure 4.4d). Electroplating/oxidation, on the other hand, produced either very large grains or clumps of Cr_2O_3 (Figure 4.4f). It occurs to everyone that 'how much the uniformity the Cr_2O_3 molecules were deep inside the film?' as this directly affects its protective property.

Another thing worth noted is that although it was carefully selected to minimize Fe/Ni contamination while maximize the formation of Cr_2O_3 (see Section 4.1), the oxidation condition did nothing to ensure that Cr atoms were oxidized throughout its entire thickness. Deeper Cr atoms may not be effectively oxidized in this condition especially those that lied deep in the Cr layer prepared by electroplating which were among the thickest (see Section 4.3 for their cross-section SEM micrographs).

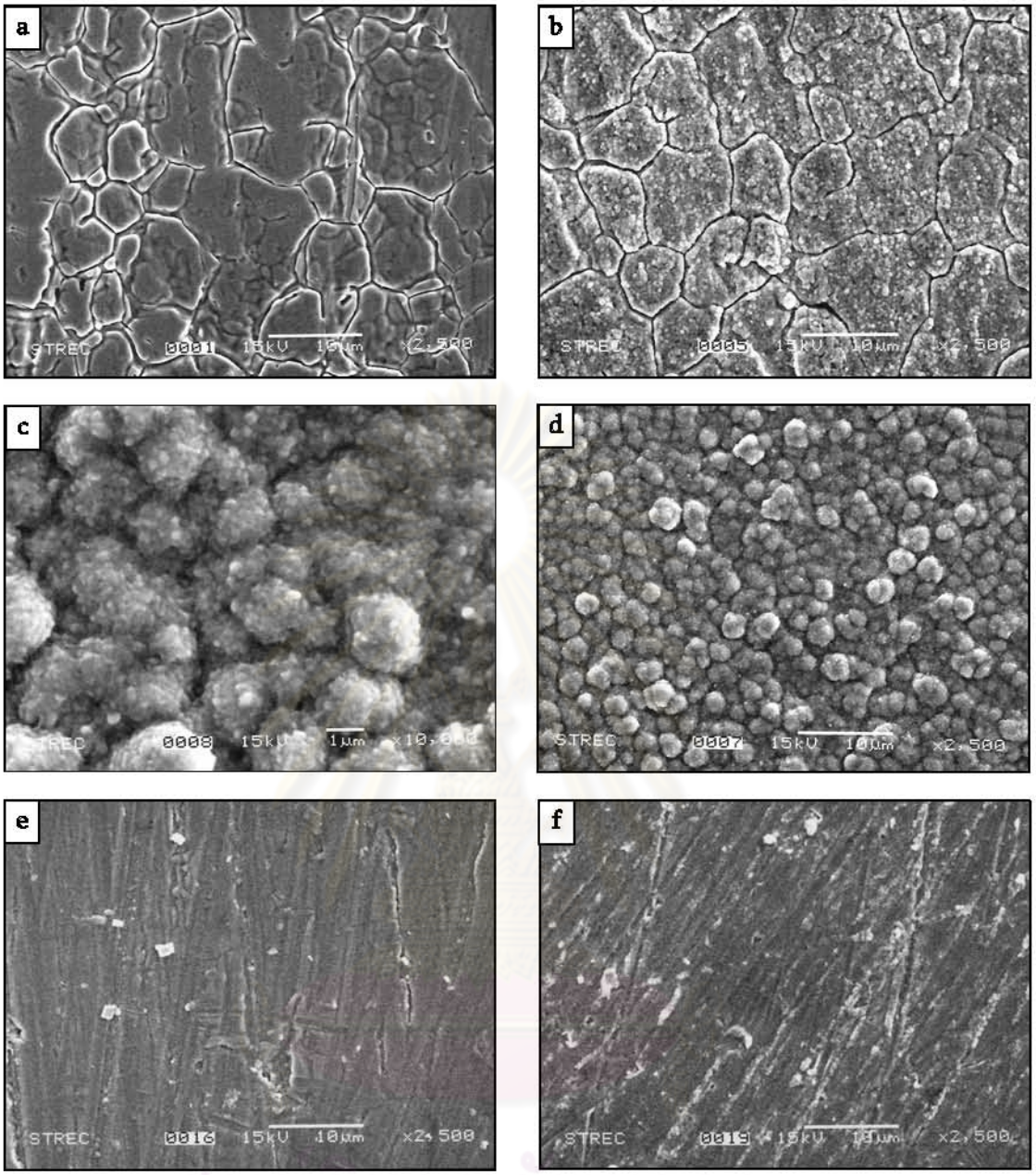

Figure 4.4 SEM micrographs of the stainless steel support with Cr_2O_3 different intermetallic diffusion barriers: **a**: plain and unoxidized stainless steel **b**: Cr_2O_3 barrier by thermal oxidation; **c**: Cr layer by Cr-electroplating; **d**: Cr_2O_3 barrier after oxidation of Cr layer shown in **c**; **e**: Cr layer by Cr-sputtering; **f**: Cr_2O_3 barrier after oxidation of Cr layer shown in **e**.

4.2.2 CrN Intermetallic Diffusion Barrier

The CrN intermetallic diffusion barrier was prepared by Cr-sputtering in nitrogen atmosphere. Nitritation [26], N_2 analogue of thermal oxidation, of the stainless steel or electroplated Cr layer was not possible in term of operation setting.

It is evident when compare the surface of CrN film (Figure 4.5b) with those of Cr_2O_3 films (Figure 4.4) that CrN film prepared at the condition of this study was thicker than Cr_2O_3 film prepared by direct oxidation but thinner than those prepared by oxidized electroplating or sputtering. The surface grooves were filled with CrN. Although the deepest grooves were not completely filled as it was the case with oxidized electroplating or sputtering, it is obvious that the CrN film was a continuous one.

One thing worth mentioned here is that sputtering produced characteristic smooth surfaces (compare Figure 4.5b and 4.4e-f with 4.4b or 4.4c-d) due to the extremely fine grains of Cr or Cr compound formed.

Another issue needs to be focus is that the CrN film produced by sputtering was free from any impurity. XPS analysis revealed that 74.9816% was Cr and the rest 25.0183% was N and XPS spectra given in Figure 4.5c-d indicated that all were in the form of CrN.

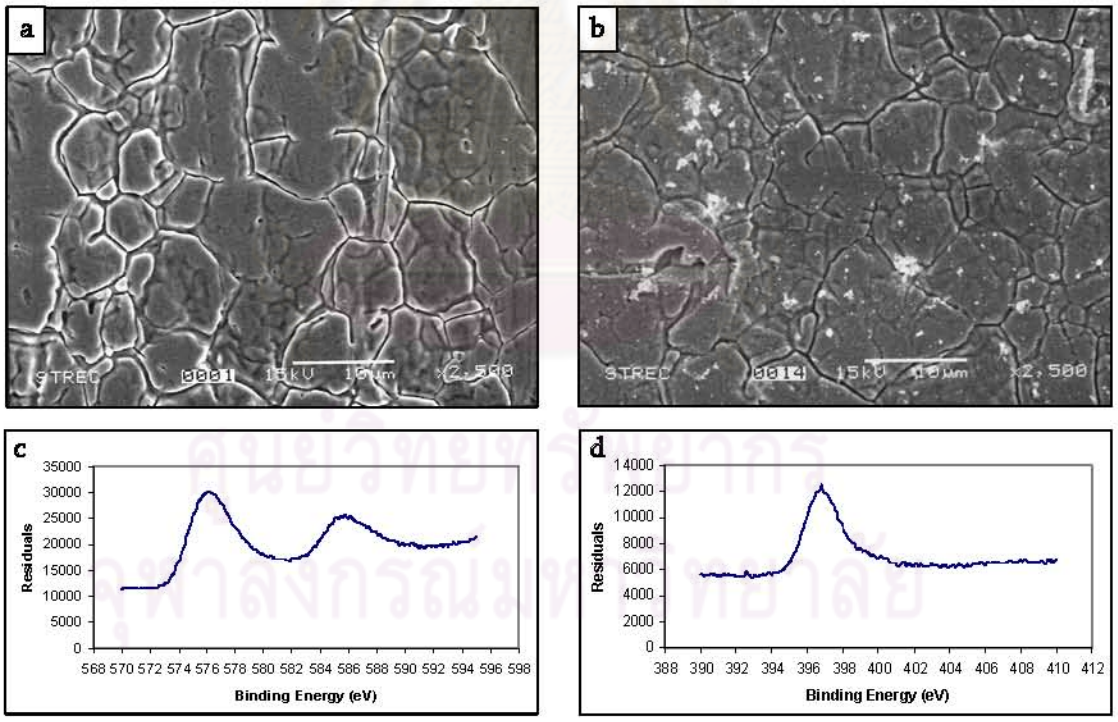

Figure 4.5 Characterization of the CrN intermetallic diffusion barrier. SEM micrographs of the unoxidized stainless steel (**a**) and the CrN film on the stainless steel support (**b**). Cr XPS spectrum of the CrN film is shown in (**c**) while N XPS spectrum is in (**d**). The characteristic peaks of Cr and N in CrN were at binding energies 376 and 386, and 395 eV, respectively.

4.3 Preparation of Palladium Membrane

The electroless plating technique (Mardilovich *et al.* [27]) was used in preparing the thin film of palladium on the stainless steel. The procedure is composed of 3 important steps: (1) surface cleaning of the support for degreasing, (2) surface activation with $SnCl_2$ and $PdCl_2$ for reducing the plating time, and (3) palladium plating with $Pd(NH_3)_4Cl_2$ solution.

4.3.1 Surface Cleaning

The stainless steel was chosen as a support since it is tougher and stronger and has higher resistance to corrosion than other materials, for example, other grade of stainless steels, ceramic and glass. The stainless steel square disks of 1 x 1 cm^2 in dimension were firstly cleaned with either an alkali solution or commercial solvents. Without this step, the palladium plating could not be deposited successfully because of grease, oil, dirt, corrosion products and others existing on the disk surface.

4.3.2 Surface Activation

Next step was to activate the surface of stainless steel disk in order to initiate an autocatalytic process of the reduction of a metastable salt complex on the target surface during electroless plating [28]. This was performed by the repeated, alternate treatments with $SnCl_2$ and $PdCl_2$ solutions. The SEM micrographs of the stainless steel surface before and after surface activation in Figure 4.6 clearly indicated that the surface was effectively activated. A large number of seeds with relatively uniform particles on the support surface were observed.

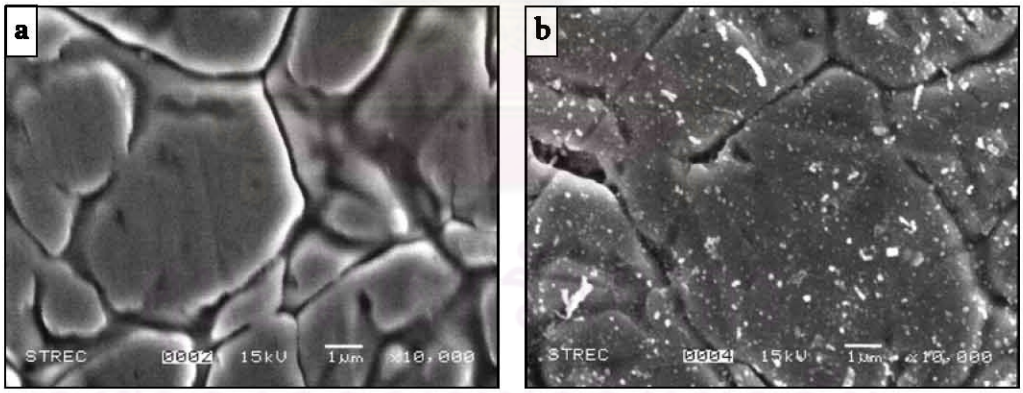

Figure 4.6 SEM micrographs of the stainless steel before (**a**) and after (**b**) surface activation.

It was proposed that tin nuclei were firstly created by decomposing of $SnCl_2$ to $Sn(OH)_{1.5}Cl_{0.5}$ with deionized water according to equation 4.1 followed by the deposition of palladium on the tin layer via the redox process described in equation 4.2 [27].

$$2SnCl_2 + 3H_2O \longrightarrow 2Sn(OH)_{1.5}Cl_{0.5} + 3HCl \quad (4.1)$$

$$Pd^{2+} + Sn^{2+} \longrightarrow Pd^{0} + Sn^{4+} \quad (4.2)$$

This phenomenon was previously proved by Shu *et al* [29]. They reported that almost no palladium seed appeared on the surface of porous stainless steel disk when it was immersed only in the acidic palladium-containing solution.

4.3.3. Palladium plating

After surface activation, the stainless steel disks were plated with palladium by electroless plating technique. The plating solution consisted of $Pd(NH_3)_4Cl_2{\cdot}H_2O$, 28% ammonia solution, and EDTA. An excess of ammonium hydroxide is necessary to stabilize the plating solution and maintain the pH at 10.

Anhydrous hydrazine, a reducing agent, was then added into the palladium plating solution when its temperature reached 60°C. During the immersion of the disks some bubbling gases were observed due to the redox reaction as shown in Figure 4.7

$$N_2H_4 + 4OH^- \longrightarrow 4H_2O + N_2 + 4e^- \qquad E^0 = -1.12\ V$$
$$2Pd(NH_3)_4^{2+} + 4e^- \longrightarrow 2Pd^0 + 8NH_3 \qquad E^0 = 0.95\ V$$
$$2Pd(NH_3)_4^{2+} + N_2H_4 + 4OH^- \longrightarrow 2Pd^0 + 4H_2O + N_2 + 8NH_3 \qquad E^0 = 2.07\ V$$

Figure 4.7 Redox reaction of palladium plating

At the end of plating step, the disk was cleaned and dried. It appeared silver-like in color which is the indication that palladium deposition had occurred. It was explained by several other research groups [29, 30] that the reaction occurred on the surface of the support, and preferentially around the palladium seeds. The occurrence was initiated by the reaction of hydrazine with hydroxide ion forming nitrogen gas and water with simultaneous release of electron. The electrons were transferred across the palladium island and used for reducing Pd^{2+} complex into palladium metal. The palladium metal was deposited onto the nuclei resulting in growth. Nitrogen and ammonia gases were concomitantly evolved as bubbles during the plating process.

The palladium plating was evident when compare the SEM micrographs of activated stainless steel disk before and after palladium plating as revealed in Figure 4.8. It obviously showed that the smooth surface was obtained resulting from palladium deposition onto the disk surface until a certain thickness was developed.

In general, the thickness of palladium layer can simply be determined by weighing. Three squares of activated stainless steel disk were weighted before the plating step and then again after palladium plating at different plating time. The calculation for the thickness of palladium layer was done by using the following equation:

$$\text{Pd thickness } (\mu m) = \left[\left(\frac{\text{plated disk weigh - initial disk weigh}}{\text{disk surface area} \times \text{palladium density}}\right)\right] \times 10^4$$

where density of palladium = 12.02 g/mL, and
surface area = $4(0.1\times1) + 2(1\times1) = 2.4\ cm^2$.

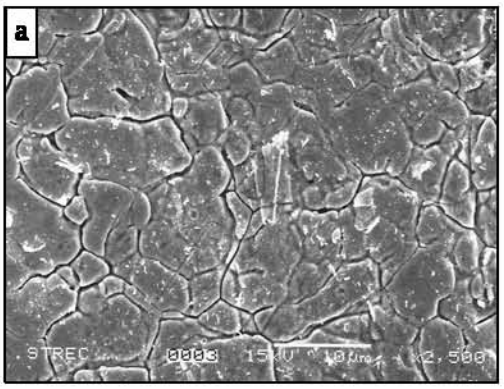

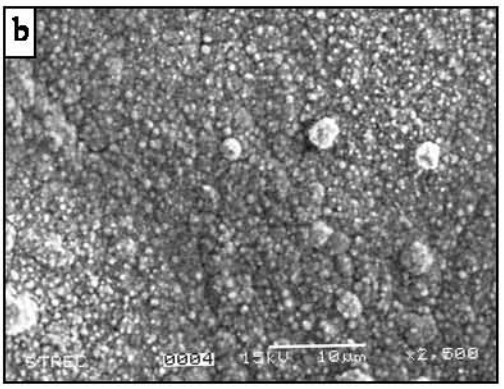

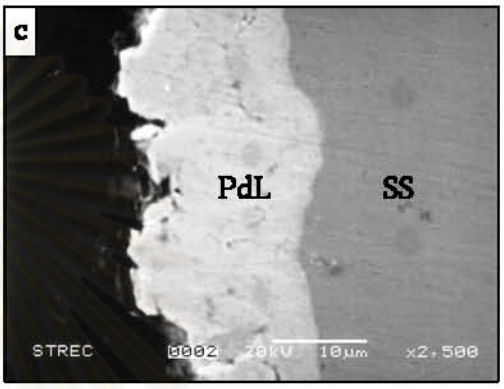

Figure 4.8 SEM micrographs of the activated surface of stainless steel before (**a**) and after (**b**) palladium plating. The cross section of (**b**) is given in (**c**). **PdL**: palladium layer; **SS**: stainless steel.

It was assumed that the gained weight of the disk came from plated palladium only and the entire disk surface was plated evenly. The reliability of the weighing method in determining the palladium layer thickness was assessed with their SEM micrographs. Both measuring methods showed that the palladium layer thickness increased with increasing plating time as illustrated in Table 4.4. It can be seen that the palladium layer thickness measured by weighing is in the range determined by SEM. Therefore, the measurement of palladium layer thickness by weighing could be acceptable.

Table 4.4 Palladium layer thickness on stainless steel disks.

Underlying Surface	Disk number	Disk weight (g)		Pd layer thickness (µm)	
		Before plating	After plating	Weighing	SEM
plain stainless steel	1	1.1825	1.1944	4.1250	4.00
	2	1.1625	1.1742	4.0557	5.16
	3	1.2020	1.2147	4.4023	8.16
Cr_2O_3 by direct oxidation	4	1.0690	1.0745	3.3277	3.50
	5	1.0246	1.0432	6.4775	5.50
	6	1.0360	1.0546	6.4775	4.50
Cr_2O_3 by oxidized Cr-electroplating	7	1.1545	1.1649	3.6051	3.83
	8	1.0103	1.0212	3.7784	3.50
	9	1.2809	1.2984	6.0662	5.16
Cr_2O_3 by oxidized Cr-sputtering	10	1.1716	1.1805	3.0851	3.00
	11	0.8841	0.8913	2.4958	2.83
	12	1.1656	1.1741	2.9464	2.66
CrN	13	1.0968	1.1024	1.9410	2.16
	14	1.0370	1.0464	3.2584	3.16
	15	1.1470	1.1565	3.2931	2.00

4.4 Prevention of Intermetallic Diffusion by Cr-Based Intermetallic Diffusion Barriers.

4.4.1 Effect of high temperature on metal diffusion

The efficacies in preventing intermetallic diffusion [31] of the barriers were assessed by annealing of the palladium membrane with either of the barriers at 450°C, 500°C, and 550°C for 24 hr under argon atmosphere and the elemental composition of the palladium layer were determined by EDS spot (Table 4.5-4.6) of their cross-section and mapped with SEM-EDS (Figure 4.11-16).

When compare among the palladium membrane without any protective barrier, elemental compositions in Table 4.5 clearly demonstrates the intermetallic diffusion of Fe, Cr and Ni from the stainless steel support to the palladium layer. The intermetallic diffusion exhibited the expected trend: diffusion increased with increasing temperatures. However, the degree in which each metal diffuses varied: more Fe and Cr accumulated at the palladium layer than Ni. In this regard, there are two factors to be considered as stated earlier:

(1) The amount of metal present in the stainless steel support, i.e. more metal percentage means more are available to diffuse, and
(2) The nature of the metal, in descending order of readiness, Cr, Fe and Ni.

EDS mapping and EDS spectra of these metals are given in Figures 4.9 and 4.10 for the representative palladium layer on an unoxidized stainless steel.

Table 4.5 Metal distribution in the palladium membrane heated at 450°C

%Metal		No barrier		Cr_2O_3 (1)		Cr_2O_3 (2)		Cr_2O_3 (3)		CrN	
		Mean	SD	Mean	SD	Mean	SD	Mean	SD	Mean	SD
Pd layer	Pd	96.43	0.59	98.72	0.58	99.20	0.26	98.30	0.36	98.72	0.48
	Fe	2.41	0.48	0.71	0.16	0.26	0.12	1.32	0.17	0.87	0.19
	Cr	0.66	0.24	0.26	0.11	0.43	0.14	0.22	0.16	0.53	0.22
	Ni	0.50	0.07	0.31	0.43	0.11	0.20	0.16	0.14	0.07	0.09
Interlayer	Pd	n/d	n/d	n/d	n/d	0.15	0.13	n/d	n/d	n/d	n/d
	Fe	n/d	n/d	n/d	n/d	0.23	0.15	n/d	n/d	n/d	n/d
	Cr	n/d	n/d	n/d	n/d	99.55	0.19	n/d	n/d	n/d	n/d
	Ni	n/d	n/d	n/d	n/d	0.07	0.09	n/d	n/d	n/d	n/d
SS	Pd	0.67	0.91	0.09	0.12	0.00	0.00	0.10	0.08	0.14	0.24
	Fe	70.71	0.43	71.21	0.05	70.54	0.30	71.09	0.42	71.36	0.25
	Cr	18.71	0.70	18.67	0.13	18.59	0.03	18.30	0.04	18.02	0.20
	Ni	9.92	0.21	10.05	0.20	10.88	0.28	10.59	0.16	10.48	0.09

(1): by direct oxidation; (2): by oxidized Cr-electroplating; (3): by oxidized Cr-sputtering; n/d: not determined due to no barrier or too thin barrier to be spotted.

Table 4.5 showed that all forms of intermetallic diffusion barrier can, at varying degrees, prevent the diffusion.

Pair-wise comparisons of the efficacies showed that:

(1) Direct oxidation barriers, oxidized Cr-electroplating, oxidized Cr-sputtering and CrN versus No barrier: The atoms of Cr and Fe in palladium layer were decreased, while atoms of palladium increased.
(2) Oxidized Cr-electroplating versus direct oxidation: The atoms of Fe in palladium layer were decreased but atoms of Cr increased, while atoms of palladium increased. The increasing of Cr atoms may be due to the diffusion of unoxidized Cr atom.
(3) Oxidized Cr-sputtering versus oxidized Cr-electroplating: The atoms of Fe in palladium layer were increased but atoms of Cr decreased, while atoms of palladium decreased. The decreasing of Cr atoms may be due to the lower thickness of sputtering layer.
(4) CrN versus oxidized Cr-sputtering: The atoms of Fe in palladium layer were decreased but atoms of Cr increased, while atoms of palladium increased. The increasing of Cr atoms may be due to the diffusion of unnitrided Cr atom.

Table 4.6 Metal distribution in the palladium membrane heated at 450, 500 and 550°C.

Barriers	% Metal	450°C						500°C						550°C					
		Pd layer		Interlayer		SS		Pd layer		Interlayer		SS		Pd layer		Interlayer		SS	
		Mean	SD	Mean	SD	Mean	SD	Mean	SD	Mean	SD	Mean	SD	Mean	SD	Mean	SD	Mean	SD
No barrier, unoxidized	Pd	96.43	0.59	n/d	n/d	0.67	0.91	87.42	0.55	n/d	n/d	0.05	0.06	73.86	1.62	n/d	n/d	0.01	0.01
	Fe	2.41	0.48	n/d	n/d	70.71	0.43	7.99	0.36	n/d	n/d	70.85	0.39	21.47	1.15	n/d	n/d	71.04	0.91
	Cr	0.66	0.24	n/d	n/d	18.71	0.70	3.70	0.27	n/d	n/d	19.37	0.06	3.45	0.76	n/d	n/d	19.47	0.13
	Ni	0.50	0.07	n/d	n/d	9.92	0.21	0.89	0.18	n/d	n/d	9.74	0.38	1.22	0.26	n/d	n/d	9.49	1.05
Cr2O3 (direct oxidation)	Pd	98.72	0.58	n/d	n/d	0.09	0.12	97.40	0.44	n/d	n/d	0.10	0.11	96.94	0.59	n/d	n/d	0.11	0.01
	Fe	0.71	0.16	n/d	n/d	71.21	0.05	1.73	0.32	n/d	n/d	70.53	0.12	2.16	0.20	n/d	n/d	71.53	0.02
	Cr	0.26	0.11	n/d	n/d	18.67	0.13	0.49	0.17	n/d	n/d	19.39	0.17	0.29	0.21	n/d	n/d	18.61	0.13
	Ni	0.31	0.43	n/d	n/d	10.05	0.20	0.38	0.27	n/d	n/d	9.995	0.03	0.63	0.25	n/d	n/d	9.76	0.15
Cr2O3 (oxidized Cr-electroplating)	Pd	99.20	0.26	0.15	0.13	0.00	0.00	98.80	0.39	0.76	0.44	0.01	0.01	98.36	0.51	0.35	0.04	0.36	0.20
	Fe	0.26	0.12	0.23	0.15	70.54	0.30	0.80	0.27	0.49	0.33	72.02	0.27	1.04	0.34	0.32	0.14	68.82	2.44
	Cr	0.43	0.14	99.55	0.19	18.59	0.03	0.25	0.07	98.59	0.31	16.37	0.78	0.30	0.09	98.40	0.25	20.68	3.64
	Ni	0.11	0.20	0.07	0.09	10.88	0.28	0.17	0.15	0.17	0.25	11.62	0.52	0.30	0.11	0.93	0.08	9.66	0.30
Cr2O3 (oxidized Cr-sputtering)	Pd	98.30	0.36	n/d	n/d	0.10	0.08	98.13	0.28	n/d	n/d	0.16	0.14	98.07	0.56	n/d	n/d	0.18	0.08
	Fe	1.32	0.17	n/d	n/d	71.09	0.42	1.22	0.43	n/d	n/d	71.54	0.17	1.02	0.40	n/d	n/d	70.60	0.18
	Cr	0.22	0.16	n/d	n/d	18.30	0.04	0.50	0.06	n/d	n/d	17.98	0.34	0.68	0.17	n/d	n/d	18.09	0.11
	Ni	0.16	0.14	n/d	n/d	10.59	0.16	0.15	0.13	n/d	n/d	10.32	0.13	0.24	0.19	n/d	n/d	11.13	0.26
CrN	Pd	98.72	0.48	n/d	n/d	0.14	0.24	96.74	0.55	n/d	n/d	0.27	0.24	94.75	2.25	n/d	n/d	0.26	0.24
	Fe	0.87	0.19	n/d	n/d	71.36	0.25	1.82	0.29	n/d	n/d	70.95	0.75	1.76	0.67	n/d	n/d	71.02	0.26
	Cr	0.53	0.22	n/d	n/d	18.02	0.20	0.88	0.09	n/d	n/d	18.15	0.12	2.43	1.07	n/d	n/d	18.32	0.39
	Ni	0.07	0.09	n/d	n/d	10.48	0.09	0.56	0.49	n/d	n/d	10.71	0.32	1.06	1.60	n/d	n/d	10.80	0.22

n/d: not determined due to no barrier or too thin barrier to be spotted.

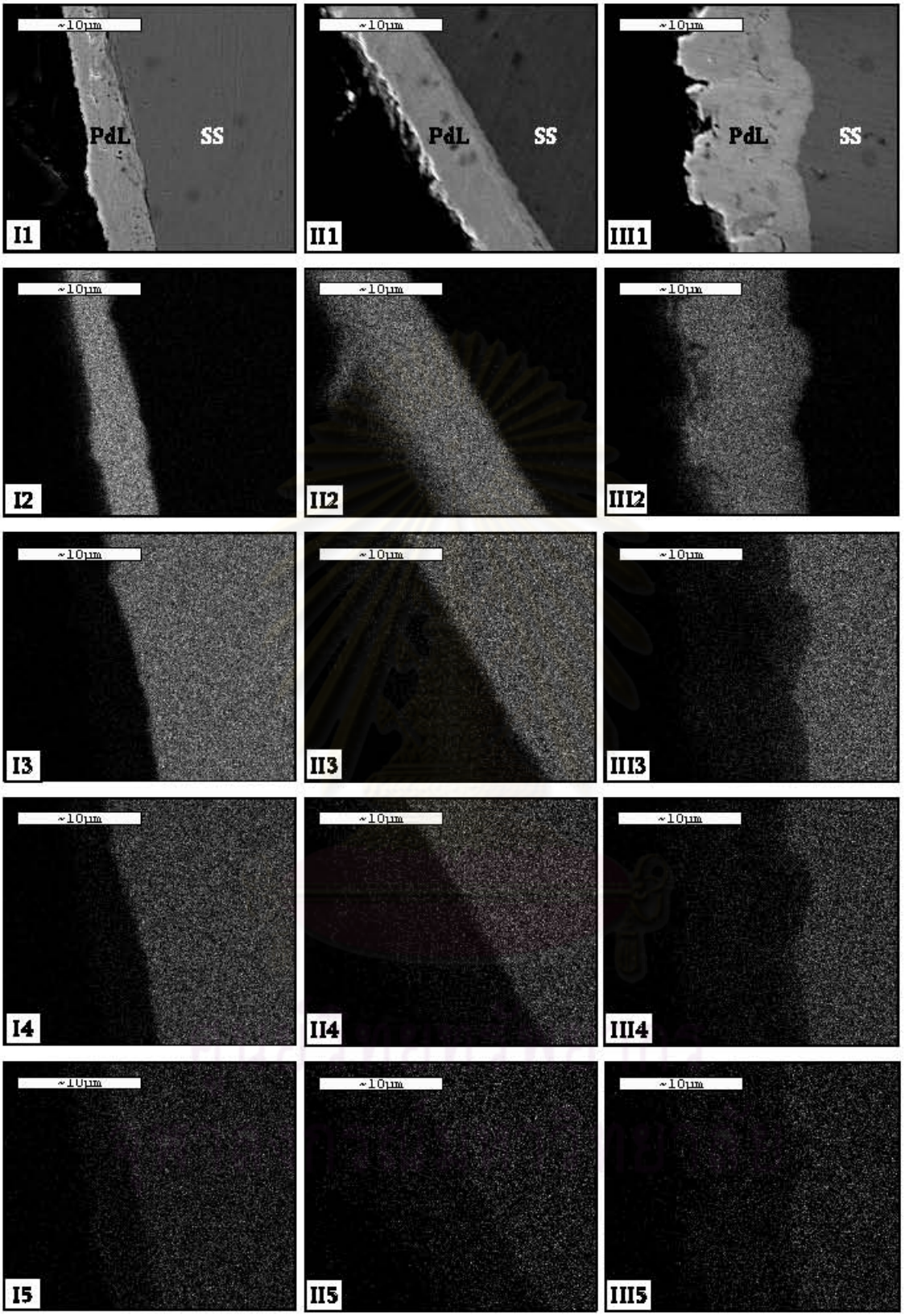

Figure 4.9 SEM micrographs (2500X) of the cross sections of palladium on an unoxidized stainless steel after heating for 24 hr at 450°C (column **I**, **I1-I5**), 500°C (column **II**, **II1-II5**) or 550°C (column **III**, **III1-III5**). Metal distribution were mapped in each row for Pd (row **2**, **I2-III**), Fe (row **3**, **I3-III3**), Cr (row **4**, **I4-III4**) and Ni (row **5**, **I5-III5**). **PdL**: Pd layer, **SS**: stainless steel.

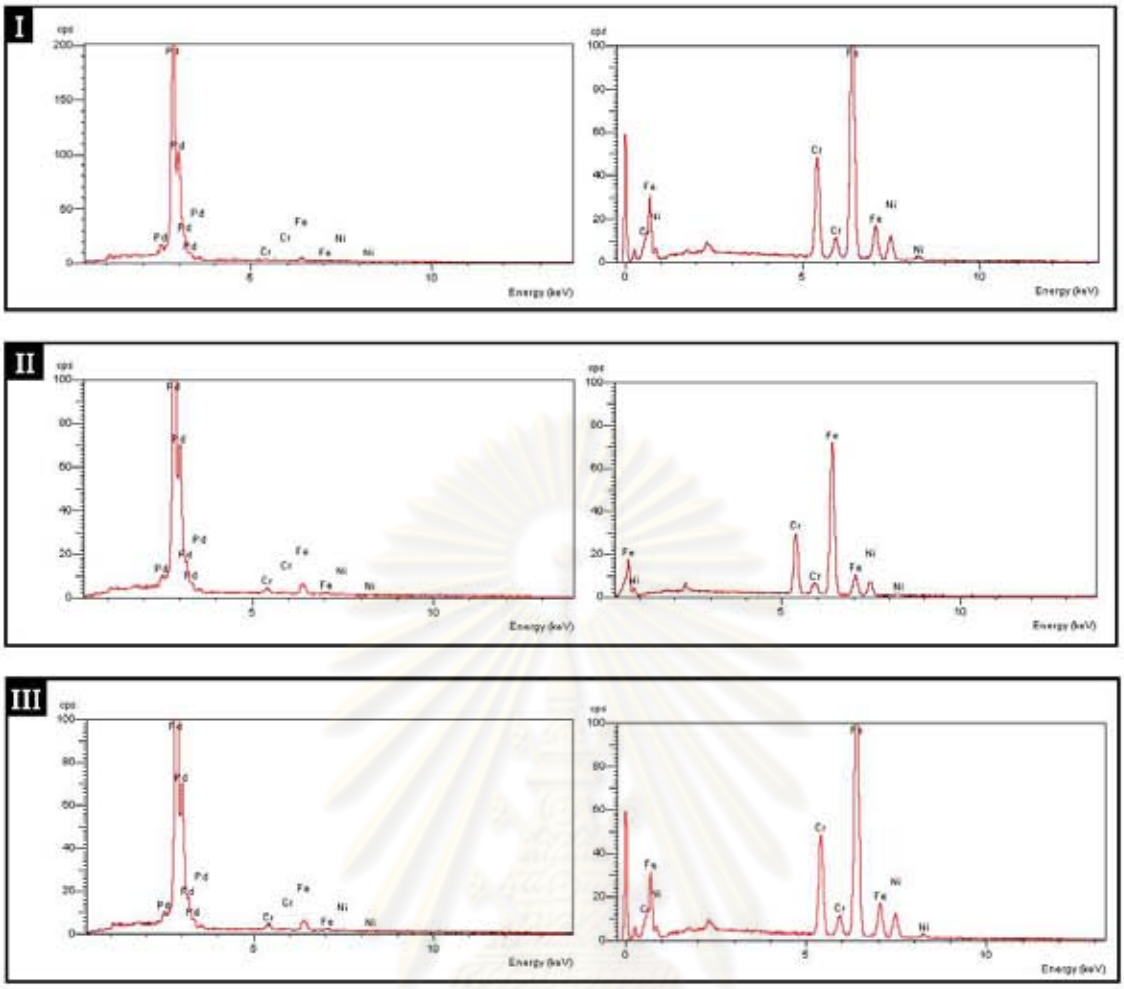

Figure 4.10 EDS spectra of the palladium membrane and unoxidized PSS support after heating for 24 hr at 450°C (**I**), 500°C (**II**) or 550°C (**III**). Shown in **I** are the EDS spectra of the untreated membrane. EDS spectra of the Pd layer are shown on the left while those of the PSS support are on the right.

4.4.2 Efficacies in preventing intermetallic diffusion

Table 4.6 showed that all forms of intermetallic diffusion barrier can, at varying degrees, prevent the diffusion. Their shielding abilities seem to be independent of temperature at least in the range of conditions tested, i.e. at 450-550°C for 24 hr. Recall that increasing temperature resulted in more diffusion and more accumulation of metal in the palladium layers. Thus, more metal contaminating in the palladium layer observed at higher incubation temperatures does not always means that the efficacy of the barrier was dropped although this is not ruled out. It may merely the result of more metals trying to penetrate the barrier to the palladium layer.

Pair-wise comparisons of the efficacies showed that:

(1) Cr_2O_3 versus CrN barriers: the Cr_2O_3 is a more effective barrier than the CrN probably because Cr_2O_3 is more stable. Even the leaky Cr_2O_3 protective barrier formed via direct oxidation was more effective than the continuous CrN film.

(2) Direct oxidation versus oxidized Cr-electroplating and direct oxidation versus oxidized Cr-sputtering: The Cr_2O_3 barriers prepared by either of the latter method in each pair are more effective than that formed by direct oxidation. The difference in their effectiveness was markedly amplified at higher temperatures. This can be explained in term of amount of Cr available to be oxidized and forms the film. The barrier formed by direct oxidation is too thin to be seen in its cross-section SEM micrograph (A1 and A2 in Figures 4.11, 4.13 and 4.15). It is evident when compare its surface with that of the unoxidized stainless steel (Figure 4.4B versus 4.4A) that the Cr atoms diffused up from the stainless steel were not adequate to form a continuous film to cover the entire surface of the stainless steel.

(3) Oxidized Cr-electroplating versus oxidized Cr-sputtering: The Cr layer was better prepared by electroplating. This is may due to
   (a) The thicker Pd layer (C1 versus D1 in figure 4.11, 4.13 and 4.15) which in turn may be a result of a rough Cr layer (Figure 4.4C versus 4.4D),
   (b) The denser Cr layer formed by chemisorptions versus the physicsorption mechanism of the sputtering.

This study ranks Cr_2O_3 thin film prepared by oxidized Cr-electroplating as the most effective intermetallic diffusion barriers in term of shielding the palladium layer. Cr_2O_3 thin film prepared by oxidized Cr-sputtering comes at the second place followed by the film formed via direct oxidation and the CrN film. However, there is one word of caution: the ranking this study suggested was made without considering of the thickness of the barriers which I found very difficult to manage to get the same. I am pretty sure that Cr_2O_3 film is a better barrier than the CrN as it is obvious from the fact that even the continuous and fairly thick CrN film was outperformed by the leaky and extremely thin Cr_2O_3 film prepared by direct oxidation. But within the group of Cr_2O_3 films, it is by no means certain that there is a significant difference in shielding effectiveness when the films are all equally thick.

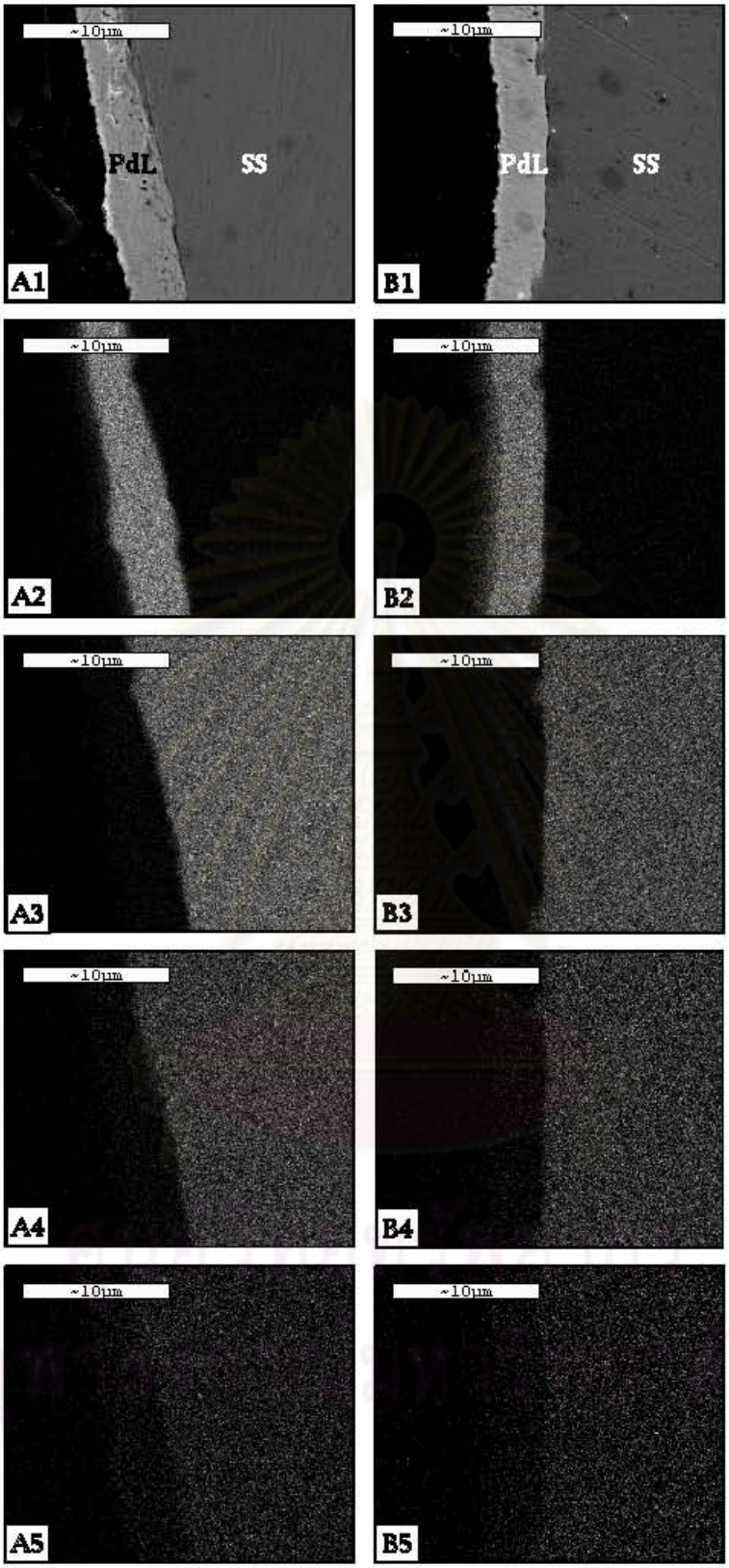

Figure 4.11 SEM micrographs (2500X) of the cross sections of palladium membrane after heating for 24 hr at 450°C. Column **A** (**A1-A5**): unoxidized, no barrier; **B** (**B1-B5**): Cr_2O_3 barrier by thermal oxidation. Metal distribution were mapped in each row: row **2** (**A2-F2**): Pd; **3** (**A3-F3**): Fe; **4** (**A4-F4**): Cr; and **5** (**A5-F5**): Ni. Arrow head: intermetallic diffusion barrier, **PdL**: Pd layer, **SS**: stainless steel.

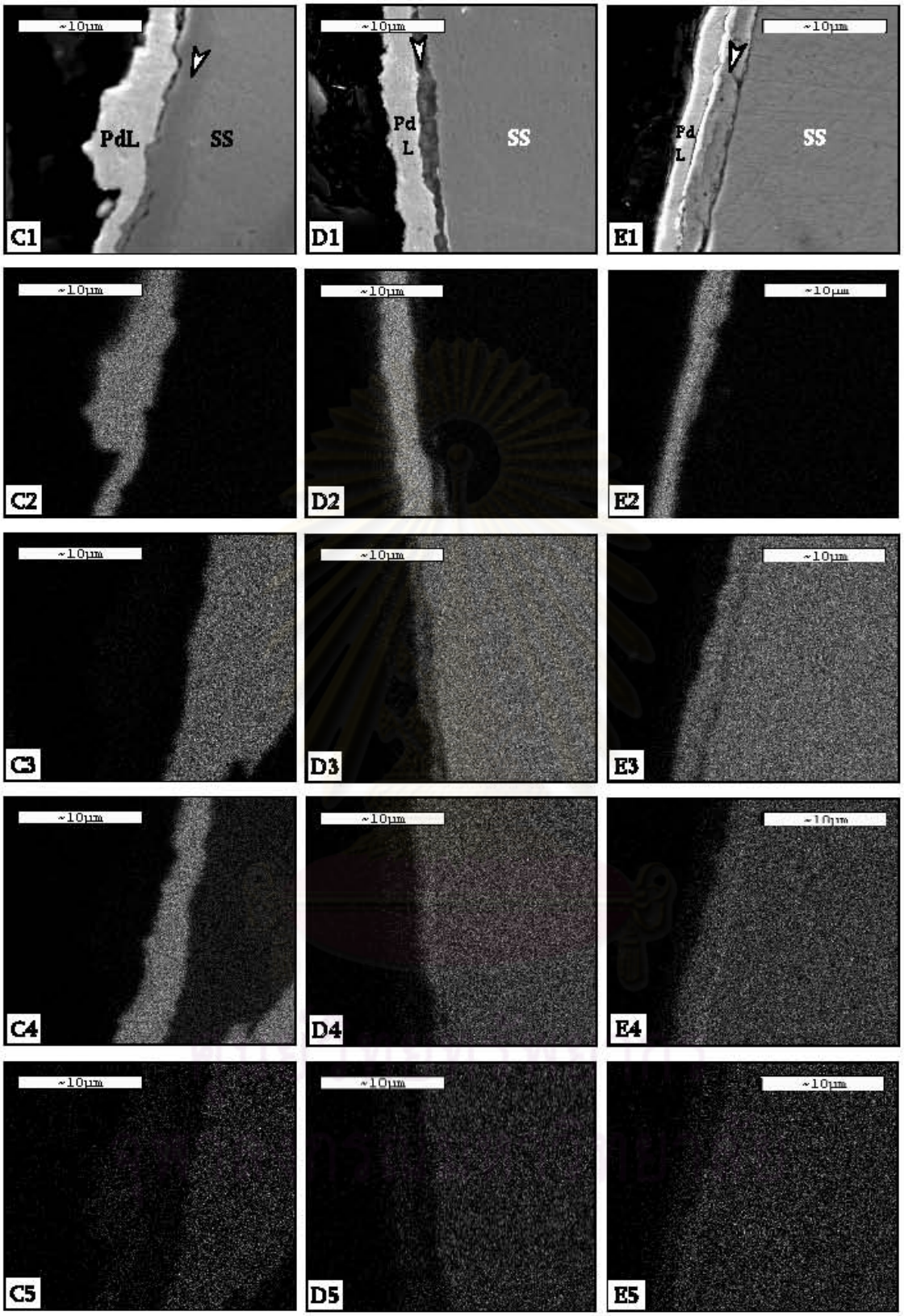

Figure 4.11 (continued) SEM micrographs (2500X) of the cross sections of palladium membrane after heating for 24 hr at 450°C. Column **C** (**C1-C5**): Cr_2O_3 barrier by Cr-electroplating/oxidation; **D** (**D1-D5**): Cr_2O_3 barrier by Cr-sputtering/oxidation; **E** (**E1-E5**): CrN barrier by sputtering. Metal distribution were mapped in each row: row **2** (**A2-F2**): Pd; **3** (**A3-F3**): Fe; **4** (**A4-F4**): Cr; and **5** (**A5-F5**): Ni. Arrow head: intermetallic diffusion barrier, **PdL**: Pd layer, **SS**: stainless steel.

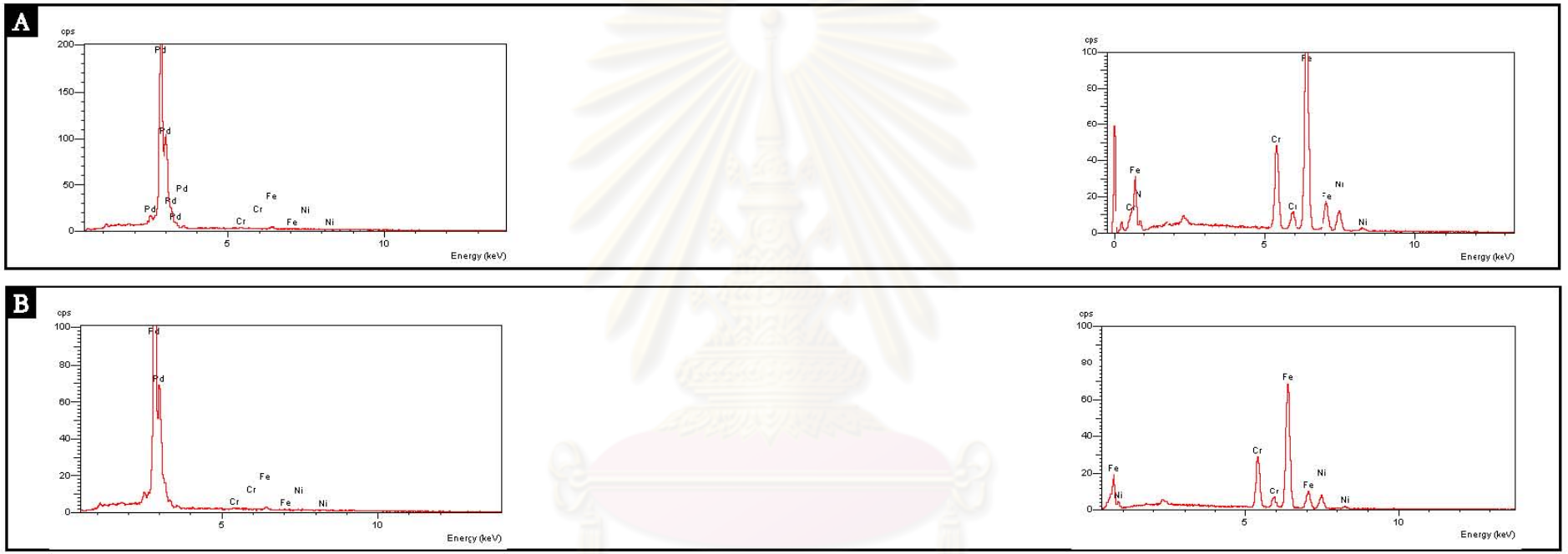

Figure 4.12 EDS spectra of the palladium membrane after heating for 24 hr at 450°C. **A**: unoxidized, no barrier; **B**: Cr_2O_3 barrier by thermal oxidation. EDS spectra of the Pd layer are shown on the left, those of the Cr-based intermetallic diffusion barrier are in the middle and those of the stainless steel support are on the right.

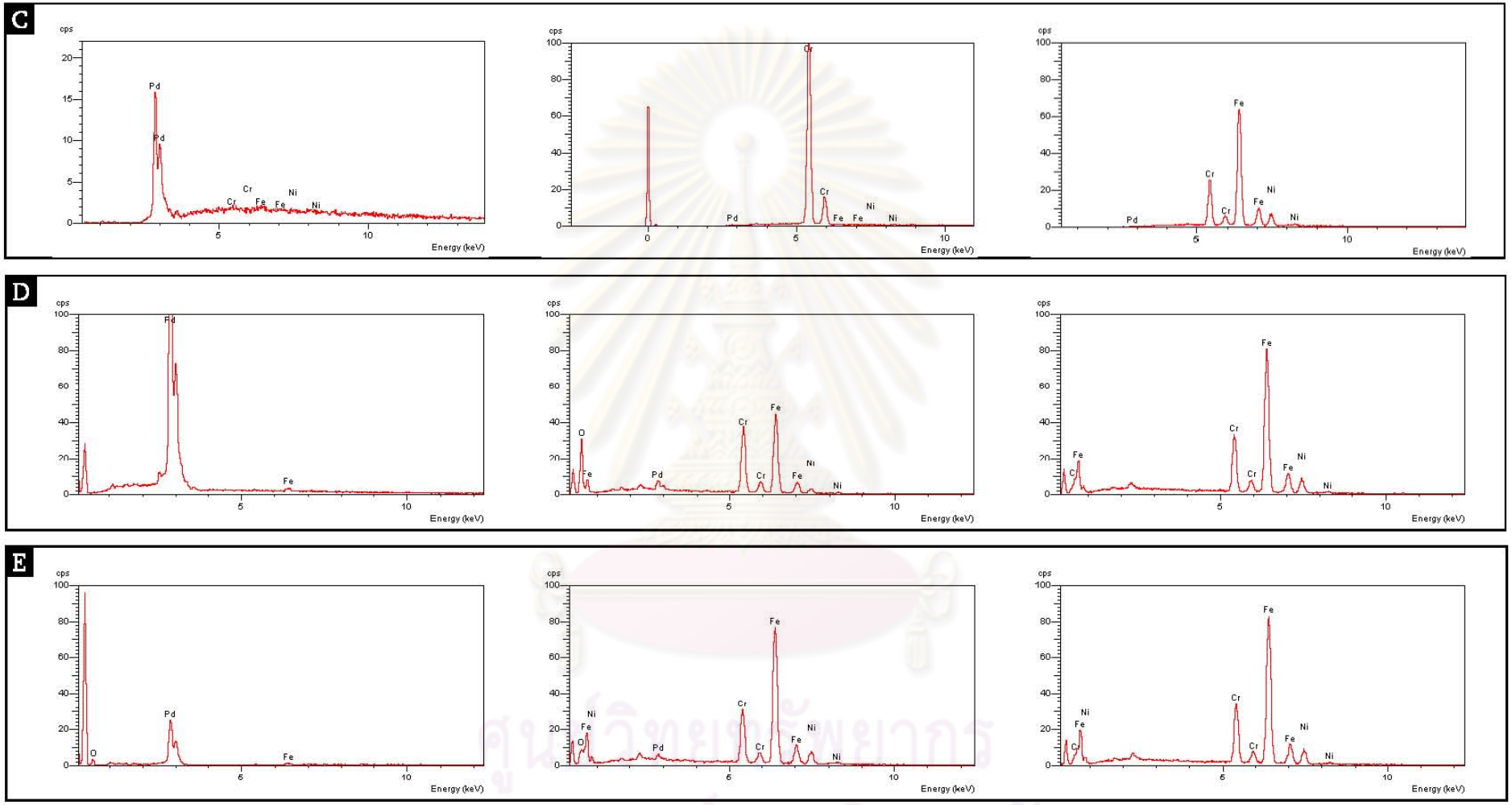

Figure 4.12 (continued) EDS spectra of the palladium membrane after heating for 24 hr at 450°C. **C**: Cr_2O_3 barrier by Cr-electroplating/oxidation; **D**: Cr_2O_3 barrier by Cr-sputtering/oxidation; **E**: CrN barrier by sputtering. EDS spectra of the Pd layer are shown on the left, those of the Cr-based intermetallic diffusion barrier are in the middle and those of the stainless steel support are on the right.

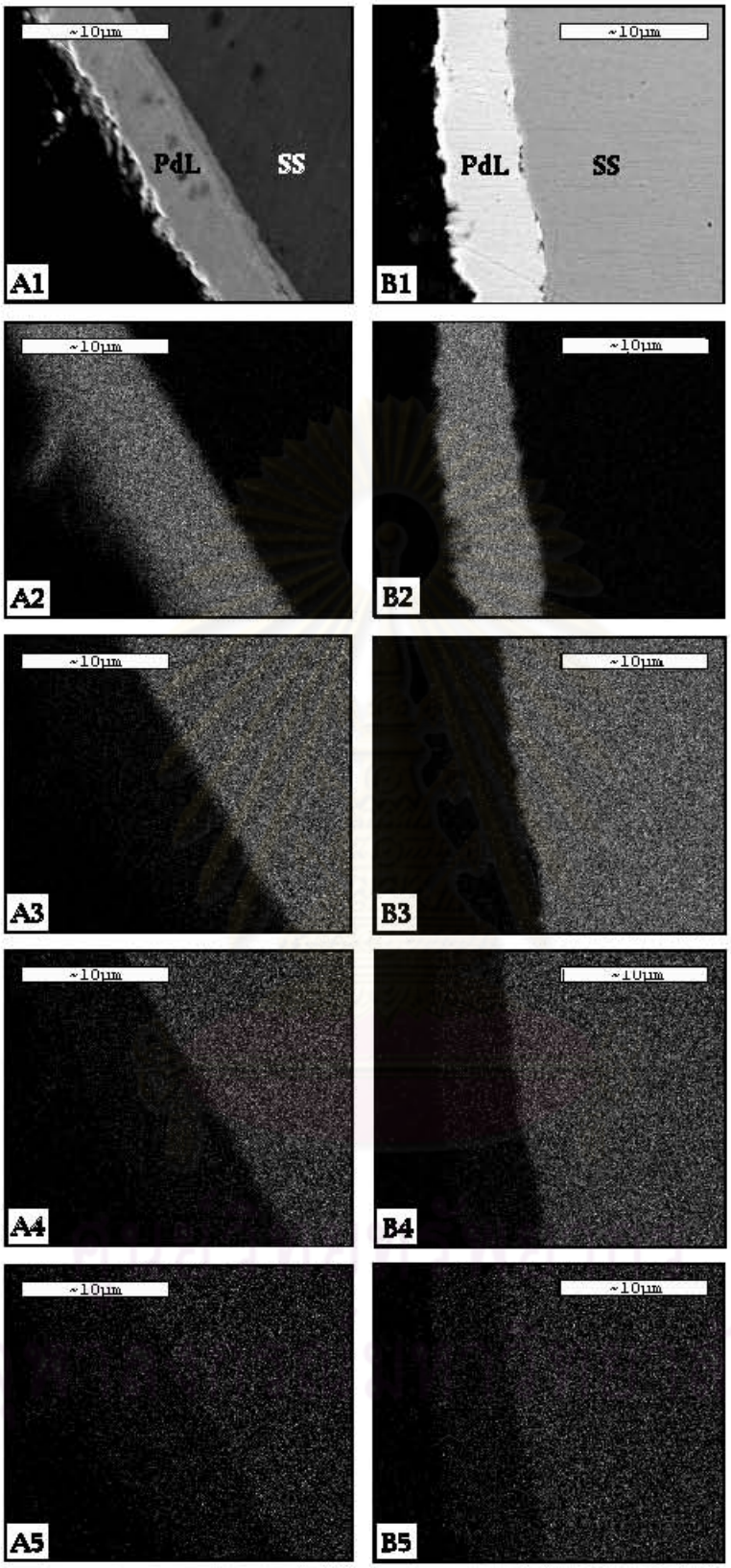

Figure 4.13 SEM micrographs (2500X) of the cross sections of palladium membrane after heating for 24 hr at 500°C. Column **A** (**A1-A5**): unoxidized, no barrier; **B** (**B1-B5**): Cr_2O_3 barrier by thermal oxidation. Metal distribution were mapped in each row: row **2** (**A2-F2**): Pd; **3** (**A3-F3**): Fe; **4** (**A4-F4**): Cr; and **5** (**A5-F5**): Ni. Arrow head: intermetallic diffusion barrier, **PdL**: Pd layer, **SS**: stainless steel.

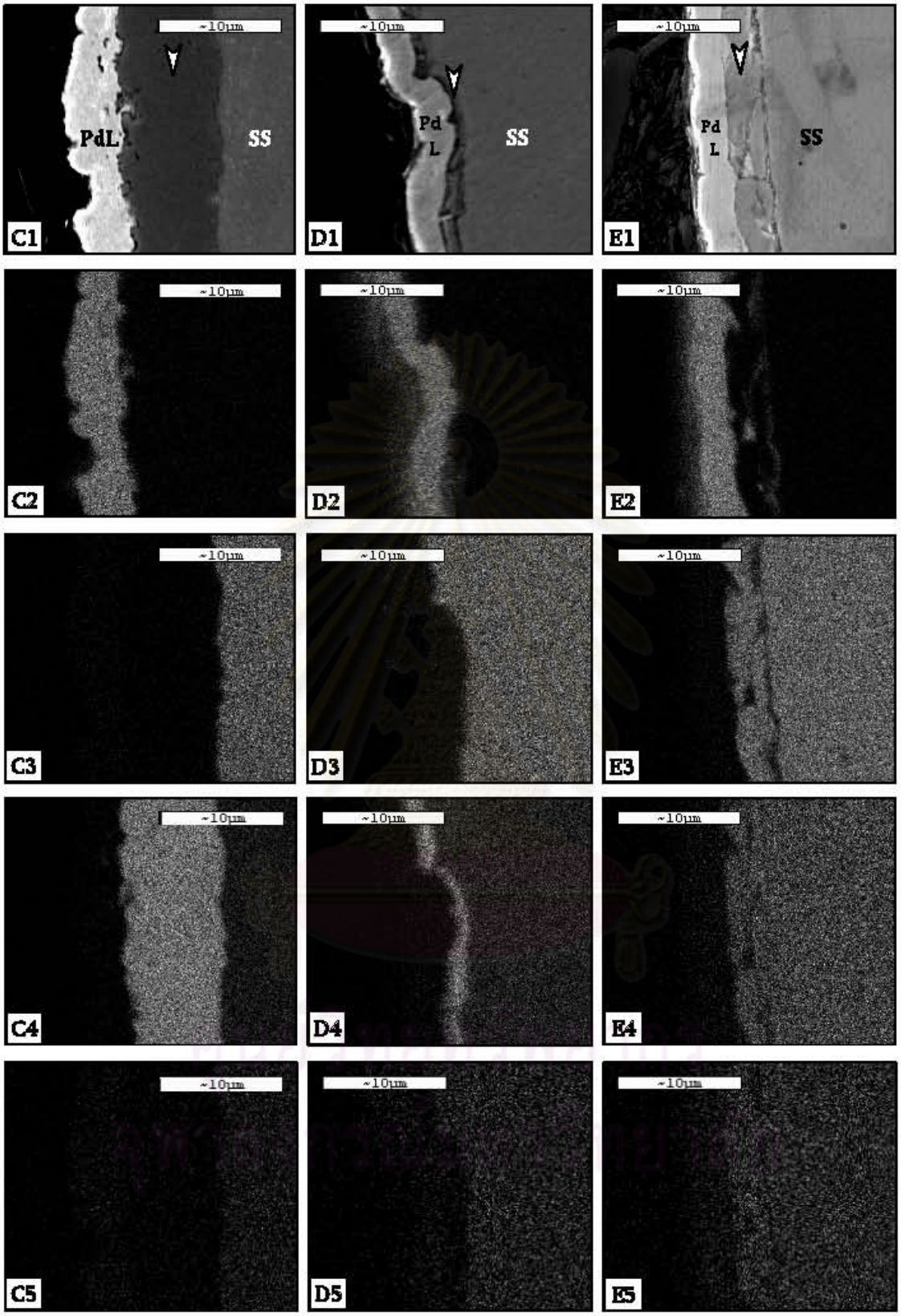

Figure 4.13 (continued) SEM micrographs (2500X) of the cross sections of palladium membrane after heating for 24 hr at 500°C. Column **C** (**C1-C5**): Cr_2O_3 barrier by Cr-electroplating/oxidation; **D** (**D1-D5**): Cr_2O_3 barrier by Cr-sputtering/oxidation; **E** (**E1-E5**): CrN barrier by sputtering. Metal distribution were mapped in each row: row **2** (**A2-F2**): Pd; **3** (**A3-F3**): Fe; **4** (**A4-F4**): Cr; and **5** (**A5-F5**): Ni. Arrow head: intermetallic diffusion barrier, **PdL**: Pd layer, **SS**: stainless steel.

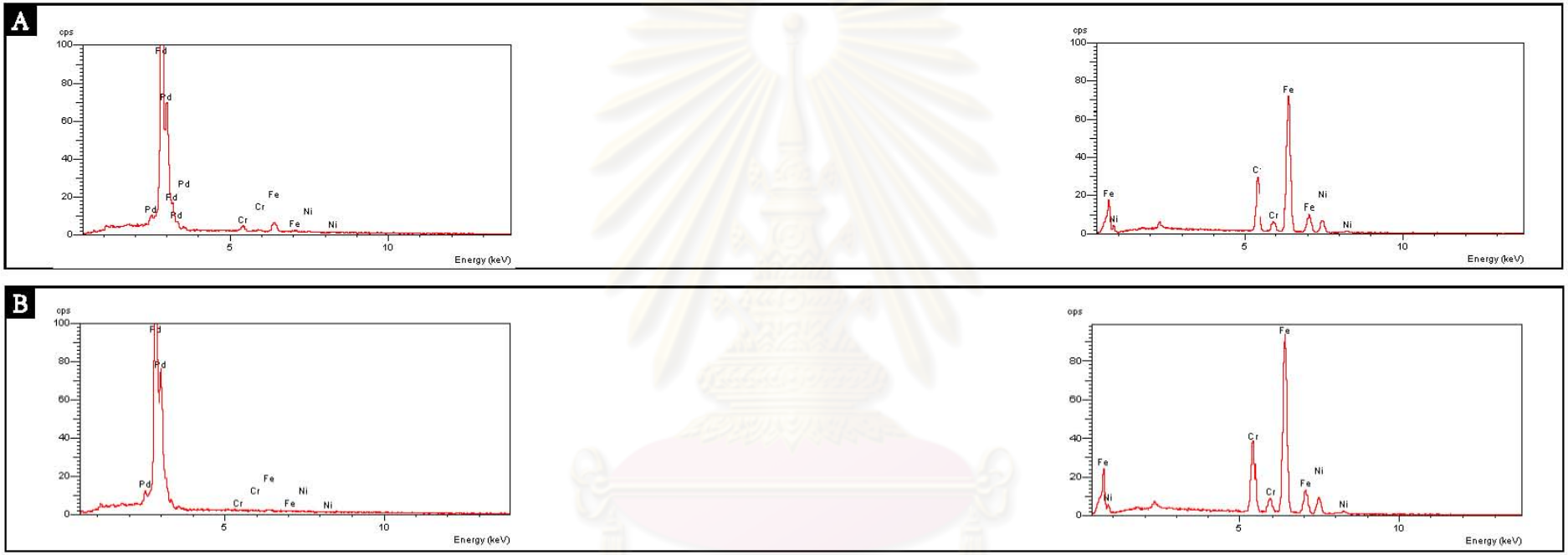

Figure 4.14 EDS spectra of the palladium membrane after heating for 24 hr at 500°C. **A**: unoxidized, no barrier; **B**: Cr_2O_3 barrier by thermal oxidation. EDS spectra of the Pd layer are shown on the left, those of the Cr-based intermetallic diffusion barrier are in the middle and those of the stainless steel support are on the right.

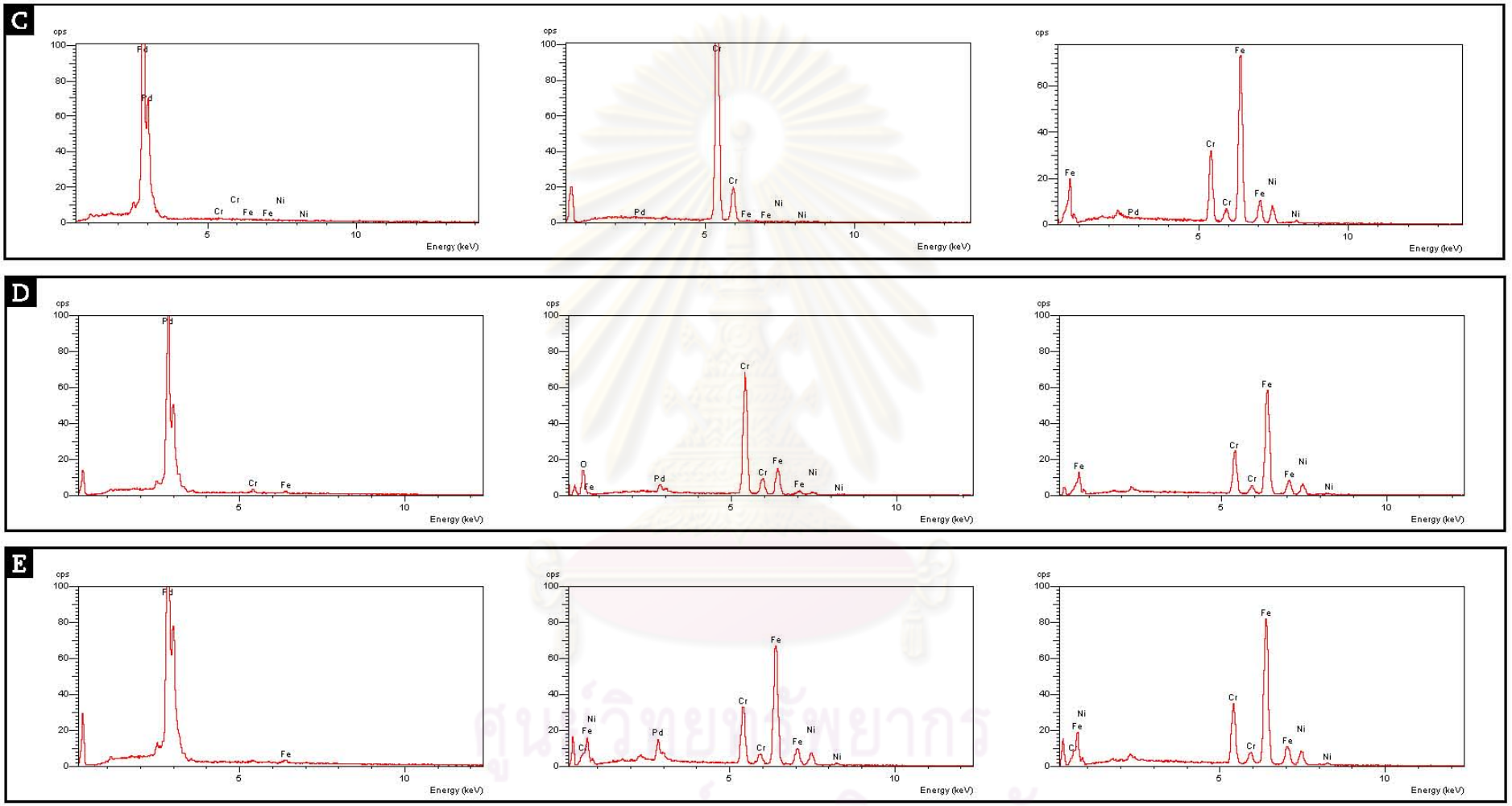

Figure 4.14 (continued) EDS spectra of the palladium membrane after heating for 24 hr at 500°C. **C**: Cr_2O_3 barrier by Cr-electroplating/oxidation; **D**: Cr_2O_3 barrier by Cr-sputtering/oxidation; **E**: CrN barrier by sputtering. EDS spectra of the Pd layer are shown on the left, those of the Cr-based intermetallic diffusion barrier are in the middle and those of the stainless steel support are on the right.

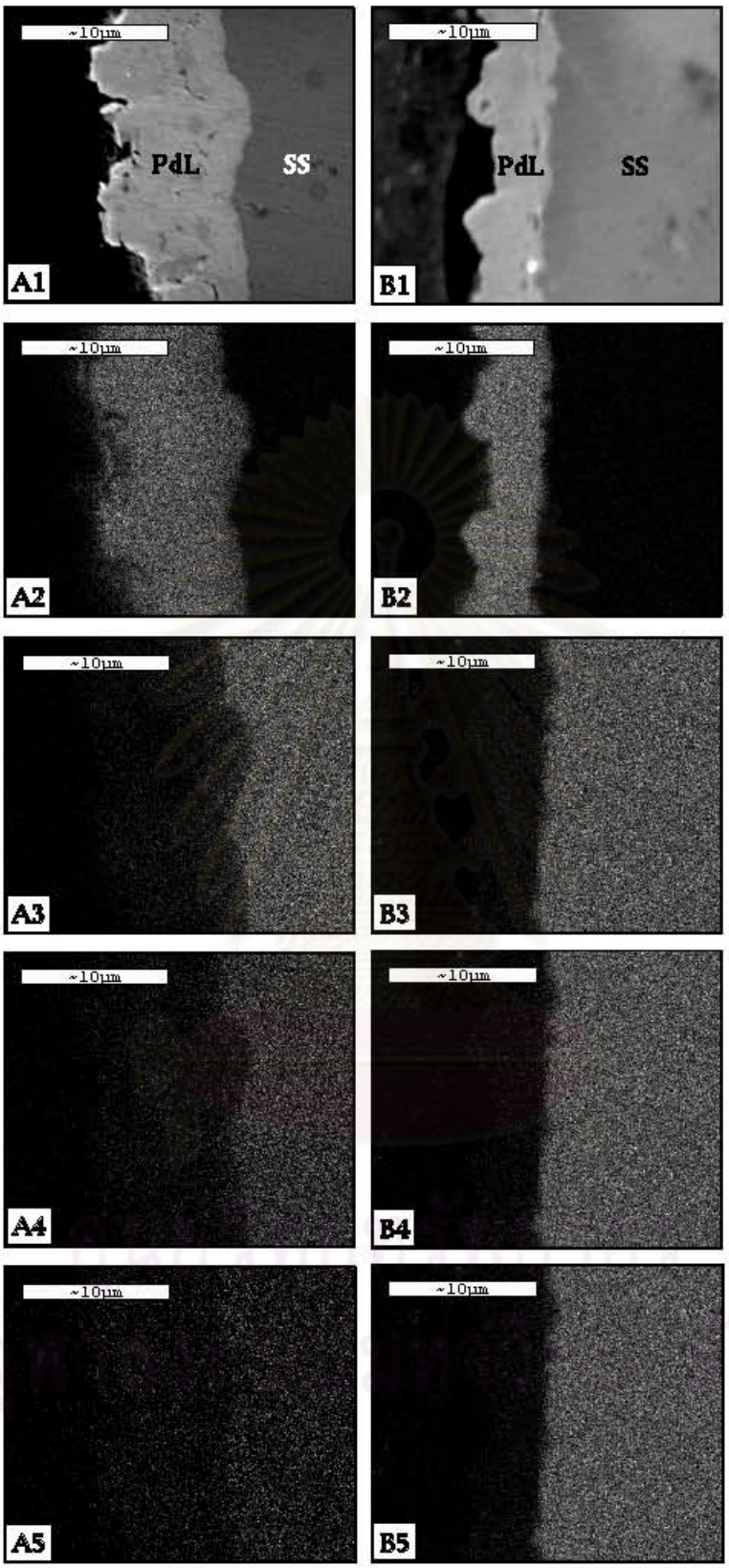

Figure 4.15 SEM micrographs (2500X) of the cross sections of palladium membrane after heating for 24 hr at 550°C. Column **A** (**A1-A5**): unoxidized, no barrier; **B** (**B1-B5**): Cr_2O_3 barrier by thermal oxidation. Metal distribution were mapped in each row: row **2** (**A2-F2**): Pd; **3** (**A3-F3**): Fe; **4** (**A4-F4**): Cr; and **5** (**A5-F5**): Ni. Arrow head: intermetallic diffusion barrier, **PdL**: Pd layer, **SS**: stainless steel.

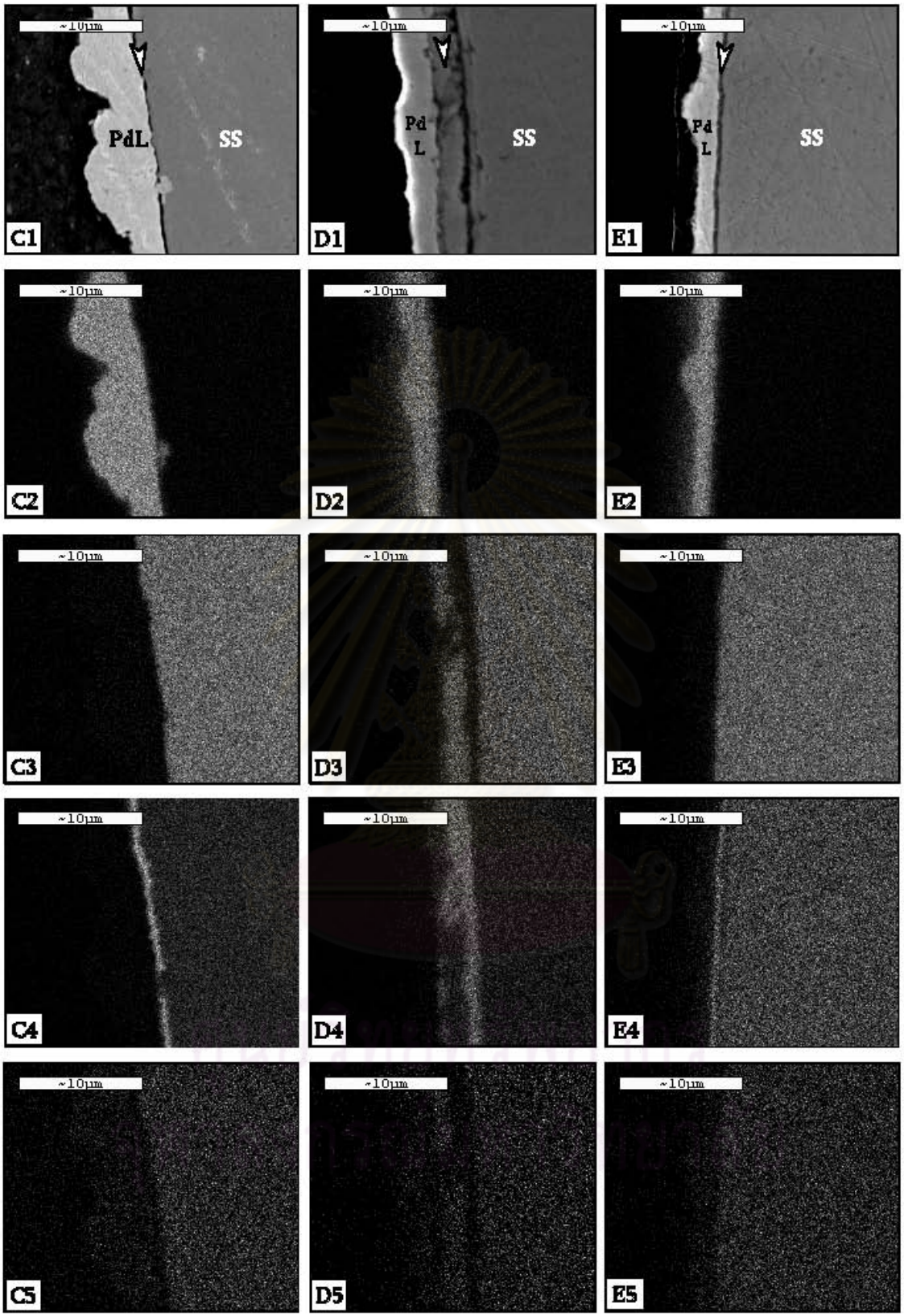

Figure 4.15 (continued) SEM micrographs (2500X) of the cross sections of palladium membrane after heating for 24 hr at 550°C. Column **C** (**C1-C5**): Cr_2O_3 barrier by Cr-electroplating/oxidation; **D** (**D1-D5**): Cr_2O_3 barrier by Cr-sputtering/oxidation; **E** (**E1-E5**): CrN barrier by sputtering. Metal distribution were mapped in each row: row **2** (**A2-F2**): Pd; **3** (**A3-F3**): Fe; **4** (**A4-F4**): Cr; and **5** (**A5-F5**): Ni. Arrow head: intermetallic diffusion barrier, **PdL**: Pd layer, **SS**: stainless steel.

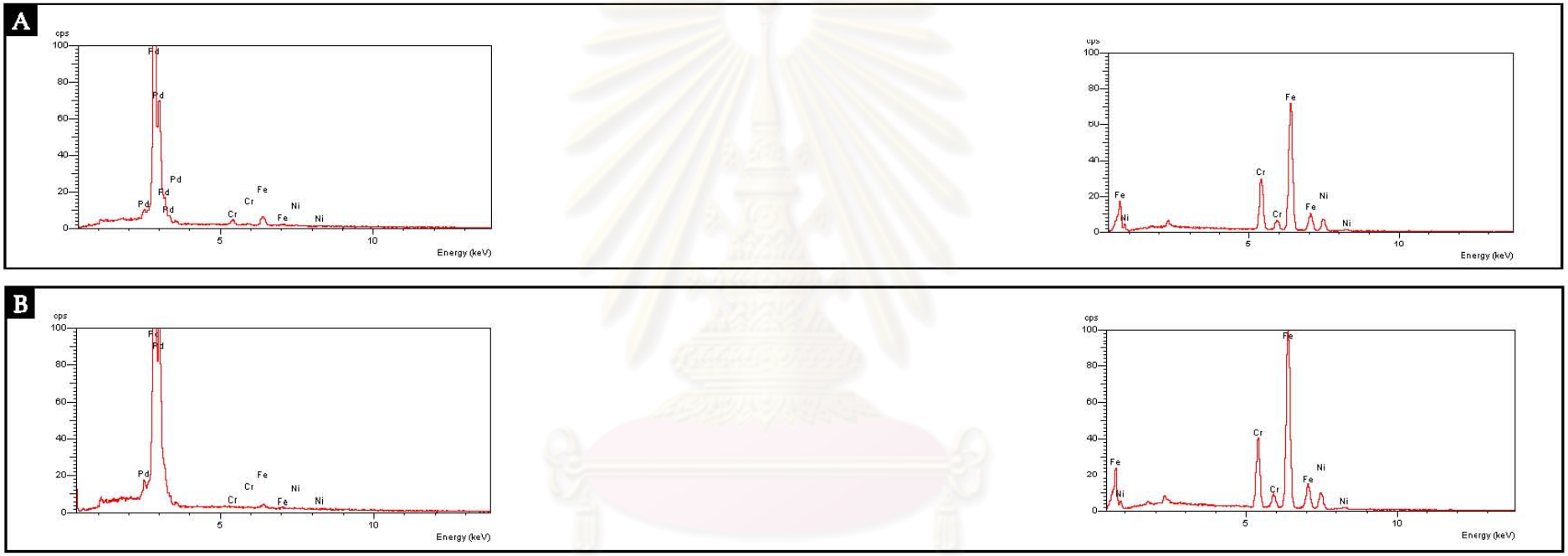

Figure 4.16 EDS spectra of the palladium membrane after heating for 24 hr at 550°C. **A**: unoxidized, no barrier; **B**: Cr_2O_3 barrier by thermal oxidation. EDS spectra of the Pd layer are shown on the left, those of the Cr-based intermetallic diffusion barrier are in the middle and those of the stainless steel support are on the right.

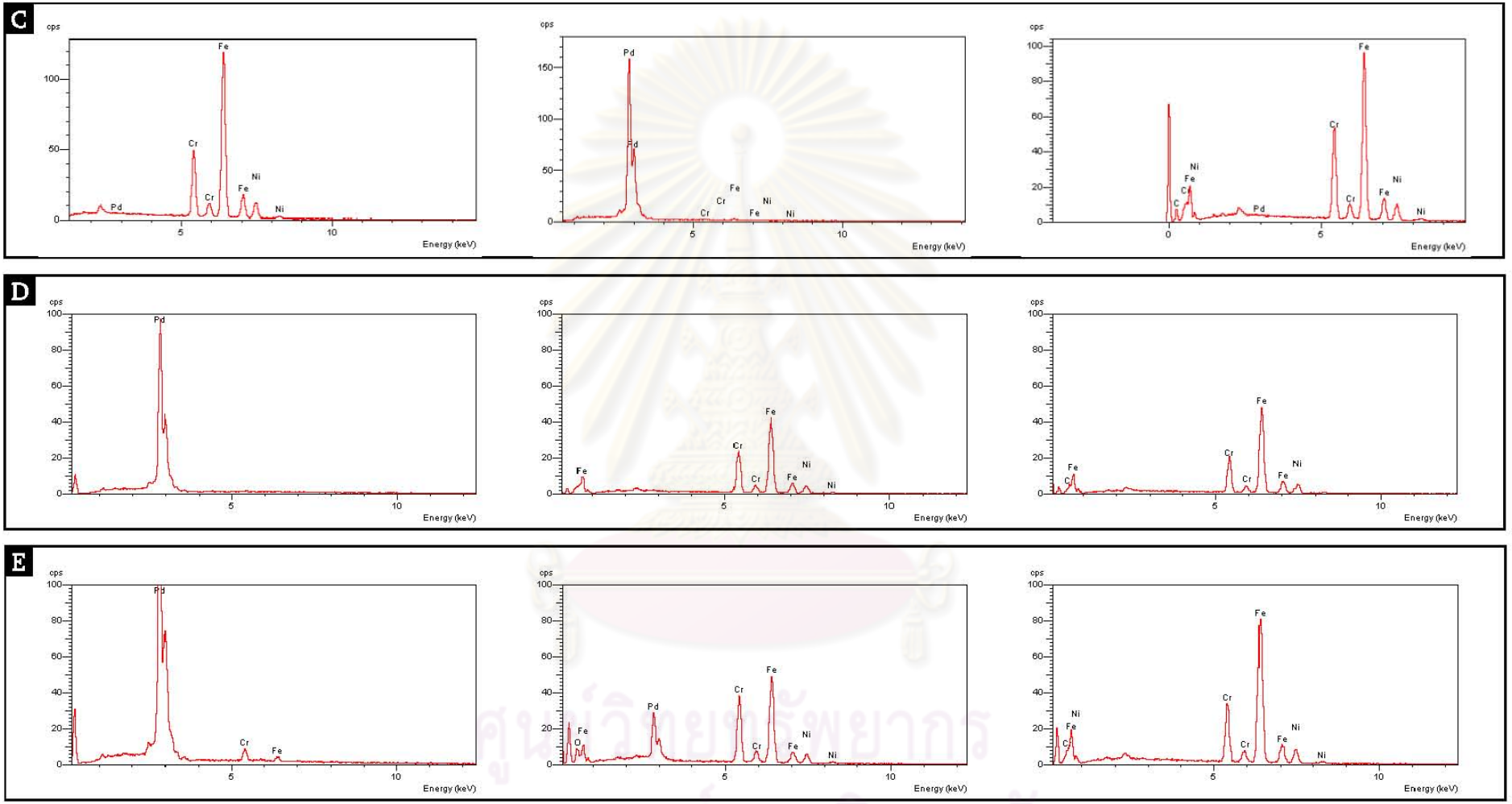

Figure 4.16 (continued) EDS spectra of the palladium membrane after heating for 24 hr at 550°C. **C**: Cr_2O_3 barrier by Cr-electroplating/oxidation; **D**: Cr_2O_3 barrier by Cr-sputtering/oxidation; **E**: CrN barrier by sputtering. EDS spectra of the Pd layer are shown on the left, those of the Cr-based intermetallic diffusion barrier are in the middle and those of the stainless steel support are on the right.

4.5 Effects of intermetallic diffusion barriers on palladium membrane morphology

The palladium layers were also melted at 500 and 550°C as revealed in Figure 4.9 by changed surface morphologies. Very little change was found at 450°C. Its trend, however, was not consistent with one another when compare with other types of support. In one case, the surface showed clumps of palladium and larger grain size but in the other meting results in finer, more even surface.

The explanations for such inconsistency do not lie in the palladium layer itself but the surface that supports them. Intermetallic diffusion barriers, to different degrees, influence how palladium atoms deposit on its support. Without doubt, different surface textures resulted in different palladium layer morphologies: smoother support surface resulted in finer, more even palladium layer surface (compare Figure 4.16IA, IB and IC). However, the chemical nature of the support surface does no small part in directing palladium membrane morphology. When compare among the finest support surfaces, i.e. the unoxidized, the Cr_2O_3-coated by oxidized Cr-sputtering and the CrN-coated, no one expects that the palladium layer was on a support of comparable level of fineness if they use the surface texture as a sole criterion.

My point in discussing this issue is not to explain why or how the two mentioned factors exert theirs influence on palladium layer morphologies. It just serves the purpose of reminding you that an effective intermetallic diffusion barrier cannot be judged alone in term of its efficacy in shielding the palladium layer. The question, Is the palladium layer still highly selective for hydrogen gas if its morphology is altered by the barrier, should be always ranked at the first place. The best intermetallic diffusion barrier in term of shielding the palladium layer could make the membrane itself the worst in term of selectivity for hydrogen gas and hence useless.

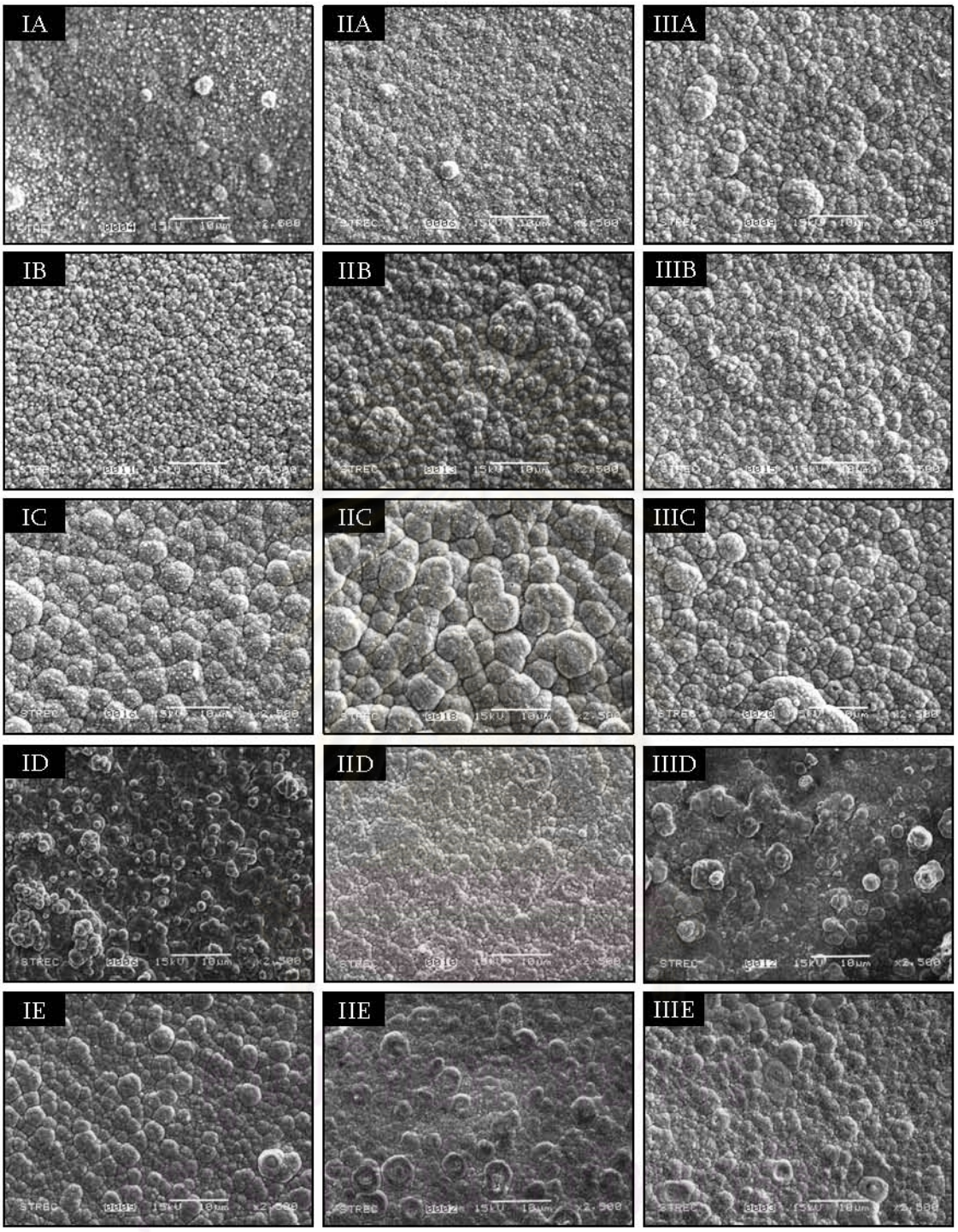

Figure 4.17 SEM micrographs (2500X) of the surface of the palladium layer on different intermetallic diffusion barrier after heating for 24 hr at 450°C (column **I**, **IA-IE**), 500°C (column **II**, **IIA-IIE**) or 550°C (column **III**, **IIIA-IIIE**). Row **A** (**IA-IIIA**): unoxidized, no barrier; **B** (**IB-IIIB**): Cr_2O_3 barrier by thermal oxidation; **C** (**IC-IIIC**): Cr_2O_3 barrier by Cr-electroplating/oxidation; **D** (**ID-IIID**): Cr_2O_3 barrier by Cr-sputtering/oxidation; **E** (**IE-IIIE**): CrN barrier by sputtering.

CHAPTER V

CONCLUSIONS AND SUGGUSTIONS

In order to extend the lifespan of the palladium membrane reactor used for the production of hydrogen gas, this study tested the efficacies in preventing intermetallic diffusion of four Cr-based films prepared by (1) direct oxidation of the stainless steel support, (2) oxidized Cr-electroplating, (3) oxidized Cr-sputtering and (4) Cr-sputtering in nitrogen atmosphere.

The most suitable condition for the oxidation step was at 600°C for 6 hours. 800°C was the upper limit of the temperature to choose from. Much more Cr was in unstable forms than in the stable Cr_2O_3 form across the range of incubation time examined. At 450°C, formation of thin film that consists almost exclusively of Cr_2O_3 can be achieved but such incubation time gave very low Cr content to be useful. Increasing the temperature to 600°C gave a better compromise between the Cr content and Cr_2O_3 content.

The film formed via direct oxidation, in spite of being extremely thin and not continuous, was more effective than the far thicker CrN film. Therefore, it can be concluded with confidence that Cr_2O_3 film is better for this function. The Cr_2O_3 film prepared by either (2) or (3) was much thicker and continuous and performed better in shielding the palladium layer.

With respect to the preparation methods of the Cr_2O_3 film, direct oxidation is not suitable due to the limited availability of Cr in the stainless steel. External source of Cr overcomes this issue. Electroplating and sputtering permitted the formation of continuous film with a range of thicknesses and the performance of the resulting films were comparable. Sputtering produced films with finer grain and was better at least in term of precision of resulting layer thickness. However, it requires expensive equipment as opposed to the general equipment setting of electroplating. To single out which one is better in term of performance of the resulting barrier, further studies that deal seriously with the barriers' thickness must be conducted.

The intermetallic diffusion barriers of all forms influence the deposition process of palladium atoms resulting in clumped, uneven surfaces of varying degrees and the properties of the membrane are, although not explicitly examined, definitely altered. Therefore, further experiments are required to fill this gap of knowledge since the best intermetallic diffusion barrier in term of shielding the palladium layer could make the membrane itself the worst in term of selectivity for hydrogen gas and hence useless.

5.1 Further Works

5.1.1 Adjust the time and temperature for the oxidation step of the Cr layer for further fine-tuning its performance.

5.1.2 Prepare Cr_2O_3 layer by Cr-reactive sputtering in oxygen atmosphere and compare its diffusion preventing efficacy with other methods.

5.1.3 Test if the selectivity of the palladium layer is altered by the intermetallic diffusion barriers.

References

[1] Lunsford, H. J. "Catalytic conversion of methane to more useful chemicals and fuels: a challenge for the 21st century". *Catalysis Today*, 63**(2000)** : 65-174.

[2] Gallucci, F.; Tosti, S.; Basile, A., Ps-Ag tubular membrane reactors for methane dry reforming: A reactive method for CO_2 consumption and H_2 production, *Journal of Membrane Science*, XX(**2007)** : xxx.

[3] Roland, D.; Hollein, V.; Kristian, D., Membrane reactors for hydrogenation and dehydrogenation processes based on supported palladium, *Journal of Molecular Catalyst*, 173**(2001)** : 135-184.

[4] Garc' la-Gabald on, M.; P'erez-Herranz, V.; Garc'la-Antón, J.; Gui'n'on, J.L., Electrochemical recovery of tin and palladium from activating solutions of the electroless plating of polymer Potentiostatic operation, *Separation and Purification Technology*, 45**(2005)** : 183-191.

[5] Adriana, D.B.; Sergio, R.D., Estanislao, A.S.; Alberto, A.C., Reforming of CH_4 with CO_2 on Pd-supported catalysts Effect of the support on the catalytic behavior, *Catalysis Today*, 107-108(**2005**) : 481-486.

[6] Sa To, I.; Takaki, M.; Arima, T.; Furuya, H.; Idemitsu, K.; Inagaki, Y.; Momoda, M.; Namekawa, T., Oxidation behavior of modified SUS316 (PNC316) stainless steel under low oxygen partial pressure, *Journal of Nuclear Materials*, 304**(2002)** : 21-28.

[7] Gustavo, V.; Kiennemann, A.; Goldwasser, M.R., Dry reforming of CH_4 over solid solution of $LaNi_{1-x}Co_xO_3$, *Catalysis Today*, xx(**2008)** : xxx-xxx.

[8] Weichun, Y.; Bo, Y.; Guiyan, C.; Liyan, D.; Chunming, W., Electrocatalytic oxidation of hydrazine compound on electroplated Pd/WO_3 film, xx **(2007)** : xxx-xxx.

[9] Surviliene, S.; Jasulaitiene, V.; Nivinskiene, O.; Cesuniene, A. Effect of hydrazine and hydroxylaminophosphate on chromeplating from trivalent electrolytes, *Applied Surface Science*, 253**(2007)** : 6738-6743.

[10] Era, H.; Ide, Y.; Nino, A.; Kishitake, K., TEM study on chromium nitride coatings deposited by reactive sputter method, *Surface & Coating Technology*, 194(2005) : 265-270.

[11] Flewitt P.E.J. and Wild R.K., PHYSICAL METHODS FOR MATERIALS CHARACTERISATION. ISBN: 0 7503 0203 8. Grear Britain : Bookcraft, 1994.

[12] Wang, P.W.; Jin-Cherng, H.; Luu-Gen H., Metallic phase formation in oxide films, *Journal of Non-crystalline Solid*, 354**(2008)** :1256-1262.

[13] Longhai, S.; Xu, S.; Sun, N.; Taimin, C.; Qiliang, Synthesis of nanocrystalline CrN by arc discharge, *Materials Letters*, 62**(2008)** : 1469-1471.

[14] Yan, H.; Roland, D., Preparation of thin palladium membranes on a porous support with rough surface, *Journal of Membrane Science*, 302(**2007)** : 160-170.

[15] Arias, D.F.; Arongo, Y.C.; Devia, A., Study of TiN and ZrN thin films grown by cathodic arc technique,*Applied Surface Science*, 253**(2006**) : 1683-1690

[16] Stefanov, P.; Stoychev, D.; Stoycheva, M.; Marinova, Ts., XPS and SEM studies of chromium oxide films chemically formed on stainless steel 316L, *Materials Chemistry and Physics*, 65**(2000)** : 212-215.

[17] Lacoste, A.; Bechu, S.; Arnal, Y.; Pelletier, J.; Gouttebaron, R., Plasma-based ion implantation of oxygen in stainless steel: influence of ion energy and dose, *Surface and Coatings Technology*, 156**(2002)** : 225-228.

[18] Huiyuan, G.; Jerry, Y.S.L.; Yongdan, L.; Baoquan Zhang., Electroless plating synthesis, characterization and permeation properties of Pd-Cu membranes supported on ZrO2 modified porous stainless steel, *Journal of Membrane Science*, 265**(2005)** : 142-152.

[19] Sabioni, A.C.S.; Huntz, A.M.; Silva, F.; Jomard, F., Diffusion of iron in Cr_2O_3: polycrystals and thin films, *Materials Science and Engineering A*, 392**(2005)** : 254-261.

[20] Huntz, A.M., Reckman A., Haut C., Severac C., Herbst M., Resende F.C.T., Sabioni., A.C.S., Oxidation of AISI 304 and AISI 439 stainless steel, *Materials Science and Engineering A*, **2007**: 266-276.

[21] Eun-Suok Oh., Kinetic and kinematic for the metal oxidation on a sphere geometry, Chemical Engineering Journal, 135(2008) : 157-167

[22] Greeff, A.P.; Swart, H.C.; Louw, C.W., The oxidation of industrial FeCrMo steel, *Corrosion Science*, 42**(2000)** : 1725-1740.

[23] De Souza, S.D.; Olzon-Dionysio, M.; Miola, E.J.; Paiva-Santo,s C.O., Plasma nitriding of sintered AISI 316L at several temperatures, *Surface and Coatings Technology*, 184**(2004**) : 176-181.

[24] Nanping, Xu.; Xue, L.; Yiqua, F.; Wanqin, J.; Yan, H.; Jun, S., Effect of EDTA on

preparation of Pd membranes by photocatalytic deposition, *Desalination*, 192**(2006)** : 177-124.

[25] Ma, L.; Gong, B., Tran, T., Wainwright, M.S., Cr2O3 promoted skeletal Cu catalysts for the reaction of methanol steam reforming and watergas shift, *Catalysis Today*, 63**(2000)** : 499-505.

[26] Navinsek, B.; Panjan, P.; Cvelbar, A., Characterization of low temperature CrN and TiN (PVD) hard coating, *Surface and Coatings Technology*, 74-75**(1995)** : 155-161.

[27] Mardilovich, I.P.; She, Y.; Ma, Y.H., Defect free palladium membrane on porous stainless steel support. 1998, *AICHE Journal*, 44(2)**(1998)** : 310-322.

[28] Keuler, J.N.; Lorenzen, L.; Sanderson, R.D.; Linkov, V., Characterization optimizing palladium conversion in electroless palladium plating of alumina membranes, *Plating and Surface Finishing*, 64**(1997)** : 215-226.

[29] Shu, J.; Grandjean, B.P.A.; Haliaguine, S., Structually stable composite Pd-Ag alloy membrane: introduction barrier, *Journal of Membrane Science*, 286**(1996)** : 72-79.

[30] Shu, J.; Adnot, A.; Grandjean, B.P.A.; Van Neste, A.; Kaliaguine, S., Simultaneous deposition of Pd and Ag on porous stainless steel by electroless plating, *Journal of Membrane Science*, 77**(1996)** : 181-195.

[31] Lee, K.H.; Num, S.E., Hydrogen separation by Pd alloy composite membranes; introduction of diffusion barrier, *Journal of Membrane Science*, 192**(2001)** : 177-185

APPENDICES

Appendix

Table 1 Operation of X-Ray photoelectron spectroscopy

No	Sample	Emss	No scan	Dwell	Step size	Lens mode
1	**Oxidized - 450°C - 4hr**					
	Eb – 1100 – 0	50	2	50	1	LAXPS
	Cr – Eb – 579 – 570	50	10	100	0.1	LAXPS
	Fe_Eb_740-700	50	5	100	0.1	LAXPS
	O_Eb_545-525	50	5	100	0.1	LAXPS
	Ni_Eb_888-848	50	20	100	0.1	LAXPS
2	**Oxidized - 450°C - 6hr**					
	Eb – 1100 – 0	50	2	50	1	LAXPS
	Cr – Eb – 579 – 570	50	10	100	0.1	LAXPS
	Fe_Eb_740-700	50	5	100	0.1	LAXPS
	O_Eb_545-525	50	5	100	0.1	LAXPS
	Ni_Eb_888-848	50	20	100	0.1	LAXPS
3	**Oxidized - 450°C - 8hr**					
	Eb – 1100 – 0	50	2	50	1	LAXPS
	Cr – Eb – 579 – 570	50	10	100	0.1	LAXPS
	Fe_Eb_740-700	50	5	100	0.1	LAXPS
	O_Eb_545-525	50	5	100	0.1	LAXPS
	Ni_Eb_888-848	50	20	100	0.1	LAXPS
4	**Oxidized - 600°C - 6hr**					
	Eb – 1100 – 0	50	2	50	1	LAXPS
	Cr – Eb – 579 – 570	50	10	100	0.1	LAXPS
	Fe_Eb_740-700	50	5	100	0.1	LAXPS
	O_Eb_545-525	50	5	100	0.1	LAXPS
	Ni_Eb_888-848	50	20	100	0.1	LAXPS
5	**Oxidized - 800°C - 4hr**					
	Eb – 1100 – 0	50	2	50	1	LAXPS
	Cr – Eb – 579 – 570	50	10	100	0.1	LAXPS
	Fe_Eb_740-700	50	5	100	0.1	LAXPS
	O_Eb_545-525	50	5	100	0.1	LAXPS
	Ni_Eb_888-848	50	20	100	0.1	LAXPS
6	**Oxidized - 800°C - 6hr**					
	Eb – 1100 – 0	50	2	50	1	LAXPS
	Cr – Eb – 579 – 570	50	10	100	0.1	LAXPS
	Fe_Eb_740-700	50	5	100	0.1	LAXPS
	O_Eb_545-525	50	5	100	0.1	LAXPS
	Ni_Eb_888-848	50	20	100	0.1	LAXPS

7	**Oxidized - 800°C - 8hr**					
	Eb – 1100 – 0	50	2	50	1	LAXPS
	Cr – Eb – 579 – 570	50	10	100	0.1	LAXPS
	Fe_Eb_740-700	50	5	100	0.1	LAXPS
	O_Eb_545-525	50	5	100	0.1	LAXPS
	Ni_Eb_888-848	50	20	100	0.1	LAXPS

Table 2 Operation of X-Ray photoelectron spectroscopy (Cons.)

No	Sample	Emss	No scan	Dwell	Step size	Lens mode
8	**Oxidized - 800°C - 12hr**	50	2	50	1	LAXPS
	Eb – 1100 – 0	50	10	100	0.1	LAXPS
	Cr – Eb – 579 – 570	50	5	100	0.1	LAXPS
	Fe_Eb_740-700	50	5	100	0.1	LAXPS
	O_Eb_545-525	50	20	100	0.1	LAXPS
	Ni_Eb_888-848					
9	**Cr Electroplsting Oxidized - 800°C - 12hr**	50	2	50	1	LAXPS
	Eb – 1100 – 0	50	10	100	0.1	LAXPS
	Cr – Eb – 579 – 570	50	5	100	0.1	LAXPS
	Fe_Eb_740-700	50	5	100	0.1	LAXPS
	O_Eb_545-525	50	20	100	0.1	LAXPS
	Ni_Eb_888-848					
10	**CrN**					
	CrN_Eb1100-O					
	CrN_Cr_ 595-570	50	20	100	0.1	LAXPS
	CrN_N ……	50	20	100	0.1	LAXPS

Table 3 shown that, elements percentage the surface of stainless steel.

Sample	Element	Area (N)			
Oxidize 450°C 4 hr	Cr2p3	32.46	Cr	=	1.5417 %
	Cr2p1	16.21	Fe	=	9.1828 %
	Cr2p3	0.44	O	=	89.2754 %
	Cr2p3	0.46			
	Fe2p1	144.42			
	Fe2p3	150.82			
	O1s	1738.96			
	O1s	1131.37			
Sample	Element	Area (N)	Cr	=	17.4273 %
Oxidize 450°C 8 hr	Fe2p1	352.35	Fe	=	1.8654 %
	Fe2p3	404.93	O	=	76.4204 %
	Fe2p3	175.16	Cr	=	4.2867 %
	Fe2p1	99.41			
	Ni2p1	55.4			
	Ni2p3	33.11			
	Ni2p1	21.94			
	O1s	2071.15			
	O1s	2453.59			
	Cr2p1	126.09			
	Cr2p3	127.72			
Sample	Element	Area (N)			
Oxidize 450°C 8 hr	Cr2p1	242.12	Cr	=	11.4900 %
	Cr2p3	273.56	Fe	=	7.8710 %
	Cr2p1	5.13	O	=	80.6389 %
	Fe2p1	151.44			
	Fe2p3	205.33			
	O1s	2945.55			
	O1s	709.58			
Sample	Element	Area (N)			
Oxidize 600°C 6 hr	Cr2p1	444.69			
	Cr2p3	434.15	Cr	=	15.1721 %
	Cr2p3	67.45	Fe	=	7.1030 %
	Fe2p1	107.6	O	=	77.7248 %
	Fe2p3	216.34			
	Fe2p1	119.08			
	O1s	4132.61			
	O1s	715.12			

Sample	Element	Area (N)			
Oxidize 800°C 4 hr	Cr2p1	369.36	Cr	=	21.7084 %
	Cr2p3	419.36	Fe	=	10.0927 %
	Cr2p1	110.57	O	=	68.1988 %
	Cr2p3	138.02			
	Fe2p1	284.63			
	Fe2p3	197.64			
	O1s	2271.92			
	O1s	986.88			
Sample	Element	Area (N)	Cr	=	11.1356 %
Oxidize 800°C 6 hr	Cr2p1	191.61	Fe	=	18.7105 %
	Cr2p3	289.56	O	=	70.1538 %
	Cr2p1	17.73			
	Fe2p1	337.57			
	Fe2p3	299.04			
	Fe2p1	103.95			
	Fe2p3	97.71			
	O1s	2626.37			
	O1s	516.67			
Sample	Element	Area (N)	Cr	=	16.9307 %
Oxidize 800°C 8 hr	Cr2p1	383.44	Fe	=	8.4709 %
	Cr2p3	325.8	O	=	74.5982 %
	Cr2p3	66.91			
	Fe2p1	177.19			
	Fe2p3	211.14			
	O1s	1946.94			
	O1s	1472.83			
Sample	Element	Area (N)	Cr	=	7.9363 %
Oxidize 800°C 12 hr Non Coat Chromium by electro plating	Cr2p1	116.03	Fe	=	16.2153 %
	Cr2p3	150.09	O	=	75.8482 %
	Cr2p1	1.68			
	Cr2p1	1.17			
	Fe2p1	251.22			
	Fe2p3	298.33			
	O1s	1442.2			
	O1s	1128.35			
Sample	Element	Area (N)	Cr	=	23.5114 %
Oxidize 800°C 12 hr Coat Chromium by electro plating	Fe2p1	256.57	Fe	=	11.5552 %
	Fe2p3	214.04	O	=	64.9333 %
	O1s	1855.3			
	O1s	789.24			
	Cr2p1	466.95			
	Cr2p3	490.6			

Sample	Element	Area (N)
CrN	Cr1p1	2997.06
	Cr2p3	679.27
	Cr2p3	342.28
	N1s	1130.57
	N1s	210.28

Cr = 74.9816 %
N = 25.0183 %

Table 4 relationship between binding energy (eV) and residuals for Cr 450°C 4 hr

Binding energy	Residuals	Binding energy	Residuals	Binding energy	Residuals	Binding energy	Residuals	Binding energy	Residuals
595	14200.5	589.7	13589.4	584.4	13391.9	579.1	13619.9	573.8	13105.1
594.9	13927.2	589.6	13732.6	584.3	13376.6	579	13680.9	573.7	12916.9
594.8	13921.6	589.5	13780.4	584.2	13235	578.9	13656.6	573.6	13138.5
594.7	14239.1	589.4	13808	584.1	13307.9	578.8	13704.4	573.5	13137
594.6	14043.5	589.3	13708.4	584	13359.9	578.7	13884	573.4	12913.2
594.5	13920	589.2	13740.3	583.9	13204	578.6	13949.6	573.3	12947.5
594.4	13935.3	589.1	13668.5	583.8	13271.1	578.5	13911.7	573.2	13136.7
594.3	13776.4	589	13714.1	583.7	13416.6	578.4	13805.5	573.1	13165.4
594.2	13985.7	588.9	13957.5	583.6	13391	578.3	13790.9	573	12982.6
594.1	13932.9	588.8	13757.8	583.5	13512.6	578.2	13773.3	572.9	12971.1
594	14016.4	588.7	13810.9	583.4	13385.7	578.1	13724.8	572.8	12835.4
593.9	13832.7	588.6	13801.8	583.3	13429.3	578	13618.4	572.7	13041.7
593.8	13784	588.5	13783.7	583.2	13257	577.9	13898.5	572.6	13051.4
593.7	13830.9	588.4	13791.5	583.1	13192.1	577.8	13927.1	572.5	13026.4
593.6	13954.5	588.3	13771.8	583	13256.2	577.7	13964.5	572.4	12927.4
593.5	13882.9	588.2	13656.7	582.9	13261.2	577.6	14102.5	572.3	12965.4
593.4	13950.1	588.1	13687.4	582.8	13222.6	577.5	13999.5	572.2	12990.8
593.3	13875.3	588	13814.9	582.7	13182.6	577.4	13818.4	572.1	12937.2
593.2	13756.5	587.9	13897.5	582.6	13299.9	577.3	13760.8	572	12795.6
593.1	13788.3	587.8	13746.2	582.5	13212.5	577.2	13769.4	571.9	12904.7
593	13736.4	587.7	13826.8	582.4	13320.7	577.1	13697.4	571.8	13000
592.9	13753.8	587.6	13696.3	582.3	13431.4	577	13705.4	571.7	13057.1
592.8	13781.9	587.5	13673.7	582.2	13550.4	576.9	13571.4	571.6	12945.3
592.7	13802.1	587.4	13806.3	582.1	13311	576.8	13574.9	571.5	12889.9
592.6	13788.9	587.3	13814.1	582	13189.5	576.7	13662.4	571.4	12882.4
592.5	13703.5	587.2	13726.1	581.9	13173.9	576.6	13586	571.3	12945.7
592.4	13692.2	587.1	13754.3	581.8	13386.8	576.5	13558.4	571.2	12942
592.3	13721.8	587	13752.2	581.7	13376.7	576.4	13559.3	571.1	12873.4
592.2	13810.6	586.9	13695.7	581.6	13315.2	576.3	13402.7	571	12936.7
592.1	13884.2	586.8	13584.9	581.5	13353.1	576.2	13358.9	570.9	12948.9
592	13805.8	586.7	13597.3	581.4	13426.2	576.1	13187.3	570.8	12805.3
591.9	13734.4	586.6	13507.2	581.3	13444.8	576	13279.8	570.7	12886.6
591.8	13806	586.5	13628.4	581.2	13305.9	575.9	13227	570.6	12673.2
591.7	13765.1	586.4	13520	581.1	13253.7	575.8	13292.6	570.5	12772.1
591.6	13725.2	586.3	13661.5	581	13218.4	575.7	13368.9	570.4	12735.1
591.5	13836.3	586.2	13560.5	580.9	13273.4	575.6	13234.8	570.3	12880
591.4	13656.1	586.1	13362.5	580.8	13352.1	575.5	13109.5	570.2	12820.1
591.3	13819.4	586	13519.4	580.7	13399.1	575.4	13294.8	570.1	12708.4
591.2	13750.2	585.9	13423	580.6	13306.9	575.3	13184.1	570	12752.3
591.1	13624.6	585.8	13385	580.5	13354.5	575.2	13209.7	573.8	13105.1
591	13808.3	585.7	13391.2	580.4	13313.5	575.1	13122.2		
590.9	13860.1	585.6	13415.5	580.3	13350.9	575	13168.4		
590.8	13642.6	585.5	13367.4	580.2	13422.9	574.9	12917.9		
590.7	13772.5	585.4	13526.3	580.1	13506.9	574.8	13168.4		
590.6	13909	585.3	13380.6	580	13516.5	574.7	12980.3		
590.5	13668.9	585.2	13365.9	579.9	13611.6	574.6	13123.4		
590.4	13677.3	585.1	13437	579.8	13516	574.5	13022.8		
590.3	13668.3	585	13310.1	579.7	13555.8	574.4	13091.2		
590.2	13627.6	584.9	13332.4	579.6	13572.5	574.3	13082.4		
590.1	13784.1	584.8	13330.4	579.5	13602	574.2	13106.1		
590	13786.6	584.7	13371.9	579.4	13571.1	574.1	12909		
589.9	13818.6	584.6	13321.7	579.3	13535.8	574	13118.9		
589.8	13684.3	584.5	13348.9	579.2	13795.7	573.9	13051.4		

Table 5 relationship between binding energy (eV) and residuals for Fe 450°C, 4 hr

Binding energy	Residuals	Binding energy	Residuals	Binding energy	Residuals	Binding energy	Residuals	Binding energy	Residuals
740	32435.7	734.7	28867.5	729.4	27442.3	724.1	27290.8	718.8	25224.3
739.9	32489	734.6	28688.7	729.3	27397.8	724	27180.6	718.7	25345.3
739.8	32268.1	734.5	28633.3	729.2	27085.9	723.9	26874.1	718.6	25553
739.7	32130.6	734.4	28649.3	729.1	27067.8	723.8	26893.6	718.5	25444
739.6	32034.4	734.3	28764.3	729	27093.9	723.7	26807.8	718.4	25281.4
739.5	31666.3	734.2	28280.2	728.9	27052.9	723.6	26754.8	718.3	25300.6
739.4	31882.9	734.1	28159.4	728.8	27372.3	723.5	26835	718.2	25353.4
739.3	31756.6	734	28103.7	728.7	27060.7	723.4	26772.6	718.1	25239.2
739.2	31638.7	733.9	28194.2	728.6	26707.1	723.3	26336.9	718	25454.9
739.1	31947	733.8	28302.3	728.5	26963.7	723.2	26099.9	717.9	25417.8
739	31511.8	733.7	28099.1	728.4	26794.6	723.1	26248.8	717.8	25264.5
738.9	31567.6	733.6	27968.7	728.3	27156.3	723	26233.8	717.7	25149
738.8	31290.3	733.5	28090.5	728.2	27287.4	722.9	26129.4	717.6	25121.7
738.7	30930.2	733.4	28262.4	728.1	27260.9	722.8	26257.7	717.5	25017.8
738.6	31023.9	733.3	28039.6	728	27224.3	722.7	25864.2	717.4	25169.5
738.5	30909.8	733.2	27928.6	727.9	26902.5	722.6	25957.1	717.3	25076
738.4	30772.1	733.1	27730.3	727.8	27214.5	722.5	25979.3	717.2	25169.3
738.3	30966.5	733	28181.6	727.7	27273.4	722.4	26011.2	717.1	25241
738.2	30565.7	732.9	28079.4	727.6	27240.8	722.3	26046.6	717	25452.8
738.1	30504.5	732.8	27376.3	727.5	27307.6	722.2	26045.7	716.9	25148.2
738	30262.2	732.7	27620.5	727.4	27213.7	722.1	25965	716.8	25140.3
737.9	30416.5	732.6	27866.5	727.3	27255.6	722	25616.1	716.7	25428.2
737.8	30636.8	732.5	27607.2	727.2	27455.3	721.9	25509.3	716.6	25167.8
737.7	30408.8	732.4	27944.2	727.1	27157.1	721.8	25577.2	716.5	25131.8
737.6	30178.9	732.3	27769.3	727	27899.8	721.7	25748.5	716.4	25017.7
737.5	29889.8	732.2	27434.8	726.9	27786.8	721.6	25360.8	716.3	25212
737.4	29514.1	732.1	27231.2	726.8	27534.8	721.5	25605.7	716.2	25237.6
737.3	29632.8	732	27386.2	726.7	27631.9	721.4	25580.5	716.1	25399.8
737.2	29902.6	731.9	27455.5	726.6	27508.8	721.3	25686.5	716	25573.8
737.1	29638.9	731.8	27379.6	726.5	27265.6	721.2	25843.6	715.9	25386.5
737	29257.4	731.7	27584.4	726.4	27363.8	721.1	25796.7	715.8	25178.7
736.9	29810.7	731.6	27664	726.3	27529.5	721	25580.2	715.7	25214.3
736.8	29586.3	731.5	27420.6	726.2	27444.7	720.9	25249.6	715.6	25254.2
736.7	29560.5	731.4	27319.2	726.1	27665.6	720.8	25402.5	715.5	25585.2
736.6	29293.3	731.3	27367.1	726	27719.7	720.7	25308	715.4	25263.4
736.5	29308.9	731.2	26979.5	725.9	27948.7	720.6	25546.6	715.3	25273.9
736.4	29491.6	731.1	27362.2	725.8	27483.3	720.5	25453.7	715.2	25624.3
736.3	29308.1	731	27729.9	725.7	27666.6	720.4	25550.6	715.1	25345.5
736.2	29252.8	730.9	27242.5	725.6	27588.2	720.3	25819.5	715	25482.4
736.1	29056.4	730.8	27017.7	725.5	27563.7	720.2	25915.2	714.9	25174.3
736	29414.6	730.7	27104.5	725.4	27422	720.1	25648.4	714.8	25731
735.9	29213	730.6	27152.7	725.3	27708.2	720	25637.4	714.7	25935.1
735.8	29092	730.5	27052.9	725.2	27539.7	719.9	25579.2	714.6	25664.1
735.7	28880	730.4	27228.2	725.1	27573.4	719.8	25477.3	714.5	25496.3
735.6	28759.1	730.3	27171.8	725	27784.5	719.7	25224.7	714.4	26009.6
735.5	29020.1	730.2	27059.9	724.9	27574.3	719.6	25333.6	714.3	26071.1
735.4	28925.7	730.1	27136.1	724.8	27820.8	719.5	25641.6	714.2	26388.6
735.3	28990.8	730	27429.8	724.7	27667.8	719.4	25549.4	714.1	26078.1
735.2	28993.3	729.9	27465.9	724.6	27476	719.3	25363.1	714	26148.5
735.1	28526.1	729.8	27237.3	724.5	27760.4	719.2	25435.1	713.9	26161.3
735	28325.8	729.7	26739.9	724.4	27378.6	719.1	25444	713.8	26170
734.9	28672.6	729.6	27137.1	724.3	27389.8	719	25532.7	713.7	26060.3
734.8	28627	729.5	27526.3	724.2	27341.6	718.9	25654.8	713.6	26280.4

Table 5 (continued) relationship between binding energy (eV) and residuals for Fe 450°C, 4 hr cons.

Binding energy	Residuals	Binding energy	Residuals	Binding energy	Residuals
713.5	26474.9	708.2	22815.7	703	22312.1
713.4	26142.7	708.1	22330.8	702.9	22517
713.3	26437.7	708	22557.7	702.8	22635.8
713.2	26690.6	707.9	22501.8	702.7	22535.6
713.1	26435.3	707.8	22367.3	702.6	22537.9
713	26605	707.7	22626.6	702.5	22378.5
712.9	26798.2	707.6	22594.3	702.4	22376.8
712.8	26981.4	707.5	22515.8	702.3	22478.6
712.7	26909.7	707.4	22673.5	702.2	22372.6
712.6	26823.1	707.3	22614.2	702.1	22338.5
712.5	27335.8	707.2	22473.5	702	22387.8
712.4	27451.5	707.1	22489.7	701.9	22053.4
712.3	26946.6	707	22200.5	701.8	22123.9
712.2	26989.4	706.9	22274.8	701.7	22351.8
712.1	27001	706.8	22626.2	701.6	22343.6
712	27108.3	706.7	22535.2	701.5	22216.3
711.9	27333.8	706.6	22420.2	701.4	22096.8
711.8	27321.4	706.5	22526.9	701.3	22048.9
711.7	27041.1	706.4	22403.2	701.2	22149.3
711.6	27334.5	706.3	22616.1	701.1	22131.9
711.5	27101.7	706.2	22265.6	701	22299.9
711.4	27200.3	706.1	22337.8	700.9	22206.4
711.3	27301.9	706	22647.7	700.8	22054.1
711.2	27324.3	705.9	22687.7	700.7	22164.9
711.1	26512.7	705.8	22591.9	700.6	22326.7
711	26421.4	705.7	22319	700.5	22240.2
710.9	26635.5	705.6	22400.4	700.4	21995.3
710.8	26747.7	705.5	22510.7	700.3	22001
710.7	26552.5	705.4	22462.9	700.2	22159.2
710.6	26431.8	705.3	22632.4	700.1	21980.9
710.5	26289.9	705.2	22620.2	700	21939.1
710.4	26112.9	705.1	22595.3		
710.3	25754.5	705	22372.5		
710.2	25405.4	704.9	22372.4		
710.1	25530.2	704.8	22450.5		
710	24941.9	704.7	22424.6		
709.9	24647	704.6	22724.6		
709.8	24693.8	704.5	22505.3		
709.7	24740	704.4	22163.7		
709.6	24621.6	704.3	22469.2		
709.5	24101.3	704.2	22438.1		
709.4	23703.3	704.1	22665.8		
709.3	23718	704	22511.6		
709.2	23340.9	703.9	22416.8		
709.1	23504.2	703.8	22371.8		
709	23882.1	703.7	22350.4		
708.9	23033.2	703.6	22565.9		
708.8	22943.3	703.5	22737.5		
708.7	22796.3	703.4	22709.8		
708.6	22516.8	703.3	22825.6		
708.5	22652.8	703.2	22610		
708.4	22457	703.1	22311.6		
708.3	22992.8	708.2	22815.7		

Table 6 relationship between binding energy (eV) and residuals for Cr 450°C, 6 hr.

Binding energy	Residuals	Binding energy	Residuals	Binding energy	Residuals	Binding energy	Residuals	Binding energy	Residuals
595	26044.1	589.7	25614.1	584.4	24226.5	579.1	25233.7	573.8	23507.4
594.9	26137.8	589.6	25424.7	584.3	24036.6	579	25306.2	573.7	23484.8
594.8	26355	589.5	25528.7	584.2	24197.5	578.9	25523.2	573.6	23539.8
594.7	26222.2	589.4	25632.1	584.1	24264.5	578.8	25352.3	573.5	23676.9
594.6	26027.6	589.3	25478.1	584	24135.9	578.7	25481.8	573.4	23863.8
594.5	25923.3	589.2	25664.2	583.9	24244	578.6	25638.6	573.3	23797.6
594.4	25821.5	589.1	25711.5	583.8	24520.4	578.5	25727.4	573.2	23652.7
594.3	26011.5	589	25595	583.7	24069.3	578.4	25800.4	573.1	23607.6
594.2	25809.4	588.9	25561.9	583.6	24259.6	578.3	25756.9	573	23632.2
594.1	25807.1	588.8	25432.8	583.5	24117.8	578.2	25561.7	572.9	23772.6
594	25748.7	588.7	25638.5	583.4	24071.3	578.1	25838.7	572.8	23504.2
593.9	25892.7	588.6	25589.7	583.3	24129.6	578	25578.8	572.7	23586.7
593.8	25889.4	588.5	25694	583.2	24319.4	577.9	25984.7	572.6	23416.4
593.7	25849.6	588.4	25597.8	583.1	24197.5	577.8	25997.1	572.5	23493.7
593.6	25790.4	588.3	25604.5	583	24091.8	577.7	25885.1	572.4	23522.1
593.5	25864	588.2	25647.8	582.9	24150.1	577.6	25903.1	572.3	23778.5
593.4	25697	588.1	25476.7	582.8	24158.7	577.5	26043.5	572.2	23502.1
593.3	25621.6	588	25448.6	582.7	24000.4	577.4	25785.7	572.1	23360.9
593.2	25443.2	587.9	25514.9	582.6	24182.2	577.3	25363.4	572	23550.6
593.1	25671.1	587.8	25780.9	582.5	24101.9	577.2	25499.7	571.9	23278.4
593	25783.1	587.7	25625.9	582.4	24136.2	577.1	25492.2	571.8	23472.7
592.9	25742.7	587.6	25553.6	582.3	24175.8	577	25347	571.7	23433.7
592.8	25537.7	587.5	25552.1	582.2	24133	576.9	25363.6	571.6	23580.1
592.7	25692.5	587.4	25242.4	582.1	24283	576.8	25478.5	571.5	23375.1
592.6	25684.5	587.3	25361.5	582	24206.4	576.7	25334.1	571.4	23494.1
592.5	25742.7	587.2	25391.1	581.9	24259.9	576.6	25165.8	571.3	23491.5
592.4	25844.3	587.1	25512.7	581.8	24246.8	576.5	25130.7	571.2	23347.9
592.3	25642.6	587	25283.7	581.7	24256.3	576.4	24817.6	571.1	23200.7
592.2	25709.4	586.9	25455.3	581.6	24274.3	576.3	24634.3	571	23287.1
592.1	25616.4	586.8	25391.4	581.5	24432.7	576.2	24684.4	570.9	23389
592	25683.6	586.7	25180	581.4	24505.6	576.1	24471.2	570.8	23555.8
591.9	25683.5	586.6	25148.9	581.3	24478.6	576	24564.4	570.7	23670.2
591.8	25452.3	586.5	24978.7	581.2	24381.5	575.9	24487.6	570.6	23470.5
591.7	25181.1	586.4	24668.8	581.1	24338.9	575.8	24345.5	570.5	23309.2
591.6	25354.2	586.3	24848.3	581	24274.1	575.7	24474.9	570.4	23233.2
591.5	25569.8	586.2	24714.2	580.9	24325.3	575.6	24438.1	570.3	23247.5
591.4	25438.7	586.1	24878.3	580.8	24495.9	575.5	23941.9	570.2	23304
591.3	25646.5	586	25079.2	580.7	24337.9	575.4	24016	570.1	23417.2
591.2	25582.6	585.9	24847.1	580.6	24317	575.3	23912.1	570	23317.2
591.1	25535.3	585.8	24712.1	580.5	24526	575.2	24021		
591	25221.3	585.7	24394.5	580.4	24568.7	575.1	23927.1		
590.9	25464.2	585.6	24459.6	580.3	24659.8	575	23971.6		
590.8	25484.6	585.5	24725.6	580.2	24606.2	574.9	23801.4		
590.7	25323.9	585.4	24517.6	580.1	24885.8	574.8	23893.6		
590.6	25517.5	585.3	24526.1	580	24858.9	574.7	23768.7		
590.5	25589.4	585.2	24525.3	579.9	24884.3	574.6	23658.1		
590.4	25402.5	585.1	24407.7	579.8	24785.2	574.5	23941.6		
590.3	25300.9	585	24345.1	579.7	24736.8	574.4	23834.3		
590.2	25477.5	584.9	24516.9	579.6	25011.7	574.3	23750.4		
590.1	25480.1	584.8	24206	579.5	24978.5	574.2	23588.3		
590	25474.4	584.7	24231.2	579.4	25064.3	574.1	23667.7		
589.9	25349.7	584.6	24368.9	579.3	25197.1	574	23656.7		
589.8	25426.3	584.5	24406.8	579.2	25243.8	573.9	23555.3		

Table 7 relationship between binding energy (eV) and residuals for Fe 450°C, 6 hr

Binding energy	Residuals	Binding energy	Residuals	Binding energy	Residuals	Binding energy	Residuals	Binding energy	Residuals
740	69903.4	734.7	62164.6	729.4	59091.4	724.1	60025.3	718.8	55554
739.9	69685	734.6	62494.7	729.3	58985.2	724	59587.1	718.7	55060.1
739.8	69418.6	734.5	61874.7	729.2	58923.5	723.9	59792.7	718.6	54989.3
739.7	69670.1	734.4	61862.9	729.1	58487.2	723.8	59597.5	718.5	54518.3
739.6	68965.6	734.3	62310.9	729	58712.4	723.7	59887.1	718.4	54572.3
739.5	68379.6	734.2	61907	728.9	58941.2	723.6	58849.7	718.3	54809.5
739.4	68001.5	734.1	61342.1	728.8	59362	723.5	58481.9	718.2	54862
739.3	68448.5	734	61741.2	728.7	59062.9	723.4	58171.4	718.1	54296
739.2	67881.5	733.9	61861.4	728.6	58576.9	723.3	58240.7	718	54315.3
739.1	67401.4	733.8	61806.2	728.5	59224.2	723.2	58357.1	717.9	54370.6
739	67150.5	733.7	61326.4	728.4	58540.4	723.1	57956.1	717.8	54659.4
738.9	67017.4	733.6	61481.3	728.3	58865.4	723	57716.9	717.7	54238.7
738.8	66998.9	733.5	61614.1	728.2	59309.5	722.9	57491.9	717.6	54482.9
738.7	66521.5	733.4	60847.2	728.1	59093.4	722.8	57185.6	717.5	54068
738.6	66308.6	733.3	61001	728	59324.2	722.7	56936.5	717.4	54381.7
738.5	66113.6	733.2	60767	727.9	59614.1	722.6	56655.8	717.3	54112.8
738.4	65866.4	733.1	60951.8	727.8	59475	722.5	57482.3	717.2	54729.8
738.3	65759	733	60932.1	727.7	59150.8	722.4	56279.2	717.1	54555.1
738.2	65608.3	732.9	60780.5	727.6	59173.4	722.3	56532	717	53856.4
738.1	65245.8	732.8	60811.9	727.5	59422.3	722.2	56214.9	716.9	53971.4
738	65665.5	732.7	60630.7	727.4	59699.9	722.1	56116.8	716.8	54194.4
737.9	64795.8	732.6	60285.4	727.3	59948.1	722	56369.2	716.7	54375.9
737.8	64522.6	732.5	60072	727.2	59815.9	721.9	56080.8	716.6	54375.2
737.7	64660.7	732.4	60106.2	727.1	60227.5	721.8	55588.1	716.5	53985.4
737.6	64385.7	732.3	59914.4	727	59998.8	721.7	55257.2	716.4	54207.3
737.5	64426.3	732.2	59725.7	726.9	59685.4	721.6	54848.6	716.3	54282.1
737.4	64216.4	732.1	59841.2	726.8	60201.1	721.5	55614	716.2	54503.7
737.3	63966.8	732	60291.2	726.7	60717.4	721.4	55673.6	716.1	54290.9
737.2	63933	731.9	59819.6	726.6	60526.1	721.3	54933.3	716	54422.2
737.1	63633.7	731.8	59660.8	726.5	60303.7	721.2	55587.8	715.9	54826.8
737	63550.7	731.7	59379.1	726.4	60289.3	721.1	55535.5	715.8	54631.8
736.9	63851.1	731.6	59400.8	726.3	60520.7	721	55585	715.7	54827.3
736.8	63658.3	731.5	59580.7	726.2	60603.7	720.9	54875	715.6	54981.2
736.7	63754.7	731.4	59824.5	726.1	60562.9	720.8	54985.8	715.5	54826.9
736.6	63010.8	731.3	59697.7	726	60519	720.7	55046.2	715.4	54461
736.5	62501.9	731.2	59529.2	725.9	60320.7	720.6	55484.7	715.3	55326.7
736.4	63074	731.1	59906.3	725.8	60701.9	720.5	55698	715.2	55520
736.3	62695.9	731	59206.9	725.7	60910	720.4	55345	715.1	55412.6
736.2	62616.1	730.9	58787.6	725.6	60648.8	720.3	55795.7	715	55473.4
736.1	62458.8	730.8	58785.2	725.5	61077.4	720.2	55777.4	714.9	55578.8
736	62854.2	730.7	58698	725.4	61263.3	720.1	55446.9	714.8	55476.7
735.9	62314.3	730.6	58999.4	725.3	60999	720	55737.8	714.7	55242.1
735.8	62658.3	730.5	59190.2	725.2	61173.2	719.9	55605.4	714.6	55465.1
735.7	62797.1	730.4	58919.2	725.1	60912.2	719.8	56221.9	714.5	56024.5
735.6	62677.2	730.3	58521.7	725	60701.4	719.7	55871.3	714.4	56169.7
735.5	62639.4	730.2	58632.8	724.9	60464.5	719.6	55384.3	714.3	56510.5
735.4	62465.9	730.1	58384.5	724.8	60693.4	719.5	55138.2	714.2	56085
735.3	62263.7	730	58559.4	724.7	60432.6	719.4	55223.4	714.1	56991
735.2	62318.1	729.9	58768	724.6	60780.2	719.3	55388	714	57250.1
735.1	62183.8	729.8	58867.5	724.5	60092.6	719.2	55526.3	713.9	56901.8
735	61665.5	729.7	59398.3	724.4	60606.5	719.1	55443.4	713.8	56704.5
734.9	61956.1	729.6	58957.7	724.3	60504.8	719	55195.5	713.7	57305.3
734.8	61766.1	729.5	58928.8	724.2	60014	718.9	55194.2	713.6	57402.8

Table 7 (continued) relationship between binding energy (eV) and residuals for Fe 450°C, 6 hr.

Binding energy	Residuals	Binding energy	Residuals	Binding energy	Residuals
713.5	57345.1	708.2	47182.9	702.9	46781.2
713.4	57774.7	708.1	47448.7	702.8	46383.6
713.3	58014	708	46812.5	702.7	46299.4
713.2	58146.2	707.9	47112.5	702.6	46502.9
713.1	58222	707.8	46844.9	702.5	46714.4
713	58111.1	707.7	47102	702.4	46661.3
712.9	58589.9	707.6	46629.4	702.3	46717.8
712.8	58940.3	707.5	46278.3	702.2	46392.4
712.7	59689	707.4	46490.8	702.1	46269.1
712.6	59373.1	707.3	46936.5	702	46548.3
712.5	59763.4	707.2	47057.8	701.9	46876.2
712.4	59890.2	707.1	46564.5	701.8	46460.2
712.3	60135.6	707	46789.5	701.7	45825.9
712.2	60141.9	706.9	46782.2	701.6	46150.8
712.1	60283.3	706.8	46687	701.5	46208.7
712	60348.1	706.7	46759.6	701.4	46087
711.9	59919.1	706.6	46600.9	701.3	45867.3
711.8	60941.1	706.5	46618.1	701.2	46351.6
711.7	60847.9	706.4	47101.9	701.1	46239.9
711.6	61119.4	706.3	46595.8	701	45873.2
711.5	60903.2	706.2	46255	700.9	45938.6
711.4	60612.1	706.1	46369.8	700.8	46225.7
711.3	60917.4	706	47050	700.7	46025.5
711.2	60895	705.9	47167.3	700.6	45575.1
711.1	60561.9	705.8	47061.1	700.5	45666.4
711	60485.3	705.7	46954.4	700.4	45298
710.9	60217.1	705.6	47090.4	700.3	45639.2
710.8	59383.3	705.5	46735.9	700.2	45505.7
710.7	59079	705.4	46210.6	700.1	45542.3
710.6	58826.9	705.3	46469.3	700	45241
710.5	58279.6	705.2	46589.6		
710.4	57901.8	705.1	46512.9		
710.3	57269.2	705	46955.6		
710.2	56887.6	704.9	46500.3		
710.1	56158.2	704.8	46591.1		
710	55384.2	704.7	46545.8		
709.9	54791.4	704.6	46793.8		
709.8	54078.3	704.5	46675		
709.7	53758	704.4	46177.1		
709.6	52724.3	704.3	46474.6		
709.5	51887.7	704.2	46952.7		
709.4	51386	704.1	46911.5		
709.3	51104.2	704	46747.3		
709.2	50485.9	703.9	46646.8		
709.1	49655.9	703.8	46466.7		
709	49386.7	703.7	46640.8		
708.9	48778	703.6	46593		
708.8	48903	703.5	46350.4		
708.7	48892.3	703.4	46474.7		
708.6	48374.7	703.3	46329.4		
708.5	47796	703.2	46536.6		
708.4	47754.7	703.1	46792.8		
708.3	47698.6	703	46886.8		

Table 8 relationship between binding energy (eV) and residuals for Cr 450°C, 8 hr

Binding energy	Residuals	Binding energy	Residuals	Binding energy	Residuals	Binding energy	Residuals	Binding energy	Residuals
595	18255.3	589.7	18540	584.4	17258.7	579.1	19182.2	573.8	15477.6
594.9	18213	589.6	18579.6	584.3	17274.6	579	19503	573.7	15634
594.8	18119.6	589.5	18545.7	584.2	17207.7	578.9	19599.5	573.6	15677.7
594.7	18143.9	589.4	18517.3	584.1	17179.8	578.8	19538	573.5	15591.7
594.6	18126.1	589.3	18462.6	584	17113	578.7	20041.2	573.4	15606.5
594.5	18254.5	589.2	18680.5	583.9	17122.6	578.6	20291.2	573.3	15596.5
594.4	18030.1	589.1	18855.6	583.8	17107.5	578.5	20214.3	573.2	15485.1
594.3	18222	589	18937.4	583.7	17031.4	578.4	20264.6	573.1	15497.8
594.2	18129.3	588.9	18846.7	583.6	16972.4	578.3	20322.3	573	15579.5
594.1	18040.8	588.8	19096.6	583.5	16858.4	578.2	20443	572.9	15463.6
594	18354.9	588.7	19157.3	583.4	16813.7	578.1	20774	572.8	15368.6
593.9	18211.4	588.6	19119.6	583.3	17008.2	578	20918	572.7	15692.5
593.8	18103.4	588.5	19109.8	583.2	17014.8	577.9	20865.9	572.6	15531.5
593.7	18024.9	588.4	19138.7	583.1	16971	577.8	20720.9	572.5	15535.5
593.6	18041.9	588.3	19341.1	583	16958.8	577.7	20841.1	572.4	15567.4
593.5	18102.3	588.2	19329.9	582.9	17030.9	577.6	20870.3	572.3	15610.5
593.4	18026.2	588.1	19411.8	582.8	17127	577.5	20921.6	572.2	15574.9
593.3	18159.1	588	19328.7	582.7	16980.8	577.4	20824.8	572.1	15465.1
593.2	18094.2	587.9	19417.1	582.6	17006.7	577.3	20696.9	572	15494.8
593.1	18048	587.8	19478	582.5	16986	577.2	20474.9	571.9	15478.6
593	18015.1	587.7	19407	582.4	17007.4	577.1	20237.3	571.8	15337.4
592.9	17950.1	587.6	19457.5	582.3	17186.5	577	20170.3	571.7	15282.8
592.8	18072.8	587.5	19651.2	582.2	16934.5	576.9	20088.6	571.6	15609.7
592.7	18064.5	587.4	19533.7	582.1	16935.3	576.8	19892.8	571.5	15337.8
592.6	18024.8	587.3	19393.1	582	17126.4	576.7	19343	571.4	15407
592.5	17988.9	587.2	19626.5	581.9	17260.7	576.6	19338.5	571.3	15396.7
592.4	17891.6	587.1	19600.1	581.8	17062.1	576.5	19011.7	571.2	15520.6
592.3	18025.8	587	19522.8	581.7	17204.8	576.4	18612.3	571.1	15407.7
592.2	17937.3	586.9	18926.3	581.6	17332.8	576.3	18415.9	571	15339.1
592.1	17962.5	586.8	19135.7	581.5	17033	576.2	18315.4	570.9	15369.4
592	18077.6	586.7	19052.1	581.4	17052.8	576.1	18108.3	570.8	15488.4
591.9	18088.2	586.6	18852.1	581.3	17161.4	576	17768.7	570.7	15498.8
591.8	18066.7	586.5	18879.6	581.2	17150.2	575.9	17545.9	570.6	15505.7
591.7	17958.6	586.4	18719.2	581.1	17209.5	575.8	17539.1	570.5	15505.6
591.6	17908.9	586.3	18564	581	17298.9	575.7	17147.3	570.4	15477.4
591.5	17910.3	586.2	18668.6	580.9	17402.9	575.6	17032.3	570.3	15710.3
591.4	17905.3	586.1	18549.4	580.8	17305.3	575.5	16796.2	570.2	15617.6
591.3	17899.6	586	18276.2	580.7	17263.7	575.4	16671.6	570.1	15591.7
591.2	18034.3	585.9	18207.5	580.6	17374	575.3	16544.8	570	15635.6
591.1	17992.7	585.8	18257.8	580.5	17686.3	575.2	16307.9		
591	18231.1	585.7	18307.8	580.4	17661.3	575.1	16169.6		
590.9	18084.1	585.6	17960.6	580.3	17800.4	575	16201.2		
590.8	18124.8	585.5	17909.7	580.2	17854	574.9	15894.4		
590.7	18046.4	585.4	17815.4	580.1	17820.5	574.8	15917.4		
590.6	18114.7	585.3	17776.3	580	17979.4	574.7	16075.8		
590.5	18418	585.2	17607.7	579.9	17887.5	574.6	16010.4		
590.4	18107.6	585.1	17486.2	579.8	18028.4	574.5	15904.3		
590.3	18252	585	17518.6	579.7	18360.2	574.4	15765.6		
590.2	18086.6	584.9	17199.3	579.6	18475.8	574.3	15830.9		
590.1	18210.2	584.8	17399.8	579.5	18561.9	574.2	15818.3		
590	18432.2	584.7	17420.5	579.4	18950.2	574.1	15677.8		
589.9	18573.3	584.6	17094.6	579.3	18924.1	574	15571.9		
589.8	18303.8	584.5	17192.5	579.2	18983.4	573.9	15482.8		

Table 9 relationship between binding energy (eV) and residuals for Fe 450°C, 8 hr

Binding energy	Residuals	Binding energy	Residuals	Binding energy	Residuals	Binding energy	Residuals	Binding energy	Residuals
740	43841.4	734.7	38261.3	729.4	36367.6	724.1	35760.5	718.8	32872.2
739.9	43769.1	734.6	38059.9	729.3	36259.9	724	35393.2	718.7	32477.4
739.8	43817.5	734.5	37899.7	729.2	36328	723.9	35884.5	718.6	32863.5
739.7	43310.2	734.4	37945.4	729.1	36675.9	723.8	35804.7	718.5	33038.8
739.6	43066.8	734.3	37639.9	729	36634.5	723.7	35533.3	718.4	32922.5
739.5	42963.5	734.2	37631.3	728.9	36217.9	723.6	35268.3	718.3	32895.5
739.4	42655	734.1	37749.8	728.8	36144.6	723.5	34940	718.2	32878.4
739.3	42360.5	734	37622	728.7	36260.8	723.4	35148.9	718.1	32647.1
739.2	42489.3	733.9	37580.5	728.6	36347.7	723.3	34833.1	718	32974.3
739.1	42450.3	733.8	37542.9	728.5	36172.5	723.2	34654.7	717.9	32684.4
739	42256.3	733.7	37683.2	728.4	36208.2	723.1	34449.4	717.8	33185.2
738.9	42065.4	733.6	37522.3	728.3	36657.9	723	34896	717.7	32410.9
738.8	41738.6	733.5	37295.1	728.2	36465.4	722.9	34201.1	717.6	32085.2
738.7	41554.9	733.4	37348.8	728.1	36144.5	722.8	34280.8	717.5	32681.7
738.6	41702.3	733.3	37316.6	728	36181.2	722.7	34273.1	717.4	32808.9
738.5	41363	733.2	37337.7	727.9	36725.5	722.6	34124.1	717.3	33055.1
738.4	40900.1	733.1	37484.1	727.8	36308.8	722.5	34464.6	717.2	32581.6
738.3	41433.9	733	37066.3	727.7	36630.7	722.4	34191.1	717.1	32261.5
738.2	41555.9	732.9	36793.3	727.6	36472.2	722.3	33798.6	717	32489.8
738.1	41278	732.8	37317	727.5	36636.6	722.2	33688	716.9	32858.4
738	41203.5	732.7	37474.6	727.4	36693.9	722.1	33735.9	716.8	32904.1
737.9	40678.8	732.6	37078.7	727.3	36597	722	33388.2	716.7	32613.2
737.8	40409.6	732.5	37147.7	727.2	36822.7	721.9	33467	716.6	32551.6
737.7	40083.2	732.4	36887.4	727.1	36587.3	721.8	33586.8	716.5	32658.2
737.6	40403.2	732.3	37139.9	727	36990.4	721.7	33794	716.4	32656.7
737.5	40526.8	732.2	37266.8	726.9	36941.5	721.6	33862.8	716.3	32535.3
737.4	40066	732.1	36884.8	726.8	36774.5	721.5	33304.9	716.2	32851.3
737.3	40289.7	732	36532.8	726.7	36962.4	721.4	33419.3	716.1	32937.6
737.2	40057.4	731.9	36937.8	726.6	36564.4	721.3	33524.7	716	32668.6
737.1	39786.7	731.8	36573.9	726.5	36563.6	721.2	33723.4	715.9	32363.4
737	39536.6	731.7	36897.8	726.4	36585.3	721.1	33461.6	715.8	32866.3
736.9	39483.7	731.6	36829.6	726.3	36370.5	721	33236.8	715.7	32510
736.8	39342.1	731.5	37127.5	726.2	36940.9	720.9	33575.2	715.6	32841
736.7	39309	731.4	37106.3	726.1	36677.9	720.8	33478.3	715.5	32727.8
736.6	39489.1	731.3	36786.5	726	36801.7	720.7	33743.2	715.4	32976.2
736.5	39434.1	731.2	36880.6	725.9	36973.8	720.6	33484.7	715.3	32944.1
736.4	39272.3	731.1	36636	725.8	36805.7	720.5	32994.2	715.2	32773.3
736.3	39146.1	731	36642.3	725.7	36600.4	720.4	33201	715.1	33090.5
736.2	39063.5	730.9	36675.9	725.6	36511.7	720.3	33619.3	715	32898.6
736.1	38959.6	730.8	36906.2	725.5	36681.2	720.2	33526.6	714.9	32752.6
736	39243.8	730.7	36428.2	725.4	36653.6	720.1	33138.2	714.8	33040.6
735.9	39195.5	730.6	36717.2	725.3	36415.1	720	33271	714.7	32895
735.8	39047.8	730.5	36944.7	725.2	36797.6	719.9	33035.6	714.6	33266.5
735.7	38918.9	730.4	36257.2	725.1	36582.4	719.8	32828	714.5	33314.1
735.6	38803.7	730.3	36737.4	725	36261.1	719.7	33048.9	714.4	33265.3
735.5	38253.3	730.2	36692.5	724.9	36258.4	719.6	33393.8	714.3	33445.7
735.4	38651.6	730.1	36417.3	724.8	36383.1	719.5	33075.1	714.2	33898.8
735.3	38410.4	730	36373.1	724.7	36275.2	719.4	33407	714.1	33703.1
735.2	38212.3	729.9	36239	724.6	36527	719.3	33128.7	714	33377.9
735.1	38630.9	729.8	36831.9	724.5	36417	719.2	33273.8	713.9	33530.8
735	38470.1	729.7	36383.1	724.4	36424.5	719.1	32795	713.8	33751.6
734.9	38330.2	729.6	36549	724.3	35890.8	719	33335.4	713.7	33716.4
734.8	38256.5	729.5	36255.3	724.2	36042.4	718.9	33371.7	713.6	33589.3

Table 9(continued) relationship between binding energy (eV) and residuals for Fe 450°C, 8 hr cont.

Binding energy	Residuals	Binding energy	Residuals	Binding energy	Residuals
713.5	33939.5	708.2	29302.3	702.9	29067.5
713.4	33970.7	708.1	29456.8	702.8	28985.5
713.3	34057.7	708	29300.3	702.7	28914.6
713.2	34370.6	707.9	29233	702.6	29341
713.1	34488.2	707.8	29120.3	702.5	29292.3
713	34377.7	707.7	29014.7	702.4	29299
712.9	34342.2	707.6	29272.9	702.3	29069.9
712.8	34492.9	707.5	28958.7	702.2	29241.2
712.7	34630.8	707.4	28963.5	702.1	29209.6
712.6	34693.3	707.3	28978.9	702	29390.7
712.5	34565.3	707.2	29320.7	701.9	29046.4
712.4	34711.1	707.1	29156.7	701.8	29494.7
712.3	34862.8	707	29172.2	701.7	29160
712.2	34659.2	706.9	29087.1	701.6	29413.1
712.1	34621.7	706.8	29302	701.5	29064.6
712	34867.2	706.7	29092.7	701.4	29004.3
711.9	35324.4	706.6	29265.7	701.3	29416.1
711.8	35050.4	706.5	29050.1	701.2	29219.7
711.7	35116.2	706.4	28993.5	701.1	29092.5
711.6	35215.6	706.3	29139.5	701	29144.6
711.5	35039.5	706.2	29460.2	700.9	28621.9
711.4	35178.7	706.1	29538.8	700.8	28913.7
711.3	35257	706	29406.9	700.7	29168.2
711.2	34914	705.9	28667.9	700.6	28853.9
711.1	34621.3	705.8	29091.2	700.5	28584.4
711	34657.9	705.7	29000.6	700.4	28640.2
710.9	34567.4	705.6	29262.6	700.3	28878.4
710.8	34464.9	705.5	29214.8	700.2	29221.3
710.7	34602.2	705.4	29346.4	700.1	28902
710.6	33841.3	705.3	29110.3	700	28737.3
710.5	33732.8	705.2	29229.1		
710.4	33431.4	705.1	29321.7		
710.3	33726.4	705	29368.2		
710.2	33344.6	704.9	29211.9		
710.1	32525	704.8	29383.7		
710	32451.8	704.7	29366.2		
709.9	32437.8	704.6	29434.7		
709.8	32266.1	704.5	29105.3		
709.7	31552.7	704.4	29077		
709.6	31501.4	704.3	29104.7		
709.5	31296.3	704.2	29299.1		
709.4	31023.2	704.1	29248.2		
709.3	30767.4	704	29390.2		
709.2	30499.9	703.9	29028.2		
709.1	30148.5	703.8	29451.8		
709	30242.1	703.7	29208.2		
708.9	30171.3	703.6	29217.7		
708.8	29960.7	703.5	29025.6		
708.7	29374.9	703.4	29257.1		
708.6	29292.9	703.3	29464.6		
708.5	29584.3	703.2	29025.2		
708.4	29306.9	703.1	29405.9		
708.3	29513.6	703	29281.5		

Table 10 relationship between binding energy (eV) and residuals for Cr 600°C, 6 hr

Binding energy	Residuals	Binding energy	Residuals	Binding energy	Residuals	Binding energy	Residuals	Binding energy	Residuals
595	24778.5	589.7	25609.3	584.4	23431.6	579.1	27438.4	573.8	20538.2
594.9	24566.6	589.6	25319.9	584.3	23471.3	579	27641	573.7	20832.8
594.8	24421.6	589.5	25615.5	584.2	23192	578.9	27783.6	573.6	20785.4
594.7	24435.1	589.4	25735.4	584.1	23181.5	578.8	27963.6	573.5	20885.1
594.6	24615.4	589.3	25922.4	584	23216.9	578.7	28296.3	573.4	20623.2
594.5	24726.2	589.2	25867	583.9	23191	578.6	28416.4	573.3	20634.5
594.4	24460.4	589.1	25777.9	583.8	23149.9	578.5	28785.2	573.2	20655.8
594.3	24482	589	26063.6	583.7	22938.4	578.4	28924.9	573.1	20792.8
594.2	24429.5	588.9	26085.4	583.6	23144.8	578.3	28880.4	573	20770.8
594.1	24398.1	588.8	26130.6	583.5	23010.1	578.2	29125.4	572.9	20632.2
594	24483.7	588.7	26404	583.4	22699.3	578.1	29510.1	572.8	20519.6
593.9	24590.3	588.6	26728.1	583.3	22977.7	578	29552.5	572.7	20706.4
593.8	24481.2	588.5	26881.5	583.2	23106.4	577.9	29468.7	572.6	20594.3
593.7	24345.9	588.4	26981.1	583.1	23001.1	577.8	29561	572.5	20593.8
593.6	24243.9	588.3	26858.9	583	23256.4	577.7	29408.4	572.4	20710.6
593.5	24199.5	588.2	26819.6	582.9	23033.3	577.6	29126.6	572.3	20646.6
593.4	24039	588.1	27316.2	582.8	23053.6	577.5	29212.6	572.2	20750.4
593.3	24178.3	588	27536.8	582.7	22971.6	577.4	29145.2	572.1	20941.6
593.2	24367.8	587.9	27444.1	582.6	23134	577.3	28616.8	572	20690.5
593.1	24287.9	587.8	27376.7	582.5	23096.3	577.2	28393.7	571.9	20601.1
593	24189.3	587.7	27493.5	582.4	23190.6	577.1	27921.9	571.8	20723.3
592.9	24527.1	587.6	27536.1	582.3	23063.8	577	27675.6	571.7	20586.7
592.8	24430.3	587.5	27269.2	582.2	22956.4	576.9	27118.4	571.6	20621.1
592.7	24269.9	587.4	27419.8	582.1	23184.7	576.8	27028.9	571.5	20403.5
592.6	24266.3	587.3	27121.3	582	23012.4	576.7	26582.5	571.4	20826.7
592.5	24071.6	587.2	26860.2	581.9	23206.1	576.6	26117.7	571.3	20646.6
592.4	24373	587.1	27147	581.8	23175.1	576.5	25586.2	571.2	20634.3
592.3	24355.3	587	26904.7	581.7	23224.3	576.4	25067.1	571.1	20387.4
592.2	24506.3	586.9	26672	581.6	23388.4	576.3	24504.5	571	20629.8
592.1	24562.8	586.8	26684.3	581.5	23470.2	576.2	24031.4	570.9	20637.9
592	24361.9	586.7	26233.1	581.4	23616.1	576.1	23470.7	570.8	20880.1
591.9	24586.9	586.6	26039.7	581.3	23755	576	23513.2	570.7	20501.5
591.8	24652.9	586.5	25845.6	581.2	23731.3	575.9	23015.2	570.6	20624.3
591.7	24570.3	586.4	25735.9	581.1	23616.4	575.8	22700.7	570.5	20688.9
591.6	24538.2	586.3	25085.9	581	23932	575.7	22420.4	570.4	20840
591.5	24591.1	586.2	25016.7	580.9	24011.7	575.6	22068.6	570.3	20850.3
591.4	24835.1	586.1	25117	580.8	24082.3	575.5	21896.9	570.2	20734.7
591.3	24748.4	586	24876.2	580.7	24084.6	575.4	21606.5	570.1	20686.2
591.2	24817.8	585.9	24846.4	580.6	24240.6	575.3	21556.4	570	20815.9
591.1	24618.6	585.8	24617	580.5	24541.8	575.2	21669.5		
591	24661.4	585.7	24324	580.4	24669.2	575.1	21214.4		
590.9	24741.5	585.6	24098.5	580.3	24884	575	21217.9		
590.8	24773	585.5	23996.7	580.2	24833.6	574.9	21124.8		
590.7	24562.8	585.4	23940.4	580.1	25135.4	574.8	21036.7		
590.6	24911.2	585.3	23664.3	580	25580	574.7	21044.5		
590.5	25245.7	585.2	23639.3	579.9	25558.4	574.6	21037.2		
590.4	24859.7	585.1	23779	579.8	25750	574.5	21313.9		
590.3	25070.7	585	23596.2	579.7	26044.4	574.4	20936.4		
590.2	25108.3	584.9	23576.8	579.6	26256.3	574.3	20836.4		
590.1	25233.5	584.8	23450	579.5	26580.9	574.2	20766.5		
590	25152.7	584.7	23274	579.4	26844.4	574.1	20743		
589.9	25241.8	584.6	23377.9	579.3	26806.2	574	20689.3		
589.8	25244.4	584.5	23497.4	579.2	27167.3	573.9	20767.1		

Table 11 relationship between binding energy (eV) and residuals for Fe 600°C, 6 hr

Binding energy	Residuals	Binding energy	Residuals	Binding energy	Residuals	Binding energy	Residuals	Binding energy	Residuals
740	58068.6	734.7	50549.1	729.4	47741.3	724.1	46502.1	718.8	43230.4
739.9	57897.4	734.6	50618.3	729.3	47827.5	724	46555.4	718.7	43048.1
739.8	57813	734.5	50625.6	729.2	47979.7	723.9	46162.9	718.6	43123.4
739.7	57990.9	734.4	50669.7	729.1	47865.3	723.8	46089.1	718.5	43256.7
739.6	57880.6	734.3	49912.8	729	48567.2	723.7	45881.7	718.4	43294.9
739.5	56721.1	734.2	50249.7	728.9	48333.8	723.6	46340.5	718.3	42782.7
739.4	56560.2	734.1	49810.3	728.8	47859.8	723.5	46065.1	718.2	42906.2
739.3	56005.7	734	50108.8	728.7	48496	723.4	46156.5	718.1	42631.5
739.2	56410.6	733.9	50334.4	728.6	47615.6	723.3	45980.8	718	42974.2
739.1	56178	733.8	49915.8	728.5	48442.9	723.2	45395.8	717.9	42941.4
739	56198.8	733.7	49917.2	728.4	48643	723.1	44841.4	717.8	42955.6
738.9	55926.8	733.6	50117.7	728.3	48485.2	723	45048.9	717.7	42842.9
738.8	55789.6	733.5	50290.7	728.2	48063.7	722.9	45031.4	717.6	42502
738.7	54935.9	733.4	49570.9	728.1	47940.5	722.8	44760.3	717.5	42376
738.6	55422.7	733.3	49648.3	728	48049.1	722.7	44929.7	717.4	42498.1
738.5	55278.8	733.2	49606.8	727.9	48199.7	722.6	44112.1	717.3	42270.6
738.4	54556	733.1	49472.9	727.8	48281	722.5	45193.9	717.2	42654.5
738.3	54738.9	733	49464.5	727.7	47930.3	722.4	44837.4	717.1	42937.2
738.2	54968.2	732.9	49952.7	727.6	47702.5	722.3	44444.6	717	42706.2
738.1	54498.2	732.8	49521.8	727.5	47273.8	722.2	44011.8	716.9	42278.2
738	54297.3	732.7	49341.2	727.4	47790.1	722.1	43991.4	716.8	42326.6
737.9	54261.5	732.6	49287.2	727.3	48177.1	722	44221.9	716.7	42550.6
737.8	54460.3	732.5	49529.4	727.2	47604.5	721.9	44099.1	716.6	42617.7
737.7	54281.8	732.4	49329.4	727.1	47662.5	721.8	43760	716.5	42422.5
737.6	53819.6	732.3	49695.5	727	47798	721.7	43743	716.4	41873.5
737.5	53565.6	732.2	49020	726.9	47700.6	721.6	43905.1	716.3	42593
737.4	53606.6	732.1	49023.4	726.8	47959.1	721.5	43938.7	716.2	42365.4
737.3	53270.8	732	49043.4	726.7	47913.2	721.4	43762	716.1	42463.1
737.2	53052.3	731.9	49110.2	726.6	48202.8	721.3	43443.1	716	41783.1
737.1	52884.9	731.8	48702.4	726.5	48310.1	721.2	43706.1	715.9	42275.1
737	52434.2	731.7	48795.5	726.4	48144.7	721.1	44008.4	715.8	42403.5
736.9	52596.4	731.6	48719.1	726.3	48065.6	721	43885.9	715.7	42385.3
736.8	52718.2	731.5	48871.2	726.2	48194.8	720.9	43487.1	715.6	41933.8
736.7	52742.8	731.4	48790	726.1	47908.1	720.8	43425.9	715.5	42202.6
736.6	52819.1	731.3	48699.2	726	47562.5	720.7	43482.6	715.4	42617.4
736.5	52344.8	731.2	48835.3	725.9	47448.5	720.6	43212.4	715.3	42820
736.4	51954.2	731.1	48504.6	725.8	47118.3	720.5	43533.7	715.2	42470.5
736.3	51997.4	731	48257.2	725.7	47569.2	720.4	43459.4	715.1	42833.8
736.2	51602.2	730.9	48401.9	725.6	48086.4	720.3	43550.9	715	42497.7
736.1	51794.4	730.8	48631.2	725.5	47597.1	720.2	43905.5	714.9	42396.4
736	51641.7	730.7	49013.4	725.4	47730.6	720.1	43998.7	714.8	42838.2
735.9	51761.8	730.6	48543	725.3	47472.2	720	43652.7	714.7	42860.9
735.8	51759.8	730.5	48644.3	725.2	47631.8	719.9	43154.4	714.6	42965
735.7	51473.4	730.4	48794.1	725.1	47670.8	719.8	43266.6	714.5	42937.8
735.6	51172.6	730.3	48187.2	725	47466.6	719.7	43642	714.4	42973.2
735.5	51251.5	730.2	48409.3	724.9	47206.9	719.6	43334.8	714.3	43148.4
735.4	50988.2	730.1	48835.7	724.8	47347.4	719.5	44023.5	714.2	43118
735.3	50703.8	730	48699.4	724.7	47089.2	719.4	43661	714.1	43275.7
735.2	50661.1	729.9	48737.7	724.6	47046.6	719.3	43254.8	714	43164.5
735.1	50544.2	729.8	48464.8	724.5	46482.7	719.2	43421.2	713.9	43049.4
735	50563.9	729.7	48621.3	724.4	46979.4	719.1	43300.9	713.8	43523.5
734.9	50903.4	729.6	48354.4	724.3	47105.6	719	43007.2	713.7	43702.6
734.8	50534.9	729.5	48235.4	724.2	46300.9	718.9	42920.6	713.6	43907.8

Table 11 (continued) relationship between binding energy (eV) and residuals for Fe 600°, 6 hr.

Binding energy	Residuals	Binding energy	Residuals	Binding energy	Residuals
713.5	43646.7	708.2	38901.6	702.9	38464.6
713.4	43272.2	708.1	38947.3	702.8	38360.8
713.3	43590.2	708	39058.4	702.7	38522.5
713.2	44210.1	707.9	38468	702.6	38406.7
713.1	43935.9	707.8	38575.5	702.5	38659.3
713	43807.5	707.7	38525.2	702.4	38907.6
712.9	44190	707.6	38772.5	702.3	38639.9
712.8	43732.5	707.5	38571.3	702.2	39012.5
712.7	44111.6	707.4	38597	702.1	38882.8
712.6	44030.4	707.3	38978.3	702	38836.1
712.5	44029.1	707.2	38577.6	701.9	38979
712.4	44422.3	707.1	38326.1	701.8	39010.7
712.3	44216.1	707	38605.2	701.7	39422.9
712.2	44300.6	706.9	38792.4	701.6	38922.8
712.1	44156.9	706.8	38763.6	701.5	38982.9
712	44778.9	706.7	38544.5	701.4	38856.5
711.9	44711.5	706.6	38504.8	701.3	38358.1
711.8	44671.4	706.5	38781.8	701.2	38422.3
711.7	44595.5	706.4	38721.9	701.1	38821.6
711.6	44691.4	706.3	39054	701	38422.6
711.5	44360.6	706.2	39040.7	700.9	38306.7
711.4	44784.5	706.1	38600.5	700.8	38513.6
711.3	44684.3	706	38848.3	700.7	38748.9
711.2	44610.7	705.9	38772.5	700.6	38522.7
711.1	44503	705.8	38599.4	700.5	38610.2
711	44242.6	705.7	38421.3	700.4	38600.3
710.9	43794	705.6	38653.6	700.3	38356.1
710.8	43841	705.5	38990	700.2	38581.7
710.7	43888.2	705.4	38978.1	700.1	38160.8
710.6	43639.8	705.3	38760.6	700	37939.1
710.5	43433.4	705.2	38538.2		
710.4	43530.5	705.1	38457.2		
710.3	43393.1	705	38531.8		
710.2	42937.8	704.9	38849		
710.1	42595.5	704.8	38626.8		
710	42274.5	704.7	38822.5		
709.9	42175.3	704.6	38564.2		
709.8	41981.3	704.5	38746.9		
709.7	41493.8	704.4	38653.1		
709.6	41115.1	704.3	38651		
709.5	41306.4	704.2	38982.4		
709.4	41109	704.1	38695		
709.3	40355.5	704	38555.8		
709.2	40471.3	703.9	39018.1		
709.1	40370.6	703.8	38851.2		
709	40103.5	703.7	38771.2		
708.9	39794	703.6	39096.2		
708.8	39634.1	703.5	38766		
708.7	39036.9	703.4	38680.4		
708.6	39320	703.3	38686.6		
708.5	39386.7	703.2	38946.7		
708.4	39113.9	703.1	38783		
708.3	39323.7	703	38935		

Table 12 relationship between binding energy (eV) and residuals for Cr 800°C, 4 hr

Binding energy	Residuals	Binding energy	Residuals	Binding energy	Residuals	Binding energy	Residuals	Binding energy	Residuals
595	20832.9	589.7	20623.9	584.4	20505.1	579.1	20611.8	573.8	16763.5
594.9	20696.5	589.6	20770.1	584.3	20164.7	579	20941.9	573.7	16645.5
594.8	20785.8	589.5	20958	584.2	19886.7	578.9	21217	573.6	16497.2
594.7	20543.2	589.4	20802.6	584.1	19846.9	578.8	21603.5	573.5	16318.9
594.6	20631.4	589.3	21121.2	584	19755.3	578.7	21647.7	573.4	16440.9
594.5	20651.1	589.2	21291	583.9	19856.3	578.6	21603.8	573.3	16300.8
594.4	20759.8	589.1	20914.4	583.8	19461.7	578.5	21915.5	573.2	16238.6
594.3	20591	589	21089.7	583.7	19276	578.4	22456.7	573.1	16049.7
594.2	20620.5	588.9	21608.3	583.6	19453.1	578.3	22351.7	573	16075.9
594.1	20476.9	588.8	21767.3	583.5	19412.9	578.2	22780.2	572.9	16099.3
594	20621.7	588.7	21703	583.4	19363.1	578.1	22892.4	572.8	16251.9
593.9	20531.7	588.6	21705.5	583.3	19204.1	578	23208.2	572.7	16135.7
593.8	20525.3	588.5	21646.8	583.2	19027.1	577.9	23682.5	572.6	16267.7
593.7	20407.3	588.4	21851.7	583.1	19174.9	577.8	23898	572.5	16120.5
593.6	20452.8	588.3	22034.3	583	18970.3	577.7	24487.8	572.4	16081.3
593.5	20436.8	588.2	22258.8	582.9	19042.9	577.6	24696.9	572.3	16164.2
593.4	20462.7	588.1	22148.8	582.8	19081.3	577.5	24956.5	572.2	15960.1
593.3	20410.6	588	22252.4	582.7	18873.7	577.4	25237.9	572.1	15964.4
593.2	20091.4	587.9	22319.7	582.6	18836.4	577.3	25642.7	572	15942.3
593.1	20248.1	587.8	22808.5	582.5	18779.4	577.2	25846.9	571.9	15842.6
593	20230.7	587.7	22858.7	582.4	18756	577.1	26005.4	571.8	15902.3
592.9	20214.6	587.6	22993.4	582.3	18882.6	577	26257.9	571.7	16022.2
592.8	20119	587.5	23102.4	582.2	19051.7	576.9	26149.4	571.6	16066.9
592.7	20141.7	587.4	23143.4	582.1	18771	576.8	26615.3	571.5	15793.1
592.6	20260.9	587.3	23076.8	582	18894.2	576.7	26708.5	571.4	15871.7
592.5	20260.9	587.2	23308.3	581.9	18923.8	576.6	26511	571.3	16100.4
592.4	20282.7	587.1	23317	581.8	18954.9	576.5	26339.5	571.2	15907.2
592.3	20098.7	587	23421.2	581.7	18977.7	576.4	26636	571.1	15868.6
592.2	20375.2	586.9	23738.2	581.6	18987.1	576.3	26738	571	15858.6
592.1	20415.2	586.8	23718.3	581.5	19060.4	576.2	26336.5	570.9	16049.3
592	20380.1	586.7	23777.1	581.4	18963.8	576.1	26025.6	570.8	16002.9
591.9	20247.6	586.6	23651.2	581.3	19239.4	576	26015.1	570.7	15947.6
591.8	20238	586.5	23739	581.2	18898.3	575.9	25457.1	570.6	16012.2
591.7	20119.3	586.4	23804.4	581.1	18947.8	575.8	25163.5	570.5	16072.9
591.6	20240	586.3	23904.4	581	19081.2	575.7	24545.7	570.4	15873.2
591.5	20105.6	586.2	23677.9	580.9	19068.8	575.6	24358.3	570.3	15920.4
591.4	20324.2	586.1	23626.5	580.8	19069.3	575.5	23883.5	570.2	16111.2
591.3	20249.7	586	23584.3	580.7	18947	575.4	23287	570.1	15972.3
591.2	20205.3	585.9	23486	580.6	19112.2	575.3	22830.9	570	16025.6
591.1	20342.1	585.8	23385.2	580.5	19202.2	575.2	22153.2		
591	20317.2	585.7	23350.8	580.4	19203.9	575.1	21511.8		
590.9	20352.5	585.6	23060.6	580.3	19374.8	575	21029.4		
590.8	20343.7	585.5	22983.2	580.2	19272.6	574.9	20624.1		
590.7	20138.2	585.4	22700.6	580.1	19503.7	574.8	19994.1		
590.6	20271.6	585.3	22528.9	580	19508.3	574.7	19306		
590.5	20397.9	585.2	22431.6	579.9	19735.1	574.6	19155.8		
590.4	20375.2	585.1	22186.5	579.8	19702	574.5	18549		
590.3	20447.1	585	21833.6	579.7	19824.2	574.4	18421.6		
590.2	20526.3	584.9	21555.9	579.6	19896.5	574.3	18013.6		
590.1	20640.6	584.8	21352.5	579.5	20143.6	574.2	17685		
590	20580	584.7	21068.7	579.4	20314.6	574.1	17451.8		
589.9	20586.4	584.6	20985.1	579.3	20516.6	574	17093.5		
589.8	20708	584.5	20651.5	579.2	20612.4	573.9	16851.7		

Table 13 relationship between binding energy (eV) and residuals for Fe 800°C, 4 hr

Binding energy	Residuals	Binding energy	Residuals	Binding energy	Residuals	Binding energy	Residuals	Binding energy	Residuals
740	47967.2	734.7	41319.9	729.4	40386.6	724.1	40434.4	718.8	35898.5
739.9	47777.3	734.6	41235.6	729.3	40474.9	724	39792.4	718.7	35461.6
739.8	47843.1	734.5	41553.9	729.2	39780.3	723.9	39963.5	718.6	35314.2
739.7	46993.2	734.4	41298	729.1	40222.3	723.8	39871.1	718.5	35462.2
739.6	46603.4	734.3	41084.8	729	40382.2	723.7	39886.9	718.4	35426.4
739.5	46743.7	734.2	40762.2	728.9	40283.2	723.6	39648.5	718.3	35135.6
739.4	46566.4	734.1	41084.7	728.8	40036.8	723.5	39370.3	718.2	35599.7
739.3	46029.1	734	40588.9	728.7	40657.6	723.4	39303.6	718.1	35210.2
739.2	46324.4	733.9	40765.8	728.6	40735.2	723.3	39053.3	718	34791.1
739.1	46454.6	733.8	41261.3	728.5	40529.1	723.2	39418.4	717.9	35360.6
739	45510.9	733.7	41444.3	728.4	40022.1	723.1	39467	717.8	34910.7
738.9	44681.6	733.6	41074.9	728.3	40361.5	723	39040.3	717.7	34622.9
738.8	44970.9	733.5	40890.2	728.2	40571.6	722.9	38529.9	717.6	34895.6
738.7	45058.7	733.4	40872.7	728.1	40265.1	722.8	38490.9	717.5	34982.1
738.6	44869.2	733.3	40991.1	728	40243.8	722.7	38037.3	717.4	35526.5
738.5	44371.6	733.2	40496.7	727.9	40531.6	722.6	38141.7	717.3	35007.7
738.4	44568.4	733.1	40649.7	727.8	40144	722.5	38155.8	717.2	34763.9
738.3	44444.2	733	40365.4	727.7	40409.4	722.4	37759.1	717.1	34889.6
738.2	44300.3	732.9	40647.7	727.6	40667.5	722.3	37728.2	717	34849.5
738.1	43760.4	732.8	40801	727.5	40600.4	722.2	37765.1	716.9	34676
738	43718.5	732.7	40576.5	727.4	40753.9	722.1	37604.8	716.8	34626.2
737.9	43642.5	732.6	40779.8	727.3	40536.9	722	37154.1	716.7	34549
737.8	43930.8	732.5	40292.4	727.2	40715.2	721.9	37442.5	716.6	34905.8
737.7	43738.6	732.4	40420.2	727.1	41055.6	721.8	37043.2	716.5	34935.3
737.6	43302.6	732.3	40386.9	727	40823.6	721.7	36496.5	716.4	34825.3
737.5	43356.3	732.2	40044.1	726.9	40919.1	721.6	36815.5	716.3	34878.2
737.4	43016.1	732.1	39981.3	726.8	40916.2	721.5	36995.3	716.2	34920
737.3	42903.4	732	40304.4	726.7	40729.4	721.4	36371.6	716.1	34762.9
737.2	42873.6	731.9	39901.1	726.6	40603	721.3	36422.8	716	34850.5
737.1	42573	731.8	40330.4	726.5	40932.2	721.2	36775.2	715.9	34533.4
737	42455.3	731.7	40134.8	726.4	40753.3	721.1	36379.2	715.8	34709.1
736.9	42551.1	731.6	40261.9	726.3	40793.7	721	36210.8	715.7	34987
736.8	42322.9	731.5	39918	726.2	40689.2	720.9	36557.4	715.6	34971.4
736.7	42566.8	731.4	39880.1	726.1	40584.7	720.8	36429.6	715.5	35082.8
736.6	42593	731.3	40263.6	726	41088.7	720.7	36171.4	715.4	34737.4
736.5	42295.7	731.2	39868.5	725.9	41305.5	720.6	36460.7	715.3	35044.3
736.4	42084.7	731.1	40147.8	725.8	41709.8	720.5	36261.7	715.2	34925.9
736.3	42126.2	731	39577.3	725.7	41373.2	720.4	35808.7	715.1	35324.6
736.2	42338.3	730.9	40331.3	725.6	40961.7	720.3	36167	715	35323.8
736.1	42272.4	730.8	40048.6	725.5	40924.8	720.2	36283.7	714.9	35175.7
736	41989.3	730.7	40218.6	725.4	40583.9	720.1	35973.4	714.8	35306.7
735.9	41990.3	730.6	39921.2	725.3	41019.5	720	36134.4	714.7	35325.7
735.8	41760.1	730.5	40100.9	725.2	40834.5	719.9	35491.5	714.6	35061.5
735.7	41628.5	730.4	40271.7	725.1	40777.8	719.8	35579.4	714.5	35211.2
735.6	42490.1	730.3	39747.9	725	41093.8	719.7	35614.3	714.4	35441.5
735.5	42204.9	730.2	39834.7	724.9	40901.5	719.6	35565.3	714.3	35470.6
735.4	41892.3	730.1	39579	724.8	41131.2	719.5	35467.7	714.2	35559
735.3	41625.4	730	40020.6	724.7	41066.7	719.4	35772.4	714.1	35524.4
735.2	40871.3	729.9	40500.6	724.6	40644.5	719.3	35708.8	714	35331.1
735.1	41707.2	729.8	40048.2	724.5	40722.4	719.2	35718.3	713.9	35888.7
735	42056.9	729.7	40143.4	724.4	40521.4	719.1	35435.1	713.8	35839
734.9	41423.3	729.6	40043.4	724.3	40574.1	719	35286.3	713.7	35927.6
734.8	41404.9	729.5	40363.9	724.2	40752.6	718.9	35452.7	713.6	36450.1

Table 13(continued) relationship between binding energy (eV) and residuals for Fe 800°C, 4 hr.

Binding energy	Residuals	Binding energy	Residuals	Binding energy	Residuals
713.5	36394.2	708.2	31725.3	702.9	31401.3
713.4	36247.9	708.1	31386.3	702.8	31633.2
713.3	36218.7	708	31452.1	702.7	31480.5
713.2	36457.9	707.9	31844.4	702.6	31288.9
713.1	36362.8	707.8	31320.8	702.5	31192
713	36419	707.7	31225.8	702.4	30923.4
712.9	36652.2	707.6	31236.6	702.3	31010.3
712.8	36720.8	707.5	31027.7	702.2	30904.4
712.7	36663.6	707.4	31047.2	702.1	31228.2
712.6	36788.7	707.3	30984.5	702	31023.9
712.5	36710.1	707.2	30839	701.9	30891.2
712.4	36705.3	707.1	31095.2	701.8	30948.5
712.3	37012.3	707	31024.5	701.7	31379.7
712.2	37216.6	706.9	31024.8	701.6	31568.2
712.1	36979.8	706.8	30701.2	701.5	31553
712	37030.2	706.7	31067.1	701.4	31167.6
711.9	36996.9	706.6	31085.7	701.3	31417.8
711.8	37107.9	706.5	30785.1	701.2	31161.4
711.7	37344.3	706.4	30601.7	701.1	31253.6
711.6	37668.5	706.3	31017.8	701	31294.2
711.5	37177.7	706.2	30863.4	700.9	31238.5
711.4	37154.3	706.1	30976.1	700.8	31188.8
711.3	37168.9	706	30859.2	700.7	31092.3
711.2	37681.2	705.9	30936.2	700.6	30968.8
711.1	37483.4	705.8	31212.7	700.5	31311.2
711	37444.6	705.7	31273.6	700.4	31150
710.9	37331.8	705.6	31169	700.3	31385.8
710.8	37372.1	705.5	31048.4	700.2	31005.7
710.7	36848.2	705.4	30825.8	700.1	31112.7
710.6	37170.3	705.3	30841.9	700	31323.2
710.5	37054.3	705.2	30611.9		
710.4	36428.8	705.1	30378.9		
710.3	36609.8	705	30979.4		
710.2	36285.6	704.9	30796.2		
710.1	35892.2	704.8	31042.1		
710	35923	704.7	31250.4		
709.9	35922.2	704.6	30940.3		
709.8	35757.4	704.5	30797.1		
709.7	35421.7	704.4	31196.6		
709.6	35109	704.3	31339.7		
709.5	34721.6	704.2	31293.4		
709.4	33995.5	704.1	30921.1		
709.3	34177.8	704	31100.2		
709.2	34013.2	703.9	31170.9		
709.1	33628.7	703.8	31566.7		
709	33185.2	703.7	30893.1		
708.9	33088.4	703.6	30813.4		
708.8	32909.8	703.5	31306.5		
708.7	32459	703.4	31361.9		
708.6	32028.7	703.3	31196.1		
708.5	32027.4	703.2	31081.4		
708.4	31640.7	703.1	31203.7		
708.3	31768.9	703	31353.8		

Table 14 relationship between binding energy (eV) and residuals for Cr 800°C, 6 hr

Binding energy	Residuals	Binding energy	Residuals	Binding energy	Residuals	Binding energy	Residuals	Binding energy	Residuals
595	20996.4	589.7	20492	584.4	19621.4	579.1	19995	573.8	17775.6
594.9	21006.3	589.6	20456.4	584.3	19499.5	579	20068.5	573.7	17637.5
594.8	20837.6	589.5	20509	584.2	19280.5	578.9	20323.9	573.6	17631.2
594.7	20771.3	589.4	20693	584.1	19538.4	578.8	20529	573.5	17589.4
594.6	20769.1	589.3	20633.7	584	19493.7	578.7	20516.5	573.4	17576.7
594.5	20726.7	589.2	20640.9	583.9	19456.8	578.6	20782.3	573.3	17663.5
594.4	20604.6	589.1	20667	583.8	19547.2	578.5	20970.9	573.2	17527.6
594.3	20709.2	589	20537.7	583.7	19051.6	578.4	20953.8	573.1	17630.9
594.2	20726.5	588.9	20549.5	583.6	19071.2	578.3	21129.8	573	17526.9
594.1	20600.3	588.8	20493.8	583.5	19021.5	578.2	21313.4	572.9	17579
594	20804.4	588.7	20683.8	583.4	19224.8	578.1	21386.8	572.8	17463.6
593.9	20776.9	588.6	20768.5	583.3	19214.1	578	21431	572.7	17363.8
593.8	20581.2	588.5	20734.5	583.2	19023	577.9	21881.8	572.6	17320.9
593.7	20747.6	588.4	20814.2	583.1	19169.8	577.8	21920.5	572.5	17490.4
593.6	20723.7	588.3	20915.3	583	19093.5	577.7	21978.1	572.4	17483.5
593.5	20589.2	588.2	20953.2	582.9	19056.3	577.6	22226.7	572.3	17571.6
593.4	20686.1	588.1	21048.3	582.8	18992.1	577.5	22573.3	572.2	17506.7
593.3	20382.5	588	20995.1	582.7	19005.4	577.4	22492.1	572.1	17401.3
593.2	20447.3	587.9	21438.4	582.6	19129.3	577.3	22683.1	572	17363.5
593.1	20345	587.8	21225.3	582.5	18975	577.2	23081.8	571.9	17312.1
593	20648.5	587.7	21460.1	582.4	19027.3	577.1	23014.2	571.8	17532.8
592.9	20660.8	587.6	21404.9	582.3	19129.8	577	23025.8	571.7	17575
592.8	20367.1	587.5	21362.2	582.2	18989.9	576.9	23399.6	571.6	17425.3
592.7	20427.3	587.4	21447.3	582.1	18992.1	576.8	23426.6	571.5	17511.2
592.6	20419.4	587.3	21621.3	582	19130.9	576.7	23142.9	571.4	17420.1
592.5	20197.3	587.2	21635.1	581.9	19020.6	576.6	23379.1	571.3	17541.3
592.4	20287.4	587.1	21633.8	581.8	18967.5	576.5	23378	571.2	17392
592.3	20461.2	587	21654	581.7	19084.7	576.4	22958.9	571.1	17409.9
592.2	20591.2	586.9	21447.4	581.6	19175	576.3	22964.2	571	17233.9
592.1	20544.9	586.8	21614.5	581.5	19067.6	576.2	22801.3	570.9	17556
592	20284.6	586.7	21654.9	581.4	19255.3	576.1	22512.9	570.8	17540.9
591.9	20137.4	586.6	21783.8	581.3	19166.2	576	22455.2	570.7	17605.1
591.8	20231.9	586.5	21547.6	581.2	19148.9	575.9	22409	570.6	17414.2
591.7	20428.3	586.4	21775.9	581.1	18994.1	575.8	22216.8	570.5	17540
591.6	20250	586.3	21664.5	581	19042.1	575.7	21929.4	570.4	17275.6
591.5	20486.1	586.2	21555.1	580.9	19038	575.6	21504.1	570.3	17300.8
591.4	20574.5	586.1	21589.3	580.8	19165.2	575.5	21458.9	570.2	17379.6
591.3	20492.2	586	21567.3	580.7	19387.2	575.4	20770.2	570.1	17160.3
591.2	20348.2	585.9	21687.3	580.6	19377.8	575.3	20545.2	570	17254.5
591.1	20183	585.8	21422.2	580.5	19239.9	575.2	20387.7		
591	20207.7	585.7	21226.4	580.4	19339.5	575.1	20104.3		
590.9	20427.7	585.6	21094	580.3	19449.7	575	19721.8		
590.8	20071	585.5	20938.9	580.2	19420.2	574.9	19371		
590.7	20206.5	585.4	20864.6	580.1	19263.8	574.8	19157.4		
590.6	20208.7	585.3	20749.1	580	19330.9	574.7	19000.9		
590.5	20318.9	585.2	20758.9	579.9	19224.5	574.6	18577.8		
590.4	20339	585.1	20611.2	579.8	19524.5	574.5	18492.9		
590.3	20470.2	585	20390.8	579.7	19446	574.4	18363.6		
590.2	20540.3	584.9	20203.4	579.6	19603.2	574.3	18221.8		
590.1	20381.9	584.8	20247.4	579.5	19538.6	574.2	18221.5		
590	20502.3	584.7	20026.5	579.4	19689.8	574.1	18215.5		
589.9	20332.4	584.6	19783.3	579.3	19935.9	574	17913		
589.8	20458.9	584.5	19734.2	579.2	20122.7	573.9	17861		

Table 15 relationship between binding energy (eV) and residuals for Fe 800°C, 6 hr

Binding energy	Residuals	Binding energy	Residuals	Binding energy	Residuals	Binding energy	Residuals	Binding energy	Residuals
740	55921.7	734.7	48746	729.4	46001.1	724.1	47206.4	718.8	42327.6
739.9	55068.4	734.6	48772.5	729.3	46033.1	724	47054	718.7	42133.7
739.8	54847.8	734.5	48301.1	729.2	45583.4	723.9	46827.8	718.6	41962.1
739.7	54669.6	734.4	48467.2	729.1	46119.3	723.8	46807.8	718.5	42412.4
739.6	54606.5	734.3	48255.5	729	45788.6	723.7	46084.6	718.4	42436.2
739.5	53890.1	734.2	48032.7	728.9	46052.1	723.6	45701.1	718.3	41923.5
739.4	54038.9	734.1	48062.8	728.8	46548	723.5	46099.7	718.2	42117
739.3	53342.9	734	48182.4	728.7	46447.6	723.4	45942.2	718.1	42161.7
739.2	53305.6	733.9	47837	728.6	46284.6	723.3	45504.8	718	41865.1
739.1	53048.9	733.8	48153.6	728.5	46252.2	723.2	45162.7	717.9	41938.2
739	52557.3	733.7	48099.2	728.4	46334.4	723.1	45614.1	717.8	41650.5
738.9	52706.1	733.6	47752.6	728.3	46043.1	723	45169.5	717.7	41668.6
738.8	52656	733.5	47740.6	728.2	46257.5	722.9	45070.8	717.6	41545.5
738.7	52335.3	733.4	47838.8	728.1	46394.5	722.8	45037.7	717.5	41803.2
738.6	51961.2	733.3	47727.8	728	46715.3	722.7	44683.4	717.4	41555.1
738.5	51862.2	733.2	47577.5	727.9	46229.3	722.6	44381.2	717.3	42155.3
738.4	51301.4	733.1	47419.2	727.8	46031.5	722.5	44324.6	717.2	41623.3
738.3	50824.7	733	47807	727.7	45888	722.4	43854.5	717.1	41772.3
738.2	51577.3	732.9	47142.7	727.6	46479.2	722.3	43679.7	717	41896.1
738.1	51224.7	732.8	47261.1	727.5	46842	722.2	43940.3	716.9	41821.3
738	51099.9	732.7	47078.1	727.4	46512.5	722.1	43535.6	716.8	41457.9
737.9	51211.3	732.6	47240	727.3	46771.3	722	43271.4	716.7	41284.7
737.8	51233.2	732.5	47013.6	727.2	46828.1	721.9	43414.5	716.6	41480
737.7	50797.4	732.4	46887.2	727.1	46667.8	721.8	42974	716.5	41225.6
737.6	50351.4	732.3	46524.6	727	47086.7	721.7	43040.6	716.4	41397.6
737.5	50129.4	732.2	46582.9	726.9	46741.5	721.6	43168.4	716.3	41538.1
737.4	50568.6	732.1	46801.5	726.8	46500.6	721.5	43283.9	716.2	41495.6
737.3	50367.1	732	46924.3	726.7	47058.3	721.4	42755.2	716.1	41983.2
737.2	50114	731.9	46980.8	726.6	47533.5	721.3	42513.9	716	41836.9
737.1	50041.2	731.8	46612.8	726.5	47652.8	721.2	42542.6	715.9	41459.8
737	50050.8	731.7	46678.4	726.4	47418.5	721.1	42879.3	715.8	41463.8
736.9	49754.7	731.6	46011.7	726.3	47347.3	721	42874.4	715.7	41675.9
736.8	49558.2	731.5	46521.9	726.2	47193.3	720.9	42906	715.6	41759.4
736.7	50084.9	731.4	46456.7	726.1	47436.7	720.8	42680	715.5	41990.6
736.6	49859.6	731.3	46459.9	726	47891.1	720.7	42834.2	715.4	42075.5
736.5	49432.2	731.2	46751.9	725.9	47768.3	720.6	42297.6	715.3	41774.6
736.4	49115.9	731.1	46685.4	725.8	47975.4	720.5	42674.1	715.2	42292.4
736.3	49490	731	46661.4	725.7	47541.8	720.4	42319.2	715.1	42637.5
736.2	49459.6	730.9	46620.5	725.6	47769.4	720.3	42557.7	715	41974.3
736.1	49146.9	730.8	46253.7	725.5	47681.2	720.2	42706.5	714.9	41780.2
736	48793.9	730.7	46333.5	725.4	47885.6	720.1	42944.4	714.8	42422
735.9	49451.3	730.6	46658.7	725.3	47579.2	720	42942	714.7	42570.2
735.8	48961.2	730.5	46139.3	725.2	47377.4	719.9	42763.2	714.6	42567.7
735.7	49183.9	730.4	46103.4	725.1	47732.3	719.8	42733.8	714.5	42806.7
735.6	48609.4	730.3	45686	725	47554.6	719.7	42769.7	714.4	42705.2
735.5	48787.5	730.2	45931.8	724.9	47801.2	719.6	42381.5	714.3	42889.5
735.4	48467.2	730.1	45997.6	724.8	47715	719.5	42255.6	714.2	42719.2
735.3	48807.4	730	46247.3	724.7	47348	719.4	42204.2	714.1	42894.1
735.2	48319.7	729.9	46323.9	724.6	47583.5	719.3	42231	714	43156.4
735.1	48211.4	729.8	46377.8	724.5	47742.3	719.2	42556.5	713.9	43321.4
735	48151.8	729.7	45763	724.4	47349.2	719.1	42570.1	713.8	43565.1
734.9	48536.4	729.6	45602.4	724.3	47378.4	719	41986.8	713.7	43659
734.8	48561.7	729.5	45841.3	724.2	46746.8	718.9	42064.3	713.6	43641.2

Table 15(continued) relationship between binding energy (eV) and residuals for Fe 800°C, 6 hr.

Binding energy	Residuals	Binding energy	Residuals	Binding energy	Residuals
713.5	43960.2	708.2	36411.4	702.9	35824.6
713.4	43826.5	708.1	36140.3	702.8	35699.2
713.3	44120.1	708	35993.2	702.7	35784.2
713.2	44520.6	707.9	35794.4	702.6	36023
713.1	44211	707.8	35874.1	702.5	35520.4
713	44741.6	707.7	36033.7	702.4	35310.4
712.9	45183.4	707.6	35956.4	702.3	35608.6
712.8	44699.4	707.5	35901.9	702.2	35729.1
712.7	45001	707.4	35786.2	702.1	35886.8
712.6	44803.5	707.3	35377.1	702	36041.7
712.5	45708	707.2	35673.2	701.9	35842.5
712.4	45516.9	707.1	35783.9	701.8	35983.6
712.3	45718.5	707	35855.9	701.7	35953.7
712.2	45563.6	706.9	35574.6	701.6	35620
712.1	45743.9	706.8	35467.1	701.5	35578
712	45923.7	706.7	35906.5	701.4	35756.2
711.9	45912.1	706.6	35809.1	701.3	35463
711.8	45797.2	706.5	35517.8	701.2	35559.8
711.7	46054.2	706.4	35469.9	701.1	35627.5
711.6	45983.6	706.3	35720.9	701	35719
711.5	46167.3	706.2	35925.8	700.9	35717
711.4	46094.8	706.1	35745.5	700.8	35240.2
711.3	45905	706	35307.8	700.7	35382.3
711.2	45736.4	705.9	35806.1	700.6	35038.5
711.1	45948.9	705.8	35499.5	700.5	35130.8
711	46020.7	705.7	35424.4	700.4	35021.4
710.9	46092.2	705.6	35639	700.3	35564.8
710.8	45857.7	705.5	35819.6	700.2	35214.6
710.7	45648.8	705.4	35717.1	700.1	35005.3
710.6	45546.8	705.3	35692.2	700	35225.3
710.5	45304.1	705.2	35995		
710.4	44625.1	705.1	35803.7		
710.3	44524.9	705	35689.4		
710.2	44426.9	704.9	35455.2		
710.1	44042.7	704.8	35795.7		
710	43535.1	704.7	35783.7		
709.9	43516.8	704.6	35746.6		
709.8	42979.3	704.5	35543.8		
709.7	42174.6	704.4	35765		
709.6	41804.9	704.3	36121		
709.5	41087.4	704.2	35622.4		
709.4	41056.2	704.1	35521.1		
709.3	40405.8	704	35324.3		
709.2	39266.9	703.9	35823.7		
709.1	38972.8	703.8	35620.2		
709	39149.8	703.7	35902.6		
708.9	38537.5	703.6	35624		
708.8	38076.2	703.5	35777.9		
708.7	37441.9	703.4	35699.7		
708.6	37659.3	703.3	35584		
708.5	37751.5	703.2	35813.5		
708.4	36632.9	703.1	35865.3		
708.3	36528.6	703	35963.6		

Table 16 relationship between binding energy (eV) and residuals for Cr 800°C, 8 hr

Binding energy	Residuals	Binding energy	Residuals	Binding energy	Residuals	Binding energy	Residuals	Binding energy	Residuals
595	18892.4	589.7	19015	584.4	18395.8	579.1	19284.6	573.8	15787.5
594.9	19194.2	589.6	19103.9	584.3	18307.4	579	19310.4	573.7	15525.3
594.8	19025	589.5	19147.2	584.2	18249	578.9	19200.5	573.6	15494.2
594.7	18947.6	589.4	19118.1	584.1	18070.5	578.8	19296.2	573.5	15506.8
594.6	19000.8	589.3	19082.9	584	17997.1	578.7	19488.9	573.4	15463.1
594.5	18925.7	589.2	19184.7	583.9	17818.7	578.6	19632.4	573.3	15489.5
594.4	18878	589.1	19337.9	583.8	17859.5	578.5	19925	573.2	15602.5
594.3	19002.1	589	19329.8	583.7	17759.9	578.4	20227.4	573.1	15435
594.2	18819.9	588.9	19387.4	583.6	17657.2	578.3	20346.3	573	15539.4
594.1	18855.1	588.8	19360.6	583.5	17437.1	578.2	20589.3	572.9	15663.8
594	18837	588.7	19432.2	583.4	17319	578.1	20700.2	572.8	15493.4
593.9	18788.2	588.6	19602.6	583.3	17579.7	578	20738.3	572.7	15255
593.8	18708.8	588.5	19469.5	583.2	17536	577.9	20860.1	572.6	15514.7
593.7	18638.1	588.4	19705	583.1	17520.7	577.8	21229.2	572.5	15338.7
593.6	18692.6	588.3	19811.6	583	17495.3	577.7	21139.9	572.4	15261.9
593.5	18431	588.2	19784.7	582.9	17492.1	577.6	21411.1	572.3	15517
593.4	18445.1	588.1	19995.9	582.8	17555.8	577.5	21647.6	572.2	15280
593.3	18416.4	588	20153.4	582.7	17315.5	577.4	21777.8	572.1	15400.2
593.2	18517.2	587.9	20263	582.6	17414.2	577.3	21983.3	572	15404.7
593.1	18639.6	587.8	20270.5	582.5	17333.1	577.2	22164.8	571.9	15533.2
593	18594.8	587.7	20372.2	582.4	17328.3	577.1	22382.5	571.8	15422.8
592.9	18535.7	587.6	20324.8	582.3	17391.8	577	22135.4	571.7	15461.2
592.8	18708.4	587.5	20420	582.2	17458.7	576.9	22141.9	571.6	15391
592.7	18461.9	587.4	20650.4	582.1	17418.2	576.8	22314.2	571.5	15329
592.6	18655.3	587.3	20552.3	582	17641	576.7	22254.2	571.4	15362.4
592.5	18684	587.2	20345.4	581.9	17669.7	576.6	22220.3	571.3	15414.1
592.4	18547.5	587.1	20513.1	581.8	17513.6	576.5	22087	571.2	15371
592.3	18400.6	587	20617.7	581.7	17515.9	576.4	22039.8	571.1	15283.6
592.2	18516.4	586.9	20508.6	581.6	17458.1	576.3	21969.9	571	15597.2
592.1	18796.4	586.8	20397	581.5	17517.2	576.2	21553.8	570.9	15382.8
592	18684.1	586.7	20719.9	581.4	17528.7	576.1	21494.2	570.8	15372.1
591.9	18551	586.6	20816.8	581.3	17726	576	21397.2	570.7	15245.7
591.8	18511.3	586.5	20779.6	581.2	17603.2	575.9	20942.2	570.6	15341.5
591.7	18476.8	586.4	20745.1	581.1	17461.2	575.8	20581.1	570.5	15334.5
591.6	18502.4	586.3	20604.7	581	17685.1	575.7	20436	570.4	15395
591.5	18584.2	586.2	20375.4	580.9	17709.4	575.6	20091	570.3	15297
591.4	18623.9	586.1	20457.1	580.8	17824.6	575.5	19823.5	570.2	15256
591.3	18605.8	586	20407.9	580.7	17779.7	575.4	19425.2	570.1	15335.2
591.2	18581.2	585.9	20212.6	580.6	17829.1	575.3	19293.2	570	15387.5
591.1	18617.9	585.8	20280	580.5	17914.8	575.2	18699.5		
591	18674	585.7	20127	580.4	18077.6	575.1	18353.5		
590.9	18584	585.6	19980.7	580.3	18080.1	575	18178		
590.8	18798.5	585.5	19946.7	580.2	18049.1	574.9	17908.7		
590.7	18701.2	585.4	19702.4	580.1	18224.6	574.8	17641.6		
590.6	18540.1	585.3	19517.6	580	18348.4	574.7	17383.2		
590.5	18707.9	585.2	19360.2	579.9	18337	574.6	17083.7		
590.4	19023.2	585.1	19273.7	579.8	18294.3	574.5	16821.1		
590.3	18617.7	585	19117.9	579.7	18347.1	574.4	16611.9		
590.2	18755.1	584.9	18967.7	579.6	18648.2	574.3	16538.4		
590.1	18831.9	584.8	18686.4	579.5	18647.6	574.2	16246.3		
590	18697.2	584.7	18714.1	579.4	18494.9	574.1	16149.9		
589.9	18969.7	584.6	18517.4	579.3	18888.4	574	15958.4		
589.8	18744.2	584.5	18439	579.2	19020.5	573.9	15883.7		

Table 17 relationship between binding energy (eV) and residuals for Fe 800°C, 8 hr

Binding energy	Residuals	Binding energy	Residuals	Binding energy	Residuals	Binding energy	Residuals	Binding energy	Residuals
740	43908.9	734.7	38019.5	729.4	36666.2	724.1	36471.4	718.8	32407.9
739.9	43639.9	734.6	37612.1	729.3	36284.2	724	36141.4	718.7	32371.2
739.8	43601.3	734.5	37742.7	729.2	36270.2	723.9	35712.2	718.6	32493.8
739.7	43197.5	734.4	37877.3	729.1	36557	723.8	35948.2	718.5	32653.6
739.6	43045.2	734.3	37557.4	729	36151.4	723.7	35793	718.4	32222.3
739.5	43163.7	734.2	37669.8	728.9	36199.3	723.6	35317.8	718.3	32295.8
739.4	43221.6	734.1	37806.1	728.8	36186.1	723.5	35586.3	718.2	32358.8
739.3	42756.7	734	37620.5	728.7	36001.4	723.4	35775.2	718.1	32534.1
739.2	42691.4	733.9	37524.9	728.6	36370.2	723.3	35383.5	718	32754.9
739.1	42140.8	733.8	37418	728.5	36438.9	723.2	34875.3	717.9	32332.7
739	41927.7	733.7	36969.1	728.4	36371.9	723.1	35037.6	717.8	32478.2
738.9	41997.2	733.6	37372.3	728.3	36511.2	723	34933.5	717.7	32053
738.8	41613.9	733.5	37702.4	728.2	36318.6	722.9	35039.7	717.6	32163.4
738.7	41373	733.4	37473.6	728.1	36154.9	722.8	34651.6	717.5	32097
738.6	41312.6	733.3	36953.2	728	36954.7	722.7	34436.1	717.4	31981.4
738.5	41182.4	733.2	36900.9	727.9	36502.9	722.6	34700.4	717.3	32149.9
738.4	40861.8	733.1	37006	727.8	36699.6	722.5	34672.9	717.2	31940.5
738.3	40536.3	733	37088.1	727.7	36328.3	722.4	34393.9	717.1	32142.7
738.2	40499.7	732.9	37085.8	727.6	36505.9	722.3	34452.8	717	31958.8
738.1	40730.6	732.8	36924.3	727.5	36765.3	722.2	33958.5	716.9	31623
738	40633	732.7	37103.1	727.4	36520.5	722.1	33959.8	716.8	31983.7
737.9	39921.2	732.6	36797.5	727.3	36129.9	722	34070.5	716.7	32131.3
737.8	40220.1	732.5	36852.6	727.2	36769.5	721.9	34248.5	716.6	32148.6
737.7	40278.1	732.4	36788.8	727.1	36734.8	721.8	33448.6	716.5	32194.9
737.6	39859.5	732.3	36899.4	727	36880.5	721.7	33727.7	716.4	32115.1
737.5	40182.1	732.2	36567	726.9	36904.6	721.6	33348.7	716.3	32265.5
737.4	39825.5	732.1	36176.2	726.8	36690.9	721.5	33579.9	716.2	32118.9
737.3	39158.4	732	36374.2	726.7	36700.3	721.4	33143.1	716.1	32117.4
737.2	39724.3	731.9	36182.9	726.6	37069.9	721.3	33371.1	716	32421
737.1	39334.2	731.8	36571.4	726.5	36877.6	721.2	32919.2	715.9	32387.9
737	39547.8	731.7	36590.6	726.4	37031.6	721.1	33314.5	715.8	32169.1
736.9	39152.6	731.6	36447.6	726.3	37000.6	721	33114.9	715.7	31878.4
736.8	39139.7	731.5	36666.9	726.2	36550.2	720.9	33295.6	715.6	31756.1
736.7	38927.8	731.4	36724.2	726.1	36687.6	720.8	33286.4	715.5	32214.9
736.6	39017.7	731.3	36332.4	726	36920.1	720.7	33040.3	715.4	32410.8
736.5	39112.1	731.2	36562.2	725.9	36832.7	720.6	33250.5	715.3	32236
736.4	39154.5	731.1	36138.4	725.8	36651.7	720.5	33312.3	715.2	32618.3
736.3	39078.6	731	36327.1	725.7	36740.8	720.4	33131.1	715.1	32242.5
736.2	38528.3	730.9	36209.5	725.6	37073.6	720.3	32749.2	715	32170
736.1	38622.1	730.8	36460.4	725.5	37066.4	720.2	32871.1	714.9	32505.7
736	38772.7	730.7	36575.7	725.4	37176.5	720.1	32701.6	714.8	32453
735.9	39176.3	730.6	36299.1	725.3	36567.6	720	32959.4	714.7	32474.6
735.8	38876.1	730.5	36263.1	725.2	36237.5	719.9	32724.5	714.6	32423.2
735.7	38882.5	730.4	36191	725.1	36305.3	719.8	32880.3	714.5	32629.3
735.6	38119.8	730.3	36410.8	725	36789	719.7	33092.7	714.4	32848.2
735.5	38217.6	730.2	36567.8	724.9	36997.1	719.6	32830.7	714.3	32747.7
735.4	38418.5	730.1	36137.5	724.8	36290.4	719.5	32700.5	714.2	32641.6
735.3	38344.3	730	36375.5	724.7	36662.3	719.4	33079.8	714.1	32806.9
735.2	38341.1	729.9	36751.5	724.6	36457.8	719.3	33155.9	714	32566.4
735.1	38420.5	729.8	36404.9	724.5	36025.7	719.2	32633.7	713.9	33177.9
735	38146.6	729.7	36394.9	724.4	35701.2	719.1	32898.2	713.8	33219.2
734.9	37807.6	729.6	36040.3	724.3	36441.1	719	32633.4	713.7	32903.7
734.8	37757.1	729.5	36353.2	724.2	36123.2	718.9	32567.9	713.6	32873.4

Table 17(continued) relationship between binding energy (eV) and residuals for Fe 800°C, 6 hr.

Binding energy	Residuals	Binding energy	Residuals	Binding energy	Residuals
713.5	33312.1	708.2	29454.2	702.9	28604.3
713.4	33482.5	708.1	29273.8	702.8	28589.5
713.3	33599.7	708	29164.1	702.7	28945.5
713.2	33563.6	707.9	29039.4	702.6	29171.8
713.1	33461.3	707.8	29025.3	702.5	28727.5
713	33211.6	707.7	29131.3	702.4	28817.3
712.9	32997.2	707.6	28996.9	702.3	29172.7
712.8	33614.1	707.5	28787.9	702.2	28921
712.7	33828.2	707.4	28947.9	702.1	28924.9
712.6	33708.7	707.3	28920.2	702	28864.4
712.5	33872.9	707.2	28771.6	701.9	28763.2
712.4	33820	707.1	28989.7	701.8	28577.6
712.3	34071.3	707	29047.4	701.7	28858.3
712.2	34024.3	706.9	28975.2	701.6	28706
712.1	34084.4	706.8	28961.3	701.5	28910.7
712	34060.1	706.7	28644.5	701.4	28798.7
711.9	34130.1	706.6	28828.4	701.3	29053
711.8	34234.6	706.5	28830.6	701.2	29046.1
711.7	34273.7	706.4	28467.1	701.1	29186.2
711.6	34414.6	706.3	28703	701	29038.2
711.5	34540.3	706.2	28623.7	700.9	28793.6
711.4	34070	706.1	28509.6	700.8	28664.5
711.3	34285.5	706	28845.1	700.7	28884.3
711.2	34185.5	705.9	28841.4	700.6	28829.1
711.1	33882.6	705.8	28762.3	700.5	28718.9
711	33977.4	705.7	29167.9	700.4	28759.9
710.9	34057.4	705.6	28657.8	700.3	28796.2
710.8	34354.4	705.5	28545.3	700.2	28827.1
710.7	34216.2	705.4	28792	700.1	28776.7
710.6	33628.3	705.3	28638.8	700	28437.2
710.5	33544.8	705.2	28555.4		
710.4	33237.2	705.1	28535.2		
710.3	33815.2	705	28683.4		
710.2	33358	704.9	28803.6		
710.1	32949.8	704.8	28594.5		
710	32953.9	704.7	28940.1		
709.9	32671.5	704.6	28956.2		
709.8	32368.7	704.5	29146.3		
709.7	31910.2	704.4	29041.9		
709.6	32195.7	704.3	28841.4		
709.5	32189.3	704.2	28770.6		
709.4	31759	704.1	29038.8		
709.3	31625.1	704	28803.5		
709.2	31380.6	703.9	28872.3		
709.1	31070.1	703.8	28782.5		
709	30704.3	703.7	29021.6		
708.9	30273.7	703.6	29011.3		
708.8	30338.2	703.5	28826.4		
708.7	30566.9	703.4	29172		
708.6	30228	703.3	29213.7		
708.5	29990	703.2	28601.2		
708.4	29728.3	703.1	28812.1		
708.3	29617.7	703	28817.1		

Table 18 relationship between binding energy (eV) and residuals for Cr 800°C, 12 hr

Binding energy	Residuals	Binding energy	Residuals	Binding energy	Residuals	Binding energy	Residuals	Binding energy	Residuals
595	14200.5	589.7	13589.4	584.4	13391.9	579.1	13619.9	573.8	13105.1
594.9	13927.2	589.6	13732.6	584.3	13376.6	579	13680.9	573.7	12916.9
594.8	13921.6	589.5	13780.4	584.2	13235	578.9	13656.6	573.6	13138.5
594.7	14239.1	589.4	13808	584.1	13307.9	578.8	13704.4	573.5	13137
594.6	14043.5	589.3	13708.4	584	13359.9	578.7	13884	573.4	12913.2
594.5	13920	589.2	13740.3	583.9	13204	578.6	13949.6	573.3	12947.5
594.4	13935.3	589.1	13668.5	583.8	13271.1	578.5	13911.7	573.2	13136.7
594.3	13776.4	589	13714.1	583.7	13416.6	578.4	13805.5	573.1	13165.4
594.2	13985.7	588.9	13957.5	583.6	13391	578.3	13790.9	573	12982.6
594.1	13932.9	588.8	13757.8	583.5	13512.6	578.2	13773.3	572.9	12971.1
594	14016.4	588.7	13810.9	583.4	13385.7	578.1	13724.8	572.8	12835.4
593.9	13832.7	588.6	13801.8	583.3	13429.3	578	13618.4	572.7	13041.7
593.8	13784	588.5	13783.7	583.2	13257	577.9	13898.5	572.6	13051.4
593.7	13830.9	588.4	13791.5	583.1	13192.1	577.8	13927.1	572.5	13026.4
593.6	13954.5	588.3	13771.8	583	13256.2	577.7	13964.5	572.4	12927.4
593.5	13882.9	588.2	13656.7	582.9	13261.2	577.6	14102.5	572.3	12965.4
593.4	13950.1	588.1	13687.4	582.8	13222.6	577.5	13999.5	572.2	12990.8
593.3	13875.3	588	13814.9	582.7	13182.6	577.4	13818.4	572.1	12937.2
593.2	13756.5	587.9	13897.5	582.6	13299.9	577.3	13760.8	572	12795.6
593.1	13788.3	587.8	13746.2	582.5	13212.5	577.2	13769.4	571.9	12904.7
593	13736.4	587.7	13826.8	582.4	13320.7	577.1	13697.4	571.8	13000
592.9	13753.8	587.6	13696.3	582.3	13431.4	577	13705.4	571.7	13057.1
592.8	13781.9	587.5	13673.7	582.2	13550.4	576.9	13571.4	571.6	12945.3
592.7	13802.1	587.4	13806.3	582.1	13311	576.8	13574.9	571.5	12889.9
592.6	13788.9	587.3	13814.1	582	13189.5	576.7	13662.4	571.4	12882.4
592.5	13703.5	587.2	13726.1	581.9	13173.9	576.6	13586	571.3	12945.7
592.4	13692.2	587.1	13754.3	581.8	13386.8	576.5	13558.4	571.2	12942
592.3	13721.8	587	13752.2	581.7	13376.7	576.4	13559.3	571.1	12873.4
592.2	13810.6	586.9	13695.7	581.6	13315.2	576.3	13402.7	571	12936.7
592.1	13884.2	586.8	13584.9	581.5	13353.1	576.2	13358.9	570.9	12948.9
592	13805.8	586.7	13597.3	581.4	13426.2	576.1	13187.3	570.8	12805.3
591.9	13734.4	586.6	13507.2	581.3	13444.8	576	13279.8	570.7	12886.6
591.8	13806	586.5	13628.4	581.2	13305.9	575.9	13227	570.6	12673.2
591.7	13765.1	586.4	13520	581.1	13253.7	575.8	13292.6	570.5	12772.1
591.6	13725.2	586.3	13661.5	581	13218.4	575.7	13368.9	570.4	12735.1
591.5	13836.3	586.2	13560.5	580.9	13273.4	575.6	13234.8	570.3	12880
591.4	13656.1	586.1	13362.5	580.8	13352.1	575.5	13109.5	570.2	12820.1
591.3	13819.4	586	13519.4	580.7	13399.1	575.4	13294.8	570.1	12708.4
591.2	13750.2	585.9	13423	580.6	13306.9	575.3	13184.1	570	12752.3
591.1	13624.6	585.8	13385	580.5	13354.5	575.2	13209.7		
591	13808.3	585.7	13391.2	580.4	13313.5	575.1	13122.2		
590.9	13860.1	585.6	13415.5	580.3	13350.9	575	13168.4		
590.8	13642.6	585.5	13367.4	580.2	13422.9	574.9	12917.9		
590.7	13772.5	585.4	13526.3	580.1	13506.9	574.8	13168.4		
590.6	13909	585.3	13380.6	580	13516.5	574.7	12980.3		
590.5	13668.9	585.2	13365.9	579.9	13611.6	574.6	13123.4		
590.4	13677.3	585.1	13437	579.8	13516	574.5	13022.8		
590.3	13668.3	585	13310.1	579.7	13555.8	574.4	13091.2		
590.2	13627.6	584.9	13332.4	579.6	13572.5	574.3	13082.4		
590.1	13784.1	584.8	13330.4	579.5	13602	574.2	13106.1		
590	13786.6	584.7	13371.9	579.4	13571.1	574.1	12909		
589.9	13818.6	584.6	13321.7	579.3	13535.8	574	13118.9		
589.8	13684.3	584.5	13348.9	579.2	13795.7	573.9	13051.4		

Table 19 relationship between binding energy (eV) and residuals for Cr-Chromium electroplating oxidized 800°C, 12 hr

Binding energy	Residuals	Binding energy	Residuals	Binding energy	Residuals	Binding energy	Residuals	Binding energy	Residuals
595	16349.6	589.7	15989.4	584.4	15279	579.1	15727.1	573.8	14260.5
594.9	16411.7	589.6	16068	584.3	15231.1	579	15710.7	573.7	14250.6
594.8	16391.7	589.5	16133.9	584.2	15134.2	578.9	15860.2	573.6	14267.4
594.7	16368.4	589.4	15929.8	584.1	15135	578.8	15940.1	573.5	14281.9
594.6	16476.8	589.3	16009.6	584	14993	578.7	16120.6	573.4	14313.4
594.5	16516.1	589.2	16231.8	583.9	15053.6	578.6	16110.1	573.3	14200.7
594.4	16438.3	589.1	16267	583.8	15265.3	578.5	16224.1	573.2	14147.6
594.3	16379.2	589	16179	583.7	15081.3	578.4	16246.8	573.1	14045.5
594.2	16428.5	588.9	16011	583.6	15296.6	578.3	16375.8	573	14300.4
594.1	16335.5	588.8	16146.3	583.5	15168.8	578.2	16544.7	572.9	14326
594	16337.1	588.7	16282	583.4	15021.7	578.1	16516.1	572.8	14200.8
593.9	16438.7	588.6	16099	583.3	15101.5	578	16572.9	572.7	14298.5
593.8	16218	588.5	16032.8	583.2	14863.8	577.9	16623.9	572.6	14205
593.7	16278.6	588.4	16243.3	583.1	15082.8	577.8	16761.2	572.5	14205.9
593.6	16158	588.3	16180.2	583	15064.4	577.7	16769.6	572.4	14183.9
593.5	16184.6	588.2	16108.6	582.9	15148	577.6	16742.5	572.3	14236.6
593.4	16306.8	588.1	16204.8	582.8	15073.5	577.5	16978.2	572.2	14163.1
593.3	16350.6	588	16415.7	582.7	15047.4	577.4	17066	572.1	14143.7
593.2	16247.8	587.9	16557.9	582.6	14992.9	577.3	17111.1	572	14154.3
593.1	16326.5	587.8	16442.5	582.5	14933.6	577.2	17196.1	571.9	14229.3
593	16325.5	587.7	16553.6	582.4	14995.2	577.1	17210.4	571.8	14308.1
592.9	16237.5	587.6	16790.7	582.3	15067.1	577	17236.6	571.7	14339.3
592.8	16068	587.5	16546.7	582.2	15062.8	576.9	17177.2	571.6	14234.6
592.7	16013.5	587.4	16441.9	582.1	14888.8	576.8	17152.5	571.5	14175.4
592.6	16020.3	587.3	16375.4	582	14850.3	576.7	16969.3	571.4	14237.4
592.5	16126.1	587.2	16595.5	581.9	14949.2	576.6	16959.6	571.3	14320.3
592.4	16073.3	587.1	16611.3	581.8	15074.9	576.5	16981.4	571.2	14052.5
592.3	16091.8	587	16667.8	581.7	15089.5	576.4	16931.5	571.1	14051.3
592.2	16173.4	586.9	16740.2	581.6	15100	576.3	16745.2	571	14008
592.1	16119.6	586.8	16614.1	581.5	15044.6	576.2	16657.2	570.9	14042.4
592	16067.1	586.7	16459.2	581.4	15082	576.1	16762.8	570.8	14064.3
591.9	16169.7	586.6	16358.2	581.3	14944.9	576	16596.1	570.7	14118.2
591.8	16259.8	586.5	16434.3	581.2	14939.4	575.9	16214.1	570.6	14059.9
591.7	16075.6	586.4	16473.9	581.1	15124.4	575.8	15986.2	570.5	14117.6
591.6	16058.3	586.3	16451	581	15295.3	575.7	16075.9	570.4	13962.3
591.5	16158	586.2	16368.9	580.9	15196.7	575.6	15970.5	570.3	14027
591.4	16051.6	586.1	16251.5	580.8	15132	575.5	15810.7	570.2	14124.4
591.3	15899.8	586	16361.8	580.7	15128.6	575.4	15601.3	570.1	14220.5
591.2	15976.8	585.9	16417	580.6	15215.1	575.3	15394.2	570	14123.2
591.1	16039	585.8	16090.1	580.5	15230.3	575.2	15527.2		
591	16051.2	585.7	16038.4	580.4	15073.4	575.1	15206.2		
590.9	16002	585.6	15877.6	580.3	15280	575	15162.2		
590.8	15937.3	585.5	15831.4	580.2	15172	574.9	15001.9		
590.7	16065.8	585.4	15835.6	580.1	15096.1	574.8	14829.1		
590.6	15993	585.3	15704.2	580	15142.1	574.7	14826.2		
590.5	16080.4	585.2	15664.2	579.9	15265.7	574.6	14782.1		
590.4	16015.3	585.1	15673.7	579.8	15455.2	574.5	14610.1		
590.3	15923.1	585	15696.5	579.7	15430.7	574.4	14564.1		
590.2	16019.5	584.9	15592.9	579.6	15470	574.3	14460.7		
590.1	16033.1	584.8	15466.4	579.5	15535.3	574.2	14420.3		
590	16170.6	584.7	15415.4	579.4	15589.9	574.1	14495.3		
589.9	16163.3	584.6	15201.6	579.3	15682.3	574	14333.7		
589.8	15899.2	584.5	15190.8	579.2	15797.2	573.9	14400.9		

Table 20 relationship between binding energy (eV) and residuals for Fe- Chromium electroplating oxidized 800°C, 12 hr

Binding energy	Residuals	Binding energy	Residuals	Binding energy	Residuals	Binding energy	Residuals	Binding energy	Residuals
740	46202.7	734.7	40260.3	729.4	38736.8	724.1	39485.5	718.8	35524.2
739.9	46101.7	734.6	40132.4	729.3	38628.9	724	38977.9	718.7	35631.7
739.8	45845	734.5	40179.2	729.2	38724.5	723.9	38909.9	718.6	35514.2
739.7	46280.1	734.4	40657.5	729.1	38115.2	723.8	38768.3	718.5	35570.7
739.6	45956.1	734.3	40166.1	729	38031.9	723.7	38446.3	718.4	35658
739.5	45745.2	734.2	40195.9	728.9	38445.8	723.6	38667.7	718.3	35798.6
739.4	44870	734.1	40410.9	728.8	38417.9	723.5	38470.1	718.2	35479.8
739.3	44477.4	734	40314.2	728.7	38215.5	723.4	38512.1	718.1	35542.6
739.2	44696.3	733.9	40050.5	728.6	38539.7	723.3	38203.2	718	35363.2
739.1	44539.4	733.8	40261.6	728.5	38573.7	723.2	37837.7	717.9	35340.2
739	44300.8	733.7	40379.2	728.4	38454.2	723.1	37972.8	717.8	34910.1
738.9	43859.8	733.6	40054.7	728.3	38389.4	723	37559.3	717.7	34898.2
738.8	43695.8	733.5	39802.1	728.2	38228.9	722.9	37543.1	717.6	34787.2
738.7	43615.4	733.4	40095.7	728.1	38471.3	722.8	37846.8	717.5	35433.4
738.6	43657.1	733.3	39991.9	728	38361.3	722.7	37645.5	717.4	35313.4
738.5	43522.2	733.2	39436.4	727.9	38645.4	722.6	37346	717.3	35096.7
738.4	43402.7	733.1	39605.8	727.8	38690.4	722.5	36422	717.2	35183.4
738.3	43371	733	39720	727.7	38782.3	722.4	36576.3	717.1	35442.1
738.2	43143.1	732.9	39404.6	727.6	38639.3	722.3	36564.9	717	34977.6
738.1	43295.5	732.8	39089	727.5	38866.8	722.2	36431	716.9	35222.8
738	42693.5	732.7	39340.5	727.4	38704.7	722.1	36247.2	716.8	35461.8
737.9	42528.6	732.6	39596.8	727.3	38753.1	722	36571.1	716.7	35383
737.8	42332.7	732.5	39171.7	727.2	39565.7	721.9	36563.8	716.6	34604.3
737.7	42452.6	732.4	39318.2	727.1	39272.5	721.8	36045.8	716.5	34830.7
737.6	42224.4	732.3	39579.1	727	39363.4	721.7	35848.5	716.4	35069.3
737.5	42712.5	732.2	39327.7	726.9	39043	721.6	36187.5	716.3	34621.6
737.4	42428.2	732.1	39177.3	726.8	39342.8	721.5	35714.3	716.2	34767.8
737.3	41796.2	732	38978	726.7	39507.8	721.4	35778.8	716.1	35254.2
737.2	41587.4	731.9	38892.1	726.6	39512.5	721.3	36077.1	716	35039.1
737.1	41557.5	731.8	38932.1	726.5	39159.3	721.2	36050.9	715.9	34928.6
737	41899	731.7	38815.4	726.4	39385.6	721.1	35763.7	715.8	35214.8
736.9	41943.4	731.6	38743.3	726.3	38983.9	721	36011.6	715.7	35331.3
736.8	41963.2	731.5	38482.1	726.2	39160.8	720.9	35902.7	715.6	35109.2
736.7	41439.7	731.4	38745.6	726.1	39068.3	720.8	35897.3	715.5	35121.5
736.6	41622.5	731.3	38719.6	726	39603.1	720.7	35993	715.4	35245.3
736.5	41600.1	731.2	38764.3	725.9	39587.8	720.6	35917.9	715.3	35497.2
736.4	41756.1	731.1	38793.1	725.8	39742.6	720.5	35976.2	715.2	35389
736.3	41264	731	39023.6	725.7	39383.1	720.4	35825.7	715.1	35484.2
736.2	41393.2	730.9	38750.2	725.6	39612.8	720.3	35864.4	715	35698.9
736.1	41510.7	730.8	38161.8	725.5	39684.2	720.2	35845	714.9	35519.3
736	41031.4	730.7	38445	725.4	39639.8	720.1	35517.1	714.8	35794.9
735.9	40838.8	730.6	38423.7	725.3	39860.7	720	35373.9	714.7	35200
735.8	41082.8	730.5	38233.3	725.2	40106.4	719.9	35843.8	714.6	35867.3
735.7	40792.2	730.4	38512.2	725.1	39849.8	719.8	35629.7	714.5	35969.9
735.6	40916.7	730.3	38912	725	39323.6	719.7	35732.2	714.4	35561.8
735.5	40599.4	730.2	38474.4	724.9	39577.6	719.6	35735.7	714.3	35855.1
735.4	40481.7	730.1	38747.4	724.8	39471.6	719.5	36043.9	714.2	36163.7
735.3	40416.3	730	38545.4	724.7	39746.8	719.4	35743.7	714.1	36189.7
735.2	40580.7	729.9	38568.9	724.6	39718.3	719.3	35921.2	714	36142.2
735.1	40231.8	729.8	38439.4	724.5	39786.9	719.2	35695.8	713.9	36755.5
735	40111.9	729.7	38592.3	724.4	39881.6	719.1	35493.3	713.8	36440.3
734.9	40445.5	729.6	38357.4	724.3	39815.2	719	35761.2	713.7	36717
734.8	40755	729.5	38362.2	724.2	39520.6	718.9	35609.3	713.6	37002.7

Table 20(continued) relationship between binding energy (eV) and residuals for Fe-Chromium electroplating oxidized 800°C, 12 hr.

Binding energy	Residuals	Binding energy	Residuals	Binding energy	Residuals
713.5	36758.7	708.2	30451.2	702.9	29743.6
713.4	37308.8	708.1	30461.8	702.8	29811.5
713.3	37161	708	30436.2	702.7	29664.5
713.2	37565.6	707.9	30225.7	702.6	29616.6
713.1	37274	707.8	30318.6	702.5	30100.3
713	37409.9	707.7	30079.9	702.4	30075.9
712.9	38008.8	707.6	30233.8	702.3	29742.9
712.8	37614.7	707.5	29960.9	702.2	29727.2
712.7	37486.8	707.4	29918	702.1	30037.6
712.6	38080.9	707.3	29644	702	30017.2
712.5	38158	707.2	29787.8	701.9	29677.4
712.4	38403.3	707.1	29864.5	701.8	29750.3
712.3	38439.2	707	29759.2	701.7	29757.9
712.2	38718.9	706.9	29814.6	701.6	30207.4
712.1	38496.1	706.8	29839	701.5	30015.6
712	38489	706.7	29810.3	701.4	29742.2
711.9	38508.1	706.6	29716.1	701.3	29715.2
711.8	38773.6	706.5	29705.7	701.2	29432.3
711.7	38595.6	706.4	30087.4	701.1	29624.5
711.6	38739.6	706.3	29771.6	701	29772
711.5	38874	706.2	29887.1	700.9	29377
711.4	38919.9	706.1	29840.9	700.8	29166.4
711.3	39229.3	706	29967.1	700.7	29286.7
711.2	38969.6	705.9	29833.9	700.6	29498.3
711.1	38881.9	705.8	29725.2	700.5	29168.4
711	38886.1	705.7	30021.3	700.4	29158.6
710.9	38756.3	705.6	29614	700.3	29142.5
710.8	38645.4	705.5	29806.6	700.2	29119.7
710.7	38543.3	705.4	30020.6	700.1	29112.3
710.6	38753.2	705.3	29605.2	700	29139.4
710.5	38391.7	705.2	29437		
710.4	38287.6	705.1	29879.7		
710.3	37842.3	705	29749.8		
710.2	37474.9	704.9	29976.7		
710.1	37078.2	704.8	29798.9		
710	37104.6	704.7	29683.4		
709.9	36449.2	704.6	29932.9		
709.8	35914.6	704.5	29968.9		
709.7	35593.2	704.4	29979.3		
709.6	35581.6	704.3	29549.2		
709.5	34680.2	704.2	29825.2		
709.4	33900.6	704.1	29857.9		
709.3	33789.3	704	29641		
709.2	33515.9	703.9	29500.4		
709.1	33028.7	703.8	29589.5		
709	32502.8	703.7	29533.2		
708.9	32116.8	703.6	29621.1		
708.8	31779.8	703.5	29903.6		
708.7	31525.1	703.4	30042.6		
708.6	31392	703.3	30016.8		
708.5	31115.6	703.2	29795.1		
708.4	30921.9	703.1	29833.3		
708.3	30769.3	703	29561.3		

Table 21 relationship between binding energy (eV) and residuals for Cr-CrN sputtering

Binding energy	Residuals	Binding energy	Residuals	Binding energy	Residuals	Binding energy	Residuals	Binding energy	Residuals
595	21495.4	589.7	19936.1	584.4	22472	579.1	19408.1	573.8	15346.2
594.9	21313.1	589.6	19851.7	584.3	22217.1	579	19804.7	573.7	14755.4
594.8	21097.9	589.5	20400.7	584.2	21784.7	578.9	20451.2	573.6	14245.7
594.7	21088.3	589.4	20496	584.1	21451.2	578.8	20499.8	573.5	13968.2
594.6	21041.1	589.3	20697.3	584	21093	578.7	20854.5	573.4	13275.3
594.5	20900.4	589.2	20893.1	583.9	20675.2	578.6	21150.6	573.3	13011
594.4	20521.2	589.1	20926.7	583.8	20101.1	578.5	21290.6	573.2	12645.2
594.3	20411.9	589	20923.1	583.7	19660	578.4	21676.7	573.1	12558.4
594.2	20679.6	588.9	20590.4	583.6	19745.4	578.3	22256.7	573	12456.6
594.1	20549.6	588.8	20832.4	583.5	19339.9	578.2	22570.4	572.9	12218.7
594	20532.5	588.7	21103.5	583.4	18942.1	578.1	22985	572.8	12117.7
593.9	20581.3	588.6	21104.9	583.3	18889.5	578	23201.6	572.7	12158.4
593.8	20287.9	588.5	21233.9	583.2	18528.8	577.9	23525.7	572.6	12087.6
593.7	20501.4	588.4	21220.5	583.1	17901.9	577.8	24005.7	572.5	11806.7
593.6	20068.4	588.3	21750	583	18113.7	577.7	24438.6	572.4	11791.1
593.5	20199.6	588.2	22003.2	582.9	17912.6	577.6	25038.6	572.3	11681.6
593.4	20379.8	588.1	21832.1	582.8	17877.5	577.5	25404.4	572.2	11682.6
593.3	20304.1	588	22258.1	582.7	17713.5	577.4	26040.3	572.1	11792.2
593.2	20061.1	587.9	22443	582.6	17707.3	577.3	26527.9	572	11772.1
593.1	19975.1	587.8	22684.1	582.5	17486.3	577.2	26986	571.9	11672.2
593	19641.1	587.7	22409.5	582.4	17313.9	577.1	27503.8	571.8	11448.6
592.9	19915.3	587.6	22469.1	582.3	17245.2	577	27777.1	571.7	11644.4
592.8	19917.2	587.5	22867.4	582.2	17072.5	576.9	28192.1	571.6	11529.6
592.7	19862.5	587.4	23411.5	582.1	17315.2	576.8	28718.4	571.5	11702.1
592.6	19582.4	587.3	23269.3	582	17196.2	576.7	28951.4	571.4	11665.3
592.5	19913.9	587.2	23491.8	581.9	17036.1	576.6	29492.1	571.3	11534.2
592.4	19841.3	587.1	23690.1	581.8	16842.6	576.5	29663.4	571.2	11534.3
592.3	19734.6	587	23913.5	581.7	17046.4	576.4	29733.6	571.1	11483.9
592.2	19500.2	586.9	23883.9	581.6	17063.8	576.3	29720.3	571	11486.3
592.1	19463	586.8	24034.6	581.5	17084.4	576.2	30026	570.9	11649.2
592	19729.7	586.7	24024.8	581.4	17123.7	576.1	30047.8	570.8	11616.9
591.9	19822.1	586.6	24383.7	581.3	17106.5	576	30024.6	570.7	11640.9
591.8	19590.2	586.5	24576.4	581.2	17232.5	575.9	29960.6	570.6	11548.1
591.7	19768.5	586.4	24433.4	581.1	17215.8	575.8	29587.4	570.5	11665.2
591.6	19758.1	586.3	24763.3	581	17231.4	575.7	29439.7	570.4	11593
591.5	19625.8	586.2	25284.4	580.9	17238.5	575.6	29086.8	570.3	11616.4
591.4	19489.4	586.1	25409.7	580.8	17270.1	575.5	28602.7	570.2	11798.7
591.3	19350.9	586	25412.6	580.7	17626	575.4	28187.7	570.1	11588.4
591.2	19531.8	585.9	24929.1	580.6	17467.6	575.3	27119.6	570	11381.4
591.1	19797.4	585.8	25551.9	580.5	17752.3	575.2	26723.3		
591	19637.8	585.7	25635.7	580.4	17677.2	575.1	25882.1		
590.9	19381.9	585.6	25322	580.3	17409.9	575	25476.8		
590.8	19876.9	585.5	25429.7	580.2	17640.7	574.9	24678.6		
590.7	20025.6	585.4	25306.8	580.1	17923	574.8	23794.9		
590.6	19863.2	585.3	25293.4	580	18050.1	574.7	22669.2		
590.5	20119.9	585.2	24999.2	579.9	18235.6	574.6	21824.8		
590.4	20144.8	585.1	25191.2	579.8	18115.2	574.5	20999.3		
590.3	19688.5	585	24557.5	579.7	18387.6	574.4	19824.8		
590.2	19907.9	584.9	24364.7	579.6	18532.5	574.3	18855.7		
590.1	20095.8	584.8	23977.6	579.5	18889.4	574.2	18162		
590	19909.5	584.7	23751.1	579.4	19212.6	574.1	17615.1		
589.9	19809.5	584.6	23487.1	579.3	19132.2	574	16671.3		
589.8	20127.4	584.5	22909	579.2	19488.2	573.9	16228		

Table 21 relationship between binding energy (eV) and residuals for N- CrN sputtering

Binding energy	Residuals	Binding energy	Residuals	Binding energy	Residuals	Binding energy	Residuals
410	6801.15	404.7	6351.1	399.4	7269.4	394.1	5735.05
409.9	6676.4	404.6	6432.35	399.3	7357.8	394	5594.45
409.8	6562.4	404.5	6447.7	399.2	7503.3	393.9	5762
409.7	6742.7	404.4	6277.35	399.1	7374.9	393.8	5762.75
409.6	6739.05	404.3	6170.1	399	7627.25	393.7	5596.8
409.5	6758.15	404.2	6411.2	398.9	7554.05	393.6	5660.15
409.4	6411.35	404.1	6304.3	398.8	7574	393.5	5596.6
409.3	6642.3	404	6263.6	398.7	7911.4	393.4	5547.85
409.2	6702.8	403.9	6199.45	398.6	7988.7	393.3	5493.85
409.1	6611.7	403.8	6337.6	398.5	8187.05	393.2	5515.35
409.0	6603.05	403.7	6294.05	398.4	8243.35	393.1	5529.75
408.9	6609.4	403.6	6327.45	398.3	8449.55	393	5504.9
408.8	6589.8	403.5	6188.25	398.2	8713.05	392.9	5431.3
408.7	6590.35	403.4	6200.2	398.1	8909.8	392.8	5540.6
408.6	6554.3	403.3	6317.7	398	9269.2	392.7	5693.3
408.5	6545.35	403.2	6305.2	397.9	9624.3	392.6	5891.35
408.4	6626.65	403.1	6344.8	397.8	9785.65	392.5	5570.9
408.3	6726.6	403	6520.15	397.7	10074.2	392.4	5487.3
408.2	6783.6	402.9	6380.15	397.6	10697.8	392.3	5475.15
408.1	6594	402.8	6287.1	397.5	10936.5	392.2	5486.4
408	6814.9	402.7	6300.45	397.4	11158.4	392.1	5486.35
407.9	6637.45	402.6	6272.8	397.3	11507	392	5459.7
407.8	6576.2	402.5	6345.9	397.2	11608.4	391.9	5561
407.7	6599.7	402.4	6534.8	397.1	11837.6	391.8	5534.75
407.6	6614.7	402.3	6219.1	397	11852.1	391.7	5549.75
407.5	6635.55	402.2	6342.3	396.9	11985.2	391.6	5625.85
407.4	6724.6	402.1	6475.1	396.8	12478.4	391.5	5563.75
407.3	6610.55	402	6322.1	396.7	12104	391.4	5530.45
407.2	6560.75	401.9	6298.7	396.6	11986.4	391.3	5628.05
407.1	6531.25	401.8	6485.2	396.5	11932.1	391.2	5507.3
407	6502.95	401.7	6492.6	396.4	11345.7	391.1	5603.9
406.9	6549.35	401.6	6219.05	396.3	11215.9	391	5461.25
406.8	6564.3	401.5	6484.45	396.2	10933.2	390.9	5547.65
406.7	6580.85	401.4	6617.35	396.1	10632.8	390.8	5682.8
406.6	6605.3	401.3	6437.5	396	9967.7	390.7	5540.4
406.5	6565.8	401.2	6358	395.9	9565.3	390.6	5612.65
406.4	6635.1	401.1	6287.75	395.8	9236.9	390.5	5573.35
406.3	6507.8	401	6481.45	395.7	8818.35	390.4	5584.55
406.2	6595.4	400.9	6492.6	395.6	8408.9	390.3	5548.2
406.1	6578.25	400.8	6510.9	395.5	7837.6	390.2	5466.25
406	6354.85	400.7	6546.8	395.4	7542.9	390.1	5649.8
405.9	6466.15	400.6	6801.8	395.3	7347.4	390	5671.15
405.8	6598.9	400.5	6864.4	395.2	6925.25		
405.7	6481.35	400.4	6853.15	395.1	6708.45		
405.6	6396.15	400.3	6890.2	395	6479.65		
405.5	6470.45	400.2	6934.95	394.9	6315.4		
405.4	6508.4	400.1	7018.85	394.8	6239.1		
405.3	6434.6	400	6896.9	394.7	6130.15		
405.2	6282.95	399.9	6964.2	394.6	5953.4		
405.1	6250.75	399.8	7072.45	394.5	5891.55		
405	6403.75	399.7	7157.35	394.4	5849.9		
404.9	6238.45	399.6	7051.3	394.3	5749.5		
404.8	6163.95	399.5	7234.35	394.2	5835.95		

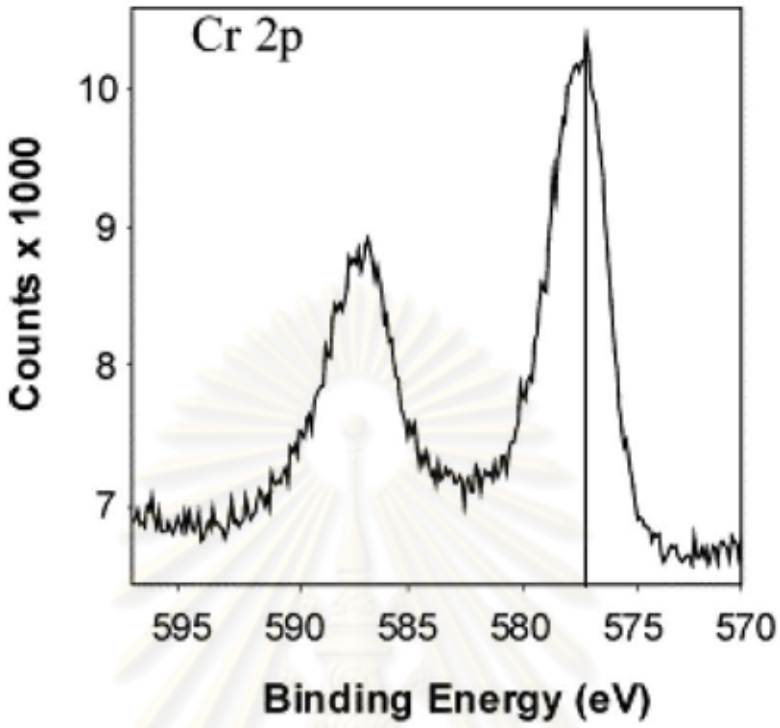

Fig. A-1. Narrow scan XPS spectrum of Cr 2p for promoted skeletal Cr sample.

As standard Cr2p3 peak binding energy given at 577.5

Table 22 Metal distribution in the palladium membrane heated at 450, 500 and 550°C.

Support			Pd layer (%)				Interlayer (%)				Stainless steel (%)			
			Pd	Fe	Cr	Ni	Pd	Fe	Cr	Ni	Pd	Fe	Cr	Ni
No barrier, unoxidized, Ar-exposed	450°C	1	96,90	2,24	0,39	0,47					1,72	70,22	17,91	10,15
		2	95,77	2,95	0,83	0,45					0,09	70,91	19,24	9,76
		3	96,61	2,03	0,77	0,58					0,19	71,01	18,97	9,84
		Av	**96,43**	**2,41**	**0,66**	**0,50**					**0,67**	**70,71**	**18,71**	**9,92**
		SD	**0,59**	**0,48**	**0,24**	**0,07**					**0,91**	**0,43**	**0,70**	**0,21**
	500°	1	88,18	7,49	3,44	0,89					0,09	70,57	19,33	10,01
		2	87,10	8,26	3,64	1,00					0,00	71,12	19,41	9,47
		3	87,48	8,25	3,63	0,64								
		4	86,93	7,97	4,07	1,03								
		Av	**87,42**	**7,99**	**3,70**	**0,89**					**0,05**	**70,85**	**19,37**	**9,74**
		SD	**0,55**	**0,36**	**0,27**	**0,18**					**0,06**	**0,39**	**0,06**	**0,38**
	550°C	1	73,06	22,58	2,96	1,40					0,01	71,68	19,56	8,75
		2	83,56	10,48	4,49	1,47					0,00	70,40	19,37	10,23
		3	72,80	21,54	4,33	1,33								
		4	75,72	20,29	3,07	0,92								
		Av	**73,86**	**21,47**	**3,45**	**1,22**					**0,01**	**71,04**	**19,47**	**9,49**
		SD	**1,62**	**1,15**	**0,76**	**0,26**					**0,01**	**0,91**	**0,13**	**1,05**
Cr_2O_3, direct oxidation, Ar-exposed	450°C	1	98,57	0,93	0,16	0,34					0,17	71,17	18,76	9,91
		2	97,97	0,72	0,40	0,91					0,00	71,24	18,58	10,19
		3	99,12	0,59	0,29	0,00								
		4	99,22	0,61	0,17	0,00								
		Av	**98,72**	**0,71**	**0,26**	**0,31**					**0,09**	**71,21**	**18,67**	**10,05**
		SD	**0,58**	**0,16**	**0,11**	**0,43**					**0,12**	**0,05**	**0,13**	**0,20**
	500°C	1	97,03	2,02	0,54	0,40					0,17	70,61	19,26	9,97
		2	97,09	1,94	0,45	0,52					0,02	70,44	19,51	10,02
		3	97,48	1,62	0,29	0,61								
		4	97,98	1,33	0,69	0,00								
		Av	**97,40**	**1,73**	**0,49**	**0,38**					**0,10**	**70,53**	**19,39**	**10,00**
		SD	**0,44**	**0,32**	**0,17**	**0,27**					**0,11**	**0,12**	**0,18**	**0,04**
	550°C	1	97,57	1,91	0,18	0,34					0,11	71,51	18,52	9,86
		2	96,91	2,28	0,27	0,54					0,10	71,54	18,70	9,65
		3	96,16	2,35	0,59	0,94								
		4	97,12	2,08	0,10	0,70								
		Av	**96,94**	**2,16**	**0,29**	**0,63**					**0,11**	**71,53**	**18,61**	**9,76**
		SD	**0,59**	**0,20**	**0,21**	**0,25**					**0,01**	**0,02**	**0,13**	**0,15**

Values in shaded cells were not used in calculation due to high deviation. Note that the Cr2O3 interlayer formed via direct oxidation was too thin to be visible under SEM therefore its metal distributions were not determined.

Table 23 (continued) Metal distribution in the palladium membrane heated at 450, 500 and 550°C.

Support			Pd layer (%)				Interlayer (%)				Stainless steel (%)			
			Pd	**Fe**	**Cr**	**Ni**	**Pd**	**Fe**	**Cr**	**Ni**	**Pd**	**Fe**	**Cr**	**Ni**
Cr_2O_3, oxidized Cr-electroplating, Ar-exposed	450°C	1	99,50	0,22	0,28	0,00	0,00	0,36	99,59	0,05	0,00	70,32	18,61	11,07
		2	99,03	0,16	0,47	0,34	0,21	0,07	99,72	0,00	0,00	70,75	18,57	10,68
		3	99,06	0,40	0,55	0,00	0,23	0,25	99,34	0,17				
		4	97,21	1,18	1,46	0,15								
		Avg	**99,20**	**0,26**	**0,43**	**0,11**	**0,15**	**0,23**	**99,55**	**0,07**	**0,00**	**70,54**	**18,59**	**10,88**
		SD	**0,26**	**0,12**	**0,14**	**0,20**	**0,13**	**0,15**	**0,19**	**0,09**	**0,00**	**0,30**	**0,03**	**0,28**
	500°C	1	98,37	1,05	0,25	0,33	0,39	0,22	98,93	0,46	0,00	71,83	16,92	11,25
		2	99,15	0,51	0,34	0,00	1,25	0,39	98,32	0,04	0,02	72,21	15,82	11,99
		3	99,11	0,63	0,18	0,08	0,63	0,85	98,52	0,00				
		4	98,55	0,99	0,21	0,25								
		Avg	**98,80**	**0,80**	**0,25**	**0,17**	**0,76**	**0,49**	**98,59**	**0,17**	**0,01**	**72,02**	**16,37**	**11,62**
		SD	**0,39**	**0,27**	**0,07**	**0,15**	**0,44**	**0,33**	**0,31**	**0,25**	**0,01**	**0,27**	**0,78**	**0,52**
	550°C	1	98,66	0,86	0,20	0,27	0,35	0,38	98,27	1,00	0,22	67,09	23,25	9,44
		2	98,61	0,87	0,34	0,18	0,38	0,41	98,25	0,96	0,50	70,54	18,10	9,87
		3	97,60	1,55	0,41	0,45	0,31	0,16	98,69	0,84				
		4	98,56	0,89	0,25	0,31								
		Avg	**98,36**	**1,04**	**0,30**	**0,30**	**0,35**	**0,32**	**98,40**	**0,93**	**0,36**	**68,82**	**20,68**	**9,66**
		SD	**0,51**	**0,34**	**0,09**	**0,11**	**0,04**	**0,14**	**0,25**	**0,08**	**0,20**	**2,44**	**3,64**	**0,30**
Cr_2O_3, oxidized Cr-sputtering, Ar-exposed	450°C	1	97,99	1,49	0,20	0,32	2,78	56,93	30,14	10,15	0,00	71,57	18,27	10,42
		2	98,22	1,32	0,38	0,08	5,69	58,17	31,23	4,91	0,14	70,92	18,30	10,64
		3	98,69	1,16	0,07	0,08	4,13	60,60	30,58	4,69	0,15	70,79	18,34	10,72
		Avg	**98,30**	**1,32**	**0,22**	**0,16**	**Err**	**Err**	**Err**	**Err**	**0,10**	**71,09**	**18,30**	**10,59**
		SD	**0,36**	**0,17**	**0,16**	**0,14**	**Err**	**Err**	**Err**	**Err**	**0,08**	**0,42**	**0,04**	**0,16**
	500°C	1	98,00	1,54	0,46	0,00	6,10	9,26	83,17	1,11	0,00	71,42	18,38	10,20
		2	97,94	1,40	0,46	0,20	4,89	23,66	68,79	2,66	0,27	71,46	17,81	10,46
		3	98,46	0,73	0,57	0,24	5,11	6,03	88,13	0,72	0,21	71,73	17,76	10,29
		Avg	**98,13**	**1,22**	**0,50**	**0,15**	**Err**	**Err**	**Err**	**Err**	**0,16**	**71,54**	**17,98**	**10,32**
		SD	**0,28**	**0,43**	**0,06**	**0,13**	**Err**	**Err**	**Err**	**Err**	**0,14**	**0,17**	**0,34**	**0,13**
	550°C	1	98,14	0,94	0,50	0,42	0,48	23,39	72,75	3,38	0,27	70,77	18,03	10,94
		2	98,60	0,67	0,69	0,05	0,44	65,54	23,95	10,07	0,14	70,41	18,03	11,43
		3	97,48	1,45	0,84	0,24	0,19	70,37	18,62	10,83	0,13	70,62	18,22	11,03
		Avg	**98,07**	**1,02**	**0,68**	**0,24**	**Err**	**Err**	**Err**	**Err**	**0,18**	**70,60**	**18,09**	**11,13**
		SD	**0,56**	**0,40**	**0,17**	**0,19**	**Err**	**Err**	**Err**	**Err**	**0,08**	**0,18**	**0,11**	**0,26**

Values in shaded cells were not used in calculation due to high deviation. Err indicates that the mean or SD is meaningless due to spotting error. In such cases, the interlayer, clearly although visible under SEM, was very thin therefore it was not possible for the probe to spot within it without covering the adjacent layers.

Table 24 (continued) Metal distribution in the palladium membrane heated at 450, 500 and 550°C.

Support			Pd layer (%)				Interlayer (%)				Stainless steel (%)			
			Pd	**Fe**	**Cr**	**Ni**	**Pd**	**Fe**	**Cr**	**Ni**	**Pd**	**Fe**	**Cr**	**Ni**
CrN, Ar-exposed	**450°C**	1	98,95	0,92	0,56	0,17	0,76	71,26	17,36	10,62	0,00	71,65	17,83	10,52
		2	98,16	1,04	0,74	0,05	8,97	62,43	19,28	9,32	0,00	71,23	18,23	10,54
		3	99,04	0,66	0,30	0,00	2,81	70,26	14,80	12,13	0,42	71,20	18,01	10,37
		Avg	**98,72**	**0,87**	**0,53**	**0,07**	**Err**	**Err**	**Err**	**Err**	**0,14**	**71,36**	**18,02**	**10,48**
		SD	**0,48**	**0,19**	**0,22**	**0,09**	**Err**	**Err**	**Err**	**Err**	**0,24**	**0,25**	**0,20**	**0,09**
	500°C	1	96,75	1,55	0,78	0,92	14,12	61,63	15,82	8,43	0,44	70,20	18,29	11,07
		2	96,19	2,13	0,93	0,75	2,68	69,86	17,03	10,44	0,38	70,97	18,05	10,60
		3	97,29	1,78	0,93	0,00	2,04	70,61	17,22	10,13	0,00	71,69	18,12	10,47
		Avg	**96,74**	**1,82**	**0,88**	**0,56**	**Err**	**Err**	**Err**	**Err**	**0,27**	**70,95**	**18,15**	**10,71**
		SD	**0,55**	**0,29**	**0,09**	**0,49**	**Err**	**Err**	**Err**	**Err**	**0,24**	**0,75**	**0,12**	**0,32**
	550°C	1	97,27	1,03	1,47	0,23	20,78	44,25	28,81	6,16	0,00	71,26	18,06	10,67
		2	94,02	2,34	3,59	0,05	20,22	47,65	24,82	7,30	0,46	70,74	18,12	10,68
		3	92,95	1,90	2,24	2,91	22,52	42,09	29,40	6,00	0,32	71,05	18,77	11,05
		Avg	**94,75**	**1,76**	**2,43**	**1,06**	**Err**	**Err**	**Err**	**Err**	**0,26**	**71,02**	**18,32**	**10,80**
		SD	**2,25**	**0,67**	**1,07**	**1,60**	**Err**	**Err**	**Err**	**Err**	**0,24**	**0,26**	**0,39**	**0,22**

Err indicates that the mean or SD is meaningless due to spotting error. In such cases, the interlayer, clearly although visible under SEM, was very thin therefore it was not possible for the probe to spot within it without covering the adjacent layers.

CURRICULUM VITAE

Name: Mr.Jaroenporn Chokboribal

Date of Birth: February 1, 1982

Residence: 681 Moo 8, Tambon Nongkronkhwang, A.Muang, Udonthani 41000

Education:

In 2004 Bachelor of Science (Chemistry), Chulalongkorn University, Bangkok, Thailand.

Presentation at the Nation Conference

In 2006 Jaroenporn Chokboribal, Supawan Tantayanon and Sukkaneste Tunkasamitra, "Chromium Oxide Formation as the Intermetallic diffusion barrier for palladium membrane, 3rd MPSGC, Faculty of Science University of Malaya Kuala Lumpur, Malaysia.